*European Journal of Taxonomy* 1021: 1–54
https://doi.org/10.5852/ejt.2025.1021.3075


europeanjournaloftaxonomy.eu
ISSN 2118-9773
2025 · Worsaae K.*et al.*

*Received: 5 January 2025* • *Accepted: 22 May 2025* • *Published: 26 September 2025*

*Topic editor: Magalie Castelin* • *Section editor: Nataliya Budaeva* • *Desk editor: Pepe Fernández*

**Monograph**

urn:lsid:zoobank.org:pub:07E3FF98-E70A-4E83-94EA-1FBCF60236D5

# High diversity and new species of meiofaunal Nerillidae (Annelida) in subtidal sediments and anchialine caves of the East China Sea

Katrine WORSAAE [1,*], Malte J. HANSEN [2], Éloïse DEFOURNEAUX [3], Jørgen OLESEN [4], Jiseon PARK [5], Taeseo PARK [6] & Yoshihisa FUJITA [7]

[1,2,3] Marine Biological Section, Department of Biology, University of Copenhagen, Universitetsparken 4, 2100-DK Copenhagen, Denmark.
[4] Natural History Museum of Denmark, University of Copenhagen, Universitetsparken 15, 2100 Copenhagen Ø, Denmark.
[5] Institute for Data Innovation in Science, Seoul National University, Seoul, 08826, Republic of Korea.
[6] Biodiversity Research Department, National Institute of Biological Resources, Incheon, 22689, Republic of Korea.
[7] Okinawa Prefectural University of Arts, 1-4 Shuri-Tounokura, Naha, Okinawa 903-8602, Japan.

* Corresponding author: kworsaae@bio.ku.dk
[2] Email: maltejarlgaard@hotmail.com
[3] Email: elo.dfx@gmail.com
[4] Email: jolesen@snm.ku.dk
[5] Email: jspark0406@hanmail.net
[6] Email: polychaeta@gmail.com
[7] Email: fujitayo@okigei.ac.jp

**Abstract.** Nerillidae is the most species-rich, meiofaunal, annelid family, but little is known about its diversity and distribution in the Northwest Pacific. Four sampling campaigns to Jeju Island, South Korea, and the Ryukyu Islands, Japan, retrieved an unexpectedly high diversity of about 17 nerillid species in subtidal and submarine cave localities of the East China sea, with only *Nipponerilla irabuensis* Worsaae, Hansen & Fujita in Worsaae *et al*., 2021 previously described. Bayesian inference and maximum likelihood methods were performed on datasets of concatenated gene sequences (18S rRNA, 28S rRNA, COI, and H3) comprising a total of 55 terminals from 11 different genera of Nerillidae. Integrating detailed morphological assessments (light-, scanning electron-, and confocal laser scanning microscopy) with molecular analyses, we here describe seven new species and a new genus, *Cirrinerilla* gen. nov. None of the species show geographical overlap between South Korea and the Ryukyu Islands, possibly due to oceanographic and anchialine dispersal barriers and poor dispersal capabilities of Nerillidae. However, two congeneric terminals of *Meganerilla* and two of *Leptonerilla* from different islands of the Ryukyus show relatively high molecular similarity, suggesting recent vicariance of these populations (or species). The anchialine caves hold a remarkably high diversity of nerillids compared to coastal subtidal localities, supporting a preadaptation of Nerillidae to these isolated habitats under freshwater influence. This study underlines the need for further exploration of the unique anchialine habitats as well

as additional subtidal meiofauna surveys in the East China Sea, for shedding further light on benthic diversifications and colonizations in this region.

**Keywords.** Interstitial, hidden biodiversity, Stygobiota, molecular phylogeny, evolution.

Worsaae K., Hansen M.J., Defourneaux É., Olesen J., Park J., Park T. & Fujita Y. 2025. High diversity and new species of meiofaunal Nerillidae (Annelida) in subtidal sediments and anchialine caves of the East China Sea. *European Journal of Taxonomy* 1021: 1–54. https://doi.org/10.5852/ejt.2025.1021.3075

## Introduction

The East China Sea covers an area of about 770 000 km$^2$ and extends from Taiwan in the south to the Korean Peninsula in the north (Liu 2013; Wang *et al*. 2014). The shallow continental shelf of East China and Korea extends across most of the East China Sea, but to the southeast, it transitions into the Okinawa Trough along the Ryukyu Islands, where depths reach down to 2700 meters (Wang *et al*. 2014; Gallagher *et al*. 2015). Within the limits of the Okinawa Trough flows the Kuroshio Current, a warm water western boundary current which enters the East China Sea east of Taiwan and exits west of South Korea (Veron 1992; Liu 2013; Wang *et al*. 2014).

While rocky coastline and tidal flats occur along the south coast of South Korea (Chough *et al*. 2000; Saito & Alino 2008; Eisma 2010), the Japanese coastline bordering the East China Sea is somewhat different, mostly with cliffs on the western coast of Kyushu Island and fringing reefs being common in the Ryukyu Islands (Veron 1992; Fujikura *et al*. 2010; Koike 2010; Nakae *et al*. 2018; Reimer *et al*. 2019). Mangrove forests also occur in the Ryukyu Archipelago, along with tidal flats, estuaries, small coves, and sandy beaches (Koike 2010; Fujita *et al*. 2015; Nakae *et al*. 2018). Limestone formations are common throughout the Ryukyu Archipelago (Takayasu 1978; Fujita *et al*. 2015), and the dissolution of this limestone has created submarine cave systems in many of the islands. Exploration of these caves and the associated fauna has mostly been performed in the central and southern regions of the archipelago (e.g., Hayami & Kase 1993; Shimomura *et al.* 2012; Fujimoto & Miyazaki 2013; Fujimoto 2015; Naruse & Fujita 2015; Chiu *et al.* 2017; Shimomura & Fujita 2017, 2021; Kakui & Fujita 2018, 2022; Komai & Fujita 2018; Okanishi & Fujita 2018; Osawa & Fujita 2019, 2022; Saito & Fujita 2022; Ise *et al.* 2023; Shimada *et al.* 2023; Fujita & Naruse 2024), covering a variety of simple euhaline to more complex anchialine cave systems (Hayami & Kase 1993; Osawa & Fujita 2019).

Meiobenthic diversity and taxonomic studies have historically been mostly focused on European and North American waters (Giere 2009). South Korean and Japanese meiobenthos studies have mainly examined hard-bodied ecdysozoans such as nematodes, harpacticoid copepods, and ostracods, presumably due to better preservation in bulk fixed samples and their high densities and diversity in meiofaunal communities (Kim *et al*. 2000; Shimada *et al*. 2009; Pavlyuk & Trebukhova 2011; Shimada & Kajihara 2014; Motokawa & Kajihara 2017; Lee *et al*. 2019; Atherton & Jondelius 2020; Kang & Kim 2020). Soft-bodied annelids have received less attention, even though they are highly abundant in most meiofauna samples (Giere 2009). Up to this day, only two species belonging to the exclusively meiofaunal families of Annelida Lamarck, 1802 are recorded from South Korea, *Pharyngocirrus uchidai* Sasaki, 1981 and *Polygordius pacificus* Uchida, 1935 (Uchida 1935; Sasaki 1981; Di Domenico *et al*. 2014). However, a recent PhD study indicates a much higher diversity of interstitial annelids in this area (Park 2023). Japan has more records and several descriptions of meiofaunal annelids, primarily from the intertidal and supratidal zones of the larger islands (i.e., Hokkaido, Honshu, and Kyushu). These include species of *Aricidea* Webster, 1879, *Dimorphilus* Worsaae, Kerbl, Vang & Gonzalez, 2021, *Diurodrilus* Remane, 1925, *Dorvillea* Parfitt, 1866, *Goniadides* Hartmann-Schröder, 1960, *Hesionides* Friedrich, 1937, *Hesionura* Hartmann-Schröder, 1958, *Microphthalmus* Mecznikow, 1865, *Ophryotrocha*

Claparède & Mecznikow, 1869, *Pharyngocirrus* Di Domenico, Martínez, Lana & Worsaae, 2014, *Pisione* Grube, 1857, *Polygordius* Schneider, 1868, *Protodrilus* Hatschek, 1881, *Trilobodrilus* Remane, 1925, *Ctenodrilus* Claparède, 1863, and *Stygocapitella* Knöllner, 1934 (see Yamanishi 1983; Jimi 2024 and references therein).

Still, the most species-rich meiofaunal family, Nerillidae Levinsen, 1883, has not been reported from South Korea except in the PhD study by Park (Park 2023), and only two nerillids have so far been found in Japanese waters (Worsaae *et al*. 2021a). The recently discovered cave species and genus, *Nipponerilla irabuensis* Worsaae, Hansen & Fujita, 2021 from the Miyako Islands (Ryukyu Archipelago) is the only nerillid described from Japan (Worsaae *et al*. 2021b). Moreover, the European *Nerilla mediterranea* Schlieper, 1925 has been reported from Japan (Yamanishi 1983); however, the exact species identity warrants further examination. Additionally, *Nerillidium orientalis* (Tzetlin & Larionov, 1988) (original genus name *Akessoniella*) is described from Sakhalin and Kunashir Island near Hokkaido (Tzetlin & Larionov 1988; Worsaae 2005a) and *Nerilla jouini* Saphonov & Tzetlin, 1988 from Popov Island in Peter the Great Gulf, Sea of Japan (Saphonov & Tzetlin 1988).

Nerillidae consists of 61 species in 15 genera (Worsaae 2020; Worsaae *et al*. 2021a, 2021b; Mendes *et al*. 2024). All nerillids are marine or brackish, except for a single limnic species (*Troglochaetus beranecki* Delachaux, 1921). The family is distributed worldwide, with species recorded from supratidal pools to the deep-sea. Most species live in the interstices of coarse subtidal sediment in coastal areas, while some prefer muddy or silty sediments. Others have been found in bacterial mats and diatom carpets on lapilli, and one species is even associated with hydrothermal vent areas (Worsaae & Kristensen 2005; Worsaae & Rouse 2009; Worsaae 2020, 2021). Anchialine cave systems have been documented to house a remarkable diversity of nerillids (Worsaae *et al*. 2004, 2009, 2019a, 2019b, 2021a, 2021b; Curini-Galletti *et al*. 2012; Martínez *et al*. 2019; Gonzalez *et al*. 2021).

Species distributions are usually limited (sometimes to the type locality) due to their small size and lack of dormant or larval dispersal stages (except in *Paranerilla* Jouin & Swedmark, 1965) (Worsaae 2005a, 2021). Climatic conditions, special habitat demands, or isolation may also affect the distribution of *Speleonerilla* Worsaae, Sterrer & Iliffe, 2018 and *Nipponerilla* Worsaae, Hansen & Fujita, 2021, only found in anchialine caves, and similar to *Leptonerilla* Westheide & Purschke, 1996 only recorded from tropical and subtropical localities (Worsaae 2021). Exceptionally, *Nerilla antennata* Schmidt, 1848 has been reported from both sides of the Atlantic and the Pacific Oceans, as well as from the Indian Ocean (Worsaae 2021 and references therein). However, for nerillids, such extensive reported geographical ranges generally reflect a lack of detailed morphological examinations or cryptic diversity (Schmidt & Westheide 1998; Worsaae *et al*. 2019a, 2021a; Worsaae 2021).

Nerillids have seven to nine segments, simple or compound chaetae, and single or double interramal parapodial cirri, the interramal cirri being an autapomorphy of the family. Paired pigmented eyes can be found on the prostomium, which furthermore carries up to three antennae and two palps or horns. The pygidium usually carries two cirri and sometimes additional pygidial lobes. The size and shape of cirri, antennae and palps vary significantly within the family. The exact combination of these traits is used to diagnose the genera (Worsaae 2021; Worsaae *et al*. 2021a, 2021b). Nerillid body length ranges from 0.3 mm (*Bathychaetus heptapous* Faubel, 1978) to 2.1 mm (*Meganerilla swedmarki* Boaden, 1961). A locomotory midventral ciliary band extending from the mouth to the pygidium facilitates gliding over surfaces, whereas longitudinal muscles and other ciliary bands may facilitate swimming. Additional ciliary groups (tufts, bands, bandlets, fields or patches) of potential systematic significance may be found on the dorsal, ventral and lateral surfaces of the head and body, typically at the level of parapodia or between parapodia, accompanied by discrete ciliation on cirri and palps and pygidial lobes (Worsaae 2005a, 2021; Westheide 2008). External ciliation and openings are best observed using scanning electron

microscopy. Nerillids can be gonochoristic or hermaphroditic and all examined species exhibit direct development (except for *Paranerilla*) (Jouin & Swedmark 1965; Jouin 1968; Worsaae & Müller 2004; Westheide 2008; Worsaae 2021). One pair of oviducts and one to three pairs of spermioducts have been detected, with either separate or common gonopores (Worsaae & Müller 2004). External brooding is seen in *Mesonerilla* Remane, 1949, *Nerillidium* Remane, 1925 and *Nerillidopsis* Jouin, 1967, with *Mesonerilla intermedia* Wilke, 1953 and *M. laerkae* Worsaae, Mikkelsen & Martínez, 2019 additionally possessing a protective brooding hood (Jouin 1968; Westheide 2008; Worsaae *et al*. 2019a). The configuration of the ciliated gonoducts can be species or clade-specific and can best be examined with confocal laser scanning microscopy of cilia labelled with immunostaining against tubulin (Worsaae & Müller 2004).

Our study unveils a high diversity of Nerillidae in the East China Sea, collected during expeditions between 2015 and 2019 to Jeju Island in South Korea and several localities of the Ryukyu Islands, Japan. Light-, scanning electron- and confocal laser scanning microscopy, as well as molecular data are used to morphologically and genetically describe seven new species, including one new genus. The lack of well-preserved material prevented a full description of nine additional, potentially new species; however, genetic data (in addition to sparse morphological information) were obtained from these individual populations for later reference. The interrelationship of all species from the East China Sea was assessed through phylogenetic analyses of four gene markers (18S rRNA, 28S rRNA, COI and H3), including a total of 55 terminals (and 11 genera) of Nerillidae. Morphological and molecular phylogenetic data are discussed in relation to the diversification and biogeography of Nerillidae in the East China Sea.

## Material and methods

### Sampling

Specimens were collected between 2015 and 2019 in the northern and southern regions of the East China Sea, south of Jeju Island, South Korea and around Iriomote, Miyako and Okinawa Islands of the Ryukyu Archipelago, Japan (see Fig. 1 for map of sampling localities). Samples of fine sand to coral rubble were collected by scuba divers in the subtidal zones of coral reefs as well as in anchialine caves. In the caves, meiofauna was further collected by towing of a 30 cm wide conical 63 or 100 µm plankton net close to the bottom and through the water column, sometimes while stirring up the upper layers of fine, silty sediment. Additionally, a slurp gun was used for sampling in crevicular spaces.

Animals were extracted from sediment samples using the $MgCl_2$ decantation technique and a 63 µm mesh (Higgins & Thiel 1988), sorted out alive using an Olympus SZX16 or SZ51 dissecting scope and, when possible, photographed via mounted cameras (IDS UI-3140CP-C-HQ Rev.2 or an iPhone X combined with iDu Optics LabCam™ microscope adapter). Samples collected by plankton towing and slurp gun were sorted out directly without prior $MgCl_2$ decantation. Sorted animals were subsequently anesthetized with a 1:1 isotonic $MgCl_2$/seawater solution and fixed for their respective microscopic or molecular analytical purposes: i) 2–4% trialdehyde solution (0.1 M cacodylate buffer with 5–7% sucrose) for 24 hrs at 4°C (stored in 0.1 M cacodylate buffer; for SEM), ii) 2% paraformaldehyde solution (in PBS (phosphate buffered saline) with 5–7% sucrose) for 18–24 h at 4°C or for 30 min–2 h at room temperature, followed by up to six rinses in PBS (stored in PBS with 0.05% $NaN_3$; for CLSM), or iii) stored in 99% ethanol (for DNA extraction).

### Molecular analyses

Genetic datasets include 55 terminals belonging to 11 different genera of Nerillidae, resulting in the most comprehensive phylogeny of the family to date. Selection of terminals was based on the availability of complete or partial sequences of at least two out of the following four genes: the nuclear gene markers 18S rRNA (1800 bp), 28S rRNA (1100 bp) and H3 (330 bp), and the mitochondrial gene marker COI (650 bp). New sequences were obtained from 17 potentially new species of Nerillidae collected from

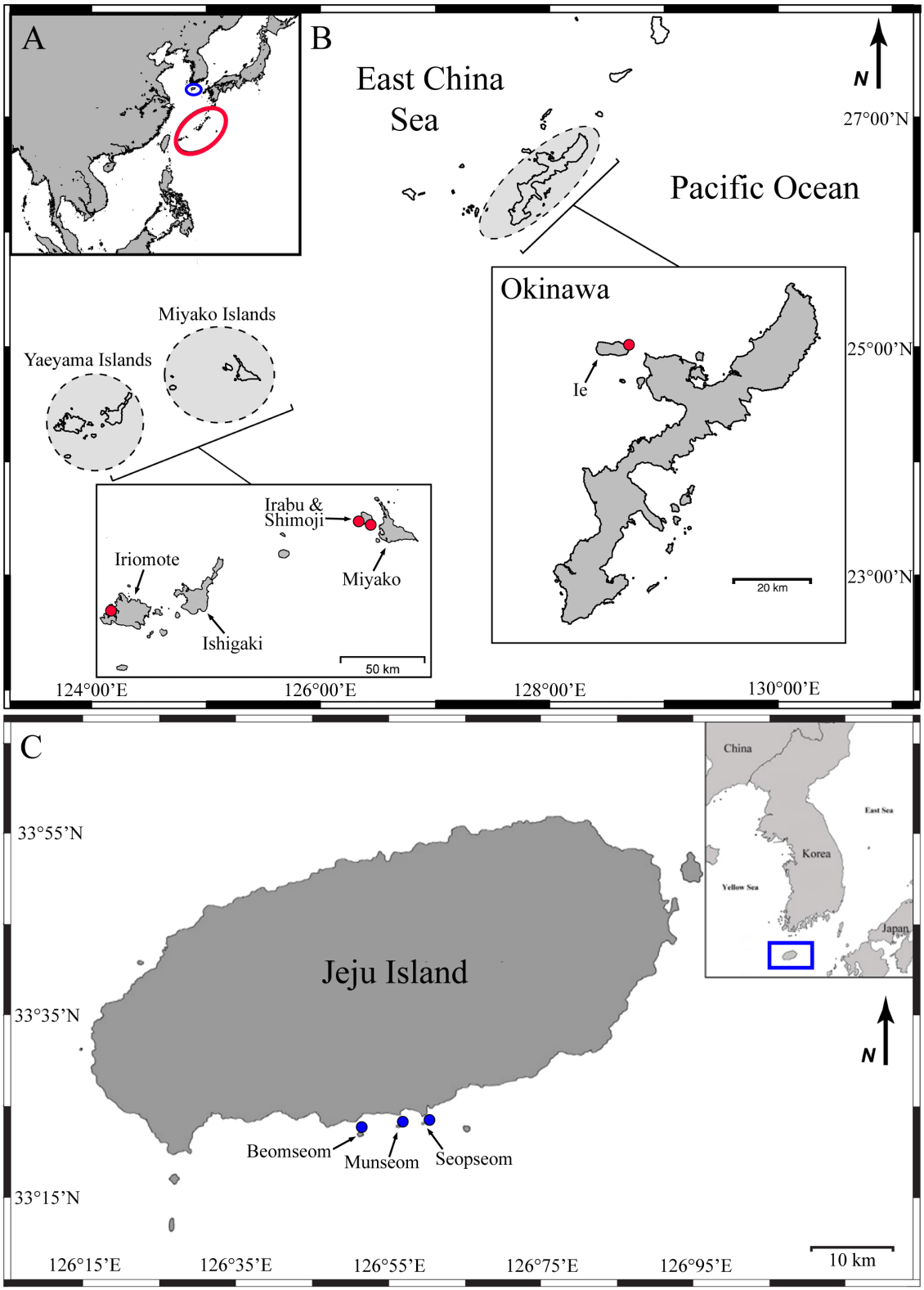


**Fig. 1.** Map of sampling localities in the East China Sea. **A**. Overview map, red and blue circles indicating study areas in Japan and South Korea (modified from Weese *et al*. 2016). **B**. Map of the Ryukyu Islands (Japan), red dots showing sampling localities (modified from Weese *et al*. 2016). **C**. Map of Jeju Island (South Korea), blue dots showing sampling localities (modified from Chan *et al*. 2018).

the East China Sea and two additional species from Trinidad and Tobago (*Aristonerilla* sp. 1) and Italy (*Micronerilla* sp. 1). These data were combined with available nerillid data from GenBank, including *Nipponerilla irabuensis* from Japan (Worsaae *et al*. 2021b). Collection sites and available sequences of the included terminals are listed in Table 1.

DNA of specimens fixed in 99% ethanol was extracted using the Qiagen DNeasy® Blood and Tissue kit, following the manufacturer's instructions. DNA elution was performed twice with 80 µl elution buffer into two separate extraction samples. Polymerase chain reaction (PCR) solutions consisted of a total volume of 25 µl with 1–1.5 µl DNA template, 4–5 µl HOT FIREPol® Blend Master Mix (Solis Biodyne, 04-25-00115), 1–1.5 µl of each primer (10 µm) and 15–17 µl UV-sterilized Milli-Q (adjusted to DNA template and primer volume). PCR protocols were performed on a Bio-Rad S100 Thermal Cycler with reaction solutions first being heated to 94°C for 13 min, followed by 35–42 cycles of denaturation (94°C for 30–40 s), annealing (45–55°C (depending on primer specificity, see Table 2) for 30–40 s) and extension (68–72°C for 45–90 s). Subsequently, a final extension phase at 72°C for 5 min was carried out. Single primer pairs were used to amplify the selected fragments of 28S rDNA, COI and H3, while two and sometimes three overlapping fragments were needed to amplify the 18S rDNA fragment. Details of primers are described in Table 2. Gel electrophoresis (1% agarose with GelRed® (Biotium, 41003)) was used to check for contamination and assess amplicons, and amplified sequences were afterwards purified with an E.Z.N.A.® Cycle Pure Kit (Omega Bio-tek). Sequencing was performed by Macrogen Europe (Amsterdam, Netherlands). Sequences were processed and examined for chromatogram misreads and contamination in Sequencher ver. 4.10.1 (GeneCodes Corporation, Ann Arbor, MI, USA) or Geneious Prime ver. 2021.2.2 (Dotmatics) (https://www.geneious.com). Consensus sequences were verified for contamination on the NCBI Standard Nucleotide Blast online platform, using the BLAST tool (Basic Local Alignment Search Tool). All newly generated sequences were deposited in GenBank®.

Sequences were aligned using MAFFT ver. 7.450 (Katoh *et al*. 2002; Katoh & Standley 2013) as implemented in Geneious. The E-INS-i algorithm was selected for nuclear markers (18S rDNA and 28S rDNA), while the G-INS-I one was used for the protein-coding genes (COI and H3). Default parameters were applied for all alignments (Gap open penalty: 1.53, Offset value: 0.123, Scoring matrix: 200 PAM/k = 2). As they show no variation in length, protein-coding gene alignments were trivial. However, to verify the presence of stop codons and indels, they were translated to amino acid sequences in Geneious. Alignments for each gene marker were edited and trimmed before being concatenated using the 'Concatenate Sequences or Alignments' tool in Geneious. The third codon of the COI alignment was excluded in the phylogenetic analyses shown in Fig. 2, due to genetic saturation, which was tested with the program DAMBE ver. 7.2.25 (Xia 2017).

Phylogenetic tree reconstructions were performed using both Maximum Likelihood (ML) and Bayesian Inference (BI) methods. ML analyses were conducted with IQ-TREE 2 ver. 2.2.6 (Minh *et al*. 2020), while BI analyses were executed using MrBayes ver. 3.2.7a (Ronquist & Huelsenbeck 2003) via the CIPRES Science Gateway online platform (Miller *et al*. 2010). To determine the most suitable nucleotide substitution models, jModelTest (Posada 2008) integrated in IQ-TREE was employed, with model selection based on the Bayesian Information Criterion (BIC), choosing the GTR+F+I+G4 model. Nodal support was calculated by ultrafast bootstrapping with 1500 replicates (Hoang *et al*. 2018). MrBayes was run twice for 15 million generations, with tree-sampling every 1000 generations and 3.75 million generations discarded as burn-in, using one cold and three heated chains. The GTR+I+ Γ model was selected. Proper convergence and parameter mixing were found using Tracer ver. 1.7.1 (Rambaut *et al*. 2018). Unrooted trees were generated and subsequently edited using FigTree ver. 1.4.4.

The pairwise sequence similarity of individual gene fragments, trimmed before primers, was calculated with MEGA X ver. 10.1.18 (Kumar *et al*. 2018). The Kimura 2-parameter distance model (Kimura 1980)

**Table 1** (continued on next page). Molecular data of nerillid species used in phylogenetic analyses and morphological techniques used to investigate each species. New sequences marked in bold.

| Species | ID extraction | Cave | Locality | GenBank accession numbers | | | | LM | SEM | CLSM |
|---|---|---|---|---|---|---|---|---|---|---|
| | | | | 18S rRNA | 28S rRNA | COI | H3 | | | |
| *Aristonerilla brevis* | KW019 | | Düsseldorf Aquarium, Germany | AY859530 | MK579428 | MK579454 | MK579473 | x | x | x |
| ***Aristonerilla*** sp. 1 | KW138 | | Tobago, Trinidad & Tobago | **PQ149833** | **PQ149815** | **PQ570583** | – | – | – | – |
| ***Cirrinerilla sulcipalpata*** gen. et sp. nov. | KW820 | 'Unnamed Cave' | Ie Isl. (island), Okinawa, Japan | **PQ149834** | **PQ149816** | **PQ570584** | **PQ421127** | x | x | x |
| ***Cirrinerilla sulcipalpata*** gen. et sp. nov. | KW826 | 'Unnamed Cave' | Ie Isl., Okinawa, Japan | **PQ149835** | **PQ149817** | **PQ570585** | **PQ421126** | x | x | x |
| ***Leptonerilla westheidei*** sp. nov. | KW708 | | Beomseom Isl., Jeju Isl., South Korea | **PQ149836** | **–** | **PQ570586** | **PQ421134** | x | x | – |
| *Leptonerilla diatomeophaga* | KW228 | Jameos del Agua | Lanzarote, Spain | MK579404 | MK579429 | MK579455 | MK579474 | x | – | – |
| *Leptonerilla prospera* | KW018 | Walsingham Cave | Bermuda | MH395342 | MH395352 | MH395369 | MH395358 | x | – | x |
| *Leptonerilla* sp. 1 | KW158 | | Scripps Aquarium, San Diego, USA | MH395340 | MH395353 | MH395370 | MH395361 | – | – | – |
| ***Leptonerilla*** sp. 2 | KW779 | Devil's Hole Cave | Shimoji Isl., Miyako Isl. Group, Japan | **PQ149837** | **PQ149818** | **PQ570587** | **PQ421129** | – | – | – |
| ***Leptonerilla*** sp. 3 | KW815 | 'Unnamed Cave' | Ie Isl., Okinawa, Japan | **PQ149838** | **PQ149819** | **PQ570588** | **PQ421128** | – | – | – |
| ***Leptonerilla purschkei*** sp. nov. | KW783 | Devil's Hole Cave | Shimoji Isl., Miyako Isl. Group, Japan | **PQ149839** | **PQ149820** | **PQ570589** | **PQ421135** | x | x | x |
| *Meganerilla cesari* | KW270 | Túnel de la Atlántida | Lanzarote, Spain | MK579405 | MK579431 | – | MK579475 | x | x | x |
| ***Meganerilla iensis*** sp. nov. | KW816 | | Ie Isl., Okinawa, Japan | **PQ149840** | **PQ149821** | **PQ570590** | **PQ421132** | x | x | – |
| ***Meganerilla*** sp. 1 | KW782 | | Irabu Isl., Miyako Isl. Group, Japan | **PQ149841** | **PQ149822** | **PQ570591** | **PQ421131** | – | – | – |
| ***Meganerilla*** sp. 2 | KW823 | | Munseom Isl., Jeju Isl., South Korea | **PQ149842** | **PQ149823** | **PQ570592** | **PQ421133** | – | – | – |
| *Mesonerilla armoricana* | KW250 | Grotta di Nereo | West Sardinia, Italy | MH395337 | MH395351 | – | MH395359 | x | x | – |
| *Mesonerilla aryae* | KW342 | | Punta del Hidalgo, Tenerife, Spain | MK579419 | MK579445 | MK579466 | MK579489 | – | x | x |
| *Mesonerilla biantennata* | KW244 | | Sardinia, Italy | MK579421 | MK579446 | MK579468 | MK579491 | x | x | x |
| *Mesonerilla* cf. *luederitzi* | KW247 | | Tenerife, Spain | MK579417 | MK579443 | MK579465 | MK579487 | x | x | x |
| *Mesonerilla* cf. *luederitzi* | KW227 | | Gran Canaria, Spain | MK579412 | MK579438 | MK579460 | MK579482 | – | x | x |
| *Mesonerilla* cf. *luederitzi* | KW240 | | Mala, Lanzarote, Spain | MK579414 | MK579440 | MK579462 | MK579484 | x | x | x |
| *Mesonerilla* cf. *luederitzi* | KW056 | | Marie Celeste Wreck, Bermuda | MK579408 | – | MK579458 | MK579478 | x | – | x |
| *Mesonerilla fagei* | KW291 | | Primel, Roscoff, France | MH395336 | MH395350 | – | MH395360 | x | x | – |
| ***Mesonerilla gamaglandulata*** sp. nov. | KW811 | 'Unnamed Cave' | Ie Isl., Okinawa, Japan | **PQ149843** | **PQ149824** | **PQ570593** | **PQ421136** | x | x | x |
| ***Mesonerilla harubangi*** sp. nov. | KW714 | | Seopseom Isl., Jeju Isl., South Korea | **PQ149844** | **–** | **PQ570594** | – | – | x | – |
| *Mesonerilla intermedia* | KW229 | | Sardinia, Italy | MK579413 | MK579439 | MK579461 | – | – | x | x |
| *Mesonerilla intermedia* | KW243 | Cueva del Palo | Mallorca, Spain | MK579415 | MK579441 | MK579463 | MK579485 | x | x | x |
| *Mesonerilla katharinae* | KW246 | | Bocas, Panama | MK579416 | MK579442 | MK579464 | MK579486 | x | x | x |
| *Mesonerilla laerkae* | KW380 | | Massachusetts, USA | MK579420 | – | MK579467 | MK579490 | x | x | x |
| *Mesonerilla peteri* | KW024 | | Tobago, Trinidad & Tobago | – | MK579433 | MK579457 | MK579477 | – | – | x |
| *Mesonerilla roscovita* | KW084 | | Trezen ar Skoden, Roscoff, France | MK579422 | – | – | MK579492 | x | – | – |
| ***Mesonerilla runae*** | KW271 | Túnel de la Atlántida | Lanzarote, Spain | – | MK579444 | **PQ570595** | MK579488 | x | x | x |
| *Mesonerilla xurxoi* | KW086 | Jameos del Agua | Lanzarote, Spain | MK579410 | MK579436 | – | MK579480 | x | x | x |
| *Mesonerilla* sp. 1 | KW057 | | Lizard Isl., Australia | MK579409 | – | MK579459 | MK579479 | x | – | x |

**Table 1** (continued). Molecular data of nerillid species used in phylogenetic analyses and morphological techniques used to investigate each species. New sequences marked in bold.

| Species | ID extraction | Cave | Locality | GenBank accession numbers | | | | LM | SEM | CLSM |
|---|---|---|---|---|---|---|---|---|---|---|
| | | | | 18S rRNA | 28S rRNA | COI | H3 | | | |
| *Mesonerilla* sp. 2 | KW023 | | Roscoff, France | MK579406 | MK579432 | MK579456 | MK579476 | – | – | x |
| ***Mesonerilla*** sp. 3 | KW814 | | Iriomote Isl., Okinawa, Japan | **PQ149845** | **PQ149825** | **PQ570596** | **PQ421139** | – | – | – |
| ***Mesonerilla*** sp. 4 | KW827 | | Ie Isl., Okinawa, Japan | **PQ149846** | **PQ149826** | **PQ570597** | **PQ421138** | – | – | – |
| ***Mesonerilla dannyi*** sp. nov. | KW824 | | Munseom Isl., Jeju Isl., South Korea | **PQ149847** | **PQ149827** | **PQ570598** | – | – | – | – |
| *Micronerilla minuta* | KW022 | | Roscoff, France | AY859533 | **PQ149828** | **PQ570599** | **PQ421130** | – | – | – |
| ***Micronerilla*** sp. 1 | KW550 | | Punta Campanella, Napoli, Italy | **PQ149848** | **PQ149829** | **PQ570600** | – | – | – | – |
| *Nerillidium gracile* | KW145 | | Gullmarsfjorden, Kristineberg, Sweden | MK579426 | MK579451 | MK579470 | MK579495 | x | x | – |
| ***Nerillidium*** sp. 2 | KW813 | | Ie Isl., Okinawa, Japan | **PQ149849** | **PQ149830** | **PQ570601** | **PQ421140** | x | – | – |
| *Nerillidium troglochaetoides* | KW151 | | Bonden Isl., Kristineberg, Sweden | MK579427 | MK579452 | MK579471 | MK579496 | x | x | – |
| ***Nerillidium*** sp. 1 | KW825 | | Munseom Isl., Jeju Isl., South Korea | **PQ149850** | **PQ149831** | **PQ570602** | – | – | – | – |
| *Nipponerilla irabuensis* | KW772 | Devil's Hole Cave | Shimoji Isl., Miyako Isl. Group, Japan | MW691176 | MW691180 | MW691186 | MW691188 | x | x | x |
| *Paranerilla* sp. | KW030 | | Disko Isl., Greenland | AY859539 | – | – | MK579497 | x | x | x |
| *Speleonerilla calypso* | KW058 | Cherokee Road Exten | Abaco, Bahamas | MH395335 | MH395345 | MH395365 | MH395355 | x | x | x |
| *Speleonerilla isa* | KW362 | Túnel de la Atlántida | Lanzarote, Spain | MH395341 | MH395346 | MH395366 | MH395357 | x | x | x |
| *Speleonerilla salsa* | KW713 | Ciénaga de Zapata | South Cuba | MH395343 | MH395349 | MH395362 | MW691189 | x | x | x |
| *Speleonerilla saltatrix* | KW017 | Roadside Cave | Bermuda | MH395334 | MH395344 | MH395363 | MH395354 | x | x | x |
| *Speleonerilla* sp. A | KW624 | Hoyo Verde Cave | Holguin, Northeast Cuba | MH395339 | MH395348 | MH395367 | MH395356 | x | x | – |
| *Speleonerilla* sp. B | KW530 | Taj Mahal & 27 Steps Cenotes | Akumal, México | MH395338 | MH395347 | MH395364 | MW691190 | x | – | x |
| *Speleonerilla* sp. C | KW775 | Conch Bar Cave | Middle Caicos, Turks & Caicos | MW691177 | MW691179 | MW691184 | MW691191 | x | x | x |
| *Trochonerilla mobilis* | KW031 | | Denmark's Aquarium, Denmark | AY834759 | MK579453 | MK579472 | – | – | – | – |
| ***Trochonerilla*** sp. 1 | KW821 | 'Unnamed Cave' | Ie Isl., Okinawa, Japan | **PQ149851** | **PQ149832** | **PQ570603** | **PQ421137** | x | – | – |

**Table 2.** List of primers used in PCR amplification of 18S rRNA, 28S rRNA, COI and H3 fragments.

| Gene | Primer name | Dir. | Primer sequence (5′→3′) | Annealing temp. (°C) | References |
|---|---|---|---|---|---|
| 18S | 18S1F | F | TACCTGGTTGATCCTGCCAGTAG | 49 | Giribet *et al*. 1996 |
| | 18S5R | R | CTTGGCAAATGCTTTCGC | | Giribet *et al*. 1996 |
| | G51 | F | GGTTGATCCTGCCAGTAG | | Hillis & Dixon 1991 |
| | G747 | R | CGGTATCTGATCGTCTTCGA | | Ibrahim *et al*. 2011 |
| | G950 | F | GTTCGATTCCGGAGAGGGA | | Giribet *et al*. 1996 |
| | G951 | R | GAGTCTCGTTCGTTATCGGA | | Cohen *et al*. 2004 |
| | G952 | F | GCGAAAGCATTTGCCAAGMA | | Cohen *et al*. 2004 |
| | G944 | R | TGATCCTTCTGCAGGTTCACCTAC | | Cohen *et al*. 2004 |
| 28S | G758 | F | ACCCGCTGAATTTAAGCAT | 53 | Brown *et al*. 1999 |
| | D3 | R | GACGATCGATTTGCACGTCA | | Vonnemann *et al*. 2005 |
| COI | dgLCO1490 | F | GGTCAACAAATCATAAAGAYATYGG | 45 | Meyer 2003 |
| | dgHCO2198 | R | TAAACTTCAGGGTGACCAAARAAYCA | | Meyer 2003 |
| | COI19f | F | CWAATCAYAAAGATATTGGAAC | | Colgan *et al*. 2001 |
| | COI726R | R | AATATAWACTTCWGGGTGACC | | Colgan *et al*. 2001 |
| H3 | af | F | ATGGCTCGTACCAAGCAGACVGC | 53–55 | Colgan *et al*. 1998 |
| | ar | R | ATATCCTTRGGCATRATRGTGAC | | Colgan *et al*. 1998 |

was employed, with nucleotide substitution rates following a gamma distribution and deletion of pairwise gaps (see Supp. file 1).

No DNA voucher material is available since the DNA was extracted from whole specimens collected at the new species' type locality.

**Morphological examination**

Light microscopy examinations of preserved specimens were done irrespective of their fixation and storage medium. Specimens were mounted on slides before being examined on an Olympus IX70 inverted compound microscope with CellSens Entry ver. 1.9 software and photographed with a mounted Olympus DP73 camera.

Preparation for scanning electron microscopy (SEM) involved post-fixation of trialdehyde-fixed specimens in 1% osmium tetroxide in demineralized water for 1 h, several rinses in Milli-Q water, dehydration through an ascending ethanol series to 100% and transfer of specimens to 100% acetone. Specimens were then critical point-dried and mounted on aluminium stubs before being sputter coated with platinum-palladium and imaged with a JEOL JSM-6335F field emission scanning electron microscope at the Natural History Museum of Denmark (NHMD), University of Copenhagen.

Immunolabelling of paraformaldehyde-fixed specimens for confocal laser scanning microscopy (CLSM) was performed by preincubating specimens in PTA (PBS rinsing buffer with 0.1% Triton X-100, 0.25% bovine serum albumin and 0.05% $NaN_3$) for 2 h followed by incubation in the primary antibody (monoclonal mouse anti-acetylated α-tubulin (Sigma-Aldrich, T6793; dilution 1:400) for 36 h. Specimens were then rinsed at least 4–6 times over a span of 4 hrs in PBS and incubated in secondary antibodies anti-mouse cyanamine (CY5, Jackson Immunoresearch, 115-175-062; dilution 1:800) and phalloidin (Alexa Flour 488; 0.33 µM) in the dark for 16 h. All antibodies and phalloidin were diluted in PTA. Specimens were then rinsed four times over 4 h in PBS rinsing buffer, taken through a series

of increasing VECTASHIELD® (Vector Laboratories, VECTH1200) concentrations and mounted between two coverslips. While all steps were conducted at room temperature, mounted slides were stored in the dark at -20°C. Mounted specimens were scanned using an Olympus Fluoview FV-1000 CSLM (Worsaae Lab, University of Copenhagen), using the Fluoview ver. 4.0 software. Measurements, maximum intensity projection of z-stacks and rendering analysis were performed in Imaris ver. 7.7 (Bitplane Scientific Software) and FIJI (Schindelin *et al*. 2012).

The morphologically examined material is preserved as voucher material and stored at the NHMD or the Natural Institute of Biological Resources, South Korea (NIBR) (museum type numbers given below).

## Results

### *Phylogenetic analyses*

Bayesian inference (BI) and maximum likelihood (ML) analyses of the 55 nerillid terminals show the same topology except for the position of *Mesonerilla harubangi* sp. nov. In the ML analysis, this species was found as a sister group to *M. laerkae* and *M.* sp. 2, while the BI analysis could not resolve this clade (Fig. 2; nodal supports given as Bayesian Posterior Probability (PP) and Maximum Likelihood Bootstrapping (BS)).

The new taxa from the East China Sea (Fig. 1) are nested within four major clades (Fig. 2A–D): the fully supported Clade A contains all previously described gonochoristic species of *Mesonerilla* with three antennae. Within clade A, *M. harubangi* sp. nov. from South Korea nests in one subclade (PP/BS: 1/97), while *Mesonerilla* sp. 3 and *M.* sp. 4 from Japan are positioned in the other fully supported subclade. The large 'sister clade' to clade A comprises the subsequently branching subclades B + C + D (PP/BS: 1/95). The fully supported clade B contains all included species of *Meganerilla*, three of which are new species from South Korea and Japan. Two new species of *Mesonerilla* nest within Clade C (PP/BS: 1/99), although with uncertain exact affinity among its members, spanning both the two anchialine genera *Speleonerilla* and *Nipponerilla* as well as a clade of hermaphroditic species of *Mesonerilla* with a shorter median antenna. Clade D (PP/BS: 0.62/57) contains subsequently branching clades of *Nerillidium*, *Paranerilla*, *Leptonerilla*, *Trochonerilla* Tzetlin & Saphonov, 1992, *Micronerilla* Jouin, 1970, *Cirrinerilla* gen. nov., and species of *Aristonerilla*. *Nerillidium* sp. 2 from Japan and *Nerillidium* sp. 1 from South Korea nest in each of their subclade of *Nerillidium* species. *Leptonerilla westheidei* sp. nov. from South Korea and *Leptonerilla purschkei* sp. nov. from Japan constitute a separate clade together with *Leptonerilla* sp. 1, whereas *Leptonerilla* sp. 2 and *L.* sp. 3 group as a sister clade to the remaining species of *Leptonerilla*. *Trochonerilla* sp. 1 from Japan groups with *Trochonerilla mobilis* Tzetlin & Saphonov, 1992, and the new genus and species from Japan, *Cirrinerilla sulcipalpata* gen. et sp. nov., is the sister group to *Aristonerilla* spp. (PP/BS: 1/92).

### *Morphological analyses*

Due to a lack of well-preserved material for detailed morphological examinations and/or close molecular resemblance to other species, we chose not to describe or name the following species of the East China Sea, otherwise positioned in the above-presented phylogenetic analyses: *Aristonerilla* sp. 1, *Leptonerilla* sp. 2, *Leptonerilla* sp. 3, *Meganerilla* sp. 1, *Meganerilla* sp. 2, *Mesonerilla* sp. 3, *Mesonerilla* sp. 4, *Micronerilla* sp. 1 and *Nerillidium* sp. 1. These species will not be treated further in the morphological analyses below. For seven species, our detailed morphological examinations provided enough data (in combination with the molecular phylogenetic analyses) to support their formal description and naming herein. The morphological descriptions are arranged alphabetically by genus.

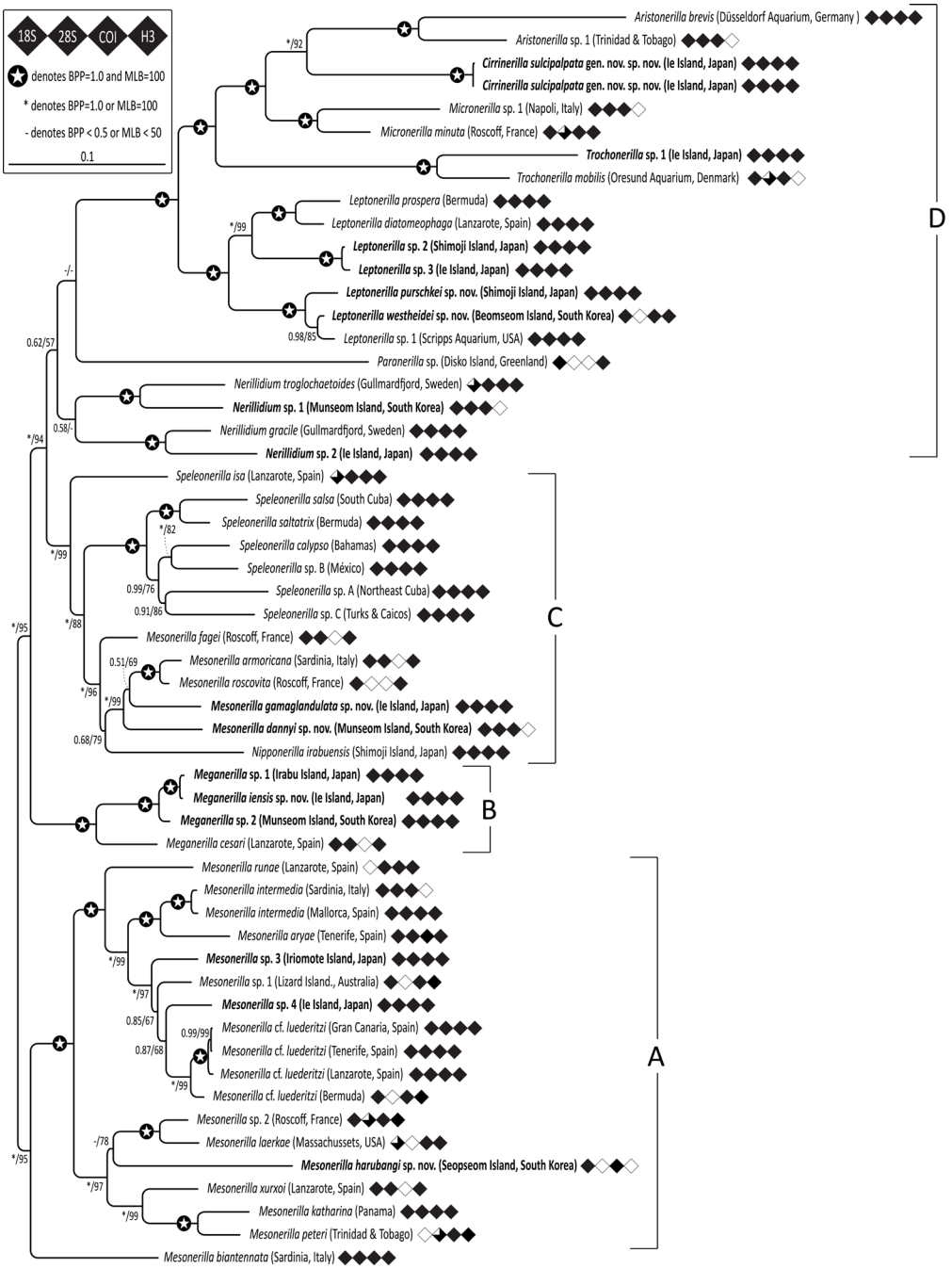


**Fig. 2.** Molecular phylogeny of 55 nerillid species using Bayesian inference (BI) and maximum likelihood (ML) analyses on four concatenated, partially sequenced genes (18S rRNA, 28S rRNA, H3, and COI (excluding saturated 3rd codon positions, see Material and methods). Terminals presented in this study are highlighted in bold and clades A–D are designated with brackets on the right. Tree topologies are largely congruent among analyses. Both Bayesian posterior probability (BPP) and maximum likelihood bootstrapping (MLB) support values are shown for each node with full support in both analyses indicated by a star, and full support in only one of the analyses being denoted with an asterisk (*). A dash (-) is assigned when nodal support is below 0.5 or 50 for BPP and MLB, respectively. Each of the four diamonds next to the terminal name indicates their genes' presence (black; diamonds lacking 25% filling = 25% incomplete fragment) or absence (white) in the analyses (i.e., 18S, 28S, COI and H3 from left to right).

## *Taxonomy*

Phylum Annelida Lamarck, 1802
Family Nerillidae Levinsen, 1883

Genus ***Cirrinerilla*** gen. nov.
urn:lsid:zoobank.org:act:55EFA3A3-D7E8-4DAB-BC8A-1A6FC39EF051

### Type species

*Cirrinerilla sulcipalpata* gen. et sp. nov.

### Diagnosis

*Cirrinerilla* gen. nov. is morphologically diagnosed by the following unique combination of characters: body cigar-shaped with eight segments. Prostomium with three, long and straight antennae and two long, cylindrical palps. Trunk segments with very long parapodial cirri. Compound chaetae in all segments. Hermaphroditic, with one pair of spermioducts opening in segment VII and one pair of oviducts in segment VIII.

### Etymology

The genus name relates to the presence of long parapodial 'cirri' and 'nerilla' refers to the type genus of Nerillidae. The Japanese name for this new genus is given here as 'Iejima-usamimi-gokai-zoku' (meaning 'Ie Island-rabbit ear-bristle worm' in English).

***Cirrinerilla sulcipalpata*** gen. et sp. nov.
urn:lsid:zoobank.org:act:1C802929-4F05-48D8-B205-38957594C97D
Figs 3–4; Table 3

### Diagnosis

*Cirrinerilla* gen. nov. with very long antennae, up to ⅔ of body length. Palps ventrally densely ciliated and dorsally with longitudinal non-ciliated furrow. Eyes absent. Long cylindrical parapodial cirri of minimum half body length in segments II–VII, longest in segment V. Maximum 12 compound chaetae per parapodium. Dorsal and ventral transverse rows of ciliary tufts on each segment.

### Etymology

'Sulcipalpata' refers to the dorsal, longitudinal furrow on each palp. The Japanese name for this new species is given here as 'Iejima-doukutsu-usamimi-gokai' (meaning 'Ie Island-cave dwelling-rabbit ear-bristle worm' in English).

### Type material

#### Holotype

JAPAN • adult; Okinawa Prefecture, Ie Island, 'Unnamed Cave' (or sometimes called 'Sho-doukutsu'); 26.72518° N, 127.83107° E; 5–12 meters depth; 9 Jun. 2019; Y. Fujita, M.J. Hansen, M.C. Allentoft-Larsen and K. Worsaae leg.; NHMD 1842011 mounted on SEM stub.

#### Paratypes

JAPAN • 4 adults; same data as for holotype; 5–17 meters depth; 2–9 Jun. 2019; NHMD 1842012 and 1842013 as permanent whole mounts, NMHD 1842014 and 1842015 mounted on SEM stub • 1 spec. examined with LM but lost during preparation for SEM; same data as for preceding.

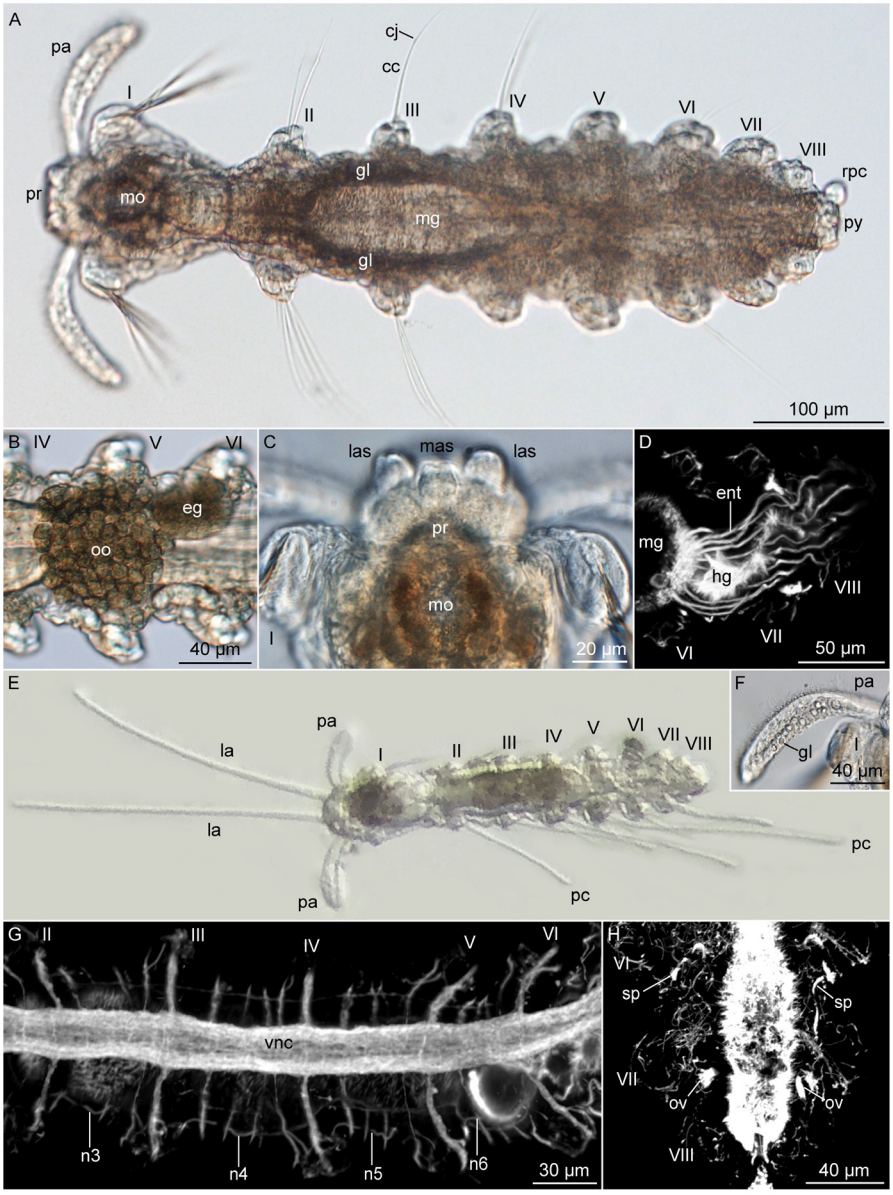


**Fig. 3.** *Cirrinerilla sulcipalpata* gen. et sp. nov. **A, C, F**. Holotype (NHMD 1842011). **B**. Paratype (NHMD 1842015). **D, G**. Paratype (NHMD 1842013). **E**. Live specimen (lost), **H**. Paratype (NHMD 1842012). **A**. Light microscopy (LM) with regenerating pygidial cirri, dorsal view. **B**. LM of oocytes and egg, dorsal view. **C**. Close-up of prostomium from A, showing lateral and median antennae scars, dorsal view. **D**. Confocal laser scanning microscopy (CLSM) of acetylated α-tubulin immunoreactivity (α-tub IR) in the cilia of ten dorsal and lateral enteronephridia running along the hindgut in adult specimen (dorsal view, Z-stack maximum intensity projection). **E**. Dissecting scope images of live specimen with palps, long lateral antennae and long parapodial cirri, dorsal view. **F**. Close-up of palp from C. **G**. CLSM of α-tub IR in ventral nerve cord and cilia of segmental nephridia (dorsal view, Z-stack maximum intensity projection). **H**. CLSM of α-tub IR in cilia of spermioducts and oviducts (NHMD 1842012). Abbreviations: cc = compound chaetae; cj = chaetal joint; eg = egg(s); ent = enteronephridium; gl = gland; hg = hindgut; la = lateral antenna; las = lateral antenna scar; mas = median antenna scar; mg = midgut; mo = mouth opening; n3–6 = nephridia in segment III–VI; oo = oocytes; ov = oviduct; pa = palp; pc = parapodial cirrus; pr = prostomium; py = pygidium; rpc = regenerating pygidial cirrus; sp = spermioduct; vnc = ventral nerve cord; I–VIII = segments I–VIII.

**Representative DNA sequences**

GenBank accession numbers PQ149834–PQ149835 (nuclear 18S rRNA), PQ149816–PQ149817 (nuclear 28S rRNA), PQ570584–PQ570585 (nuclear H3) and PQ421126–PQ421127 (mitochondrial COI); from specimen with same collection data as holotype (Table 1).

**Description**

Measurements are based on LM of holotype, counts and ciliation from SEM of holotype; values for paratype are given in parentheses. Body about 525 µm long (500–685 µm, n = 5) with eight segments (Figs 3A, 4A). Segment I double length of following segment (n = 6); segment lengths of holotype 98, 53, 72, 70, 63, 53, 43, 28 µm, pygidium 24 µm long. Cigar-shaped body. Segment V widest, segments VII–VIII decreasing in length and width (n = 6). Maximum width of trunk segments, including parapodia, about 125 µm (115–180 µm, n = 3); about 90 µm excluding parapodia (90–125 µm, n = 3). Max length of parapodium segment I, 37 µm (35–45, n = 5); max length in segments II–VIII, 34 µm (37–48 µm, n = 5).

Prostomium carrying three antennae and two straight palps (Fig. 3A, C, E). Palps 117 µm long (121 µm, n = 2) and 18 µm in width (23 µm, n = 1) with heavy ventral ciliation and dorsal longitudinal furrow. Lateral antennae cylindrical with a length of about 400 µm, estimated relative to LM measure of total body length from dissection scope images of live holotype (la, Fig. 3E). Scars from lateral and median antennae visible in fixed holotype (las, mas, Figs 3C, 4D). Characteristics of median antenna unknown. Eyes absent. Elongated esophageal glands in segments II–IV, along foregut (Fig. 3A).

Parapodial cirri observed on live specimens on segments II–V and VII (cirri assumed lost in segment VI, absent on segment I (buccal segment) and VIII); increasing in length posteriorly until segment V. Cirri of segment V noticeably longest; maximum length of 310 µm estimated relative to LM measure of total body length from dissection scope images of live holotype (pc, Fig. 3E). Parapodial cirri lost in fixed specimens. Pygidial cirri lost in all specimens; only regenerating bud of cirrus recorded (rpc, Fig. 3A).

Compound chaetae in all segments. Up to ten chaetae in one bundle on each parapodium of segment I, pointing posteriorly, maximum 149 µm long (141 µm, n = 1). Segments II–VIII with up to 12 chaetae per parapodium (five-seven in each dorsal and ventral bundle, respectively; often broken or lost). Chaetae maximum 127 µm long (84–138 µm, n = 5) (cc, Fig. 4B, G); shaft up to 96 µm long (52–111 µm, n = 5), blade up to 31 µm long (20–63 µm, n = 5), distal extension on shaft at joint 2 µm long (n = 1).

Prostomium with anterior and posterior fields of presumed sensory cilia and lateral rows of cilia extending from insertion of lateral antenna and more than halfway towards insertion of nearest palp (lrc, Fig. 4D). Paired, densely ciliated nuchal organs on dorsolateral border between prostomium and segment I. Palps ventrally with longitudinal dense ciliary row from insertion point to tip of palps (pvc, Fig. 4D), lined by ventrolateral row of ciliary tufts (each tuft with up to six cilia). Palps lost in most specimens during SEM and CLSM preparation. Segment I with paired dorsolateral transverse rows of each three ciliary tufts (each tuft with minimum four cilia) at the level of parapodia. Trunk segments each with dorsal transverse row of up to 20 ciliary tufts (with middorsal gap in segments III–V) on slightly elevated dorsal ridges at level of parapodia (tdc, Fig. 4B–C). Ventral ciliation consisting of i) densely ciliated mouth, ii) midventral ciliary band and iii) continuous transverse rows of cilia in all segments at level of parapodia (vc, tvc, Fig. 4A, F). Multiple single cilia scattered on dorsal, lateral, and ventral sides of body.

Three to ten blind ending enteronephridia extend from transition between mid- and hindgut, posteriorly along hindgut (ent, Fig. 3D). Four pairs of segmental nephridia run laterally in segments III–VI, originating more dorsally and opening ventrolaterally (n3–n6, Fig. 3G). Hermaphroditic. One pair of spermioducts opening in segment VII, and one pair of oviducts opening in segment VIII, both with an

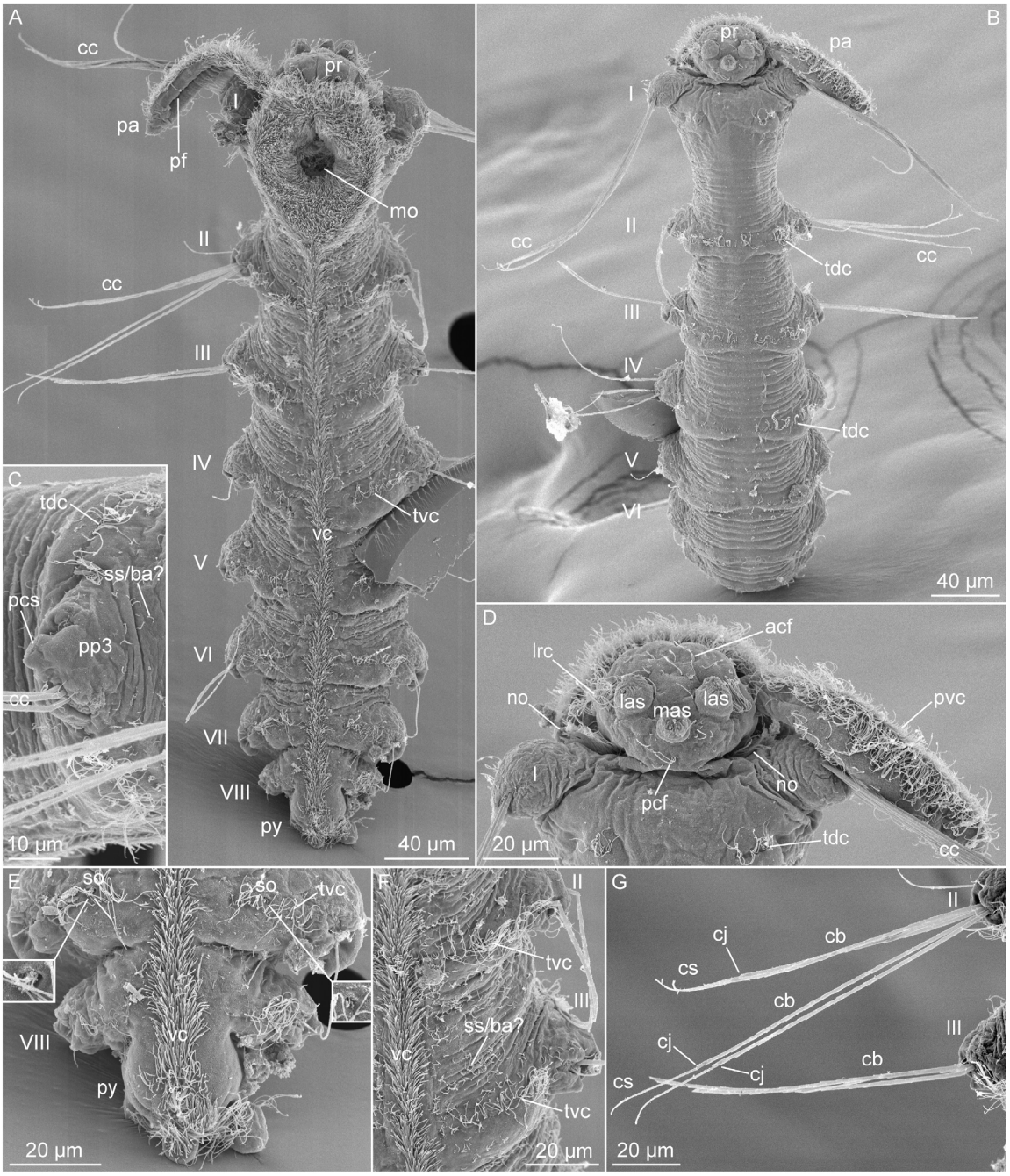


**Fig. 4.** *Cirrinerilla sulcipalpata* gen. et sp. nov., paratype (NHMD 1842015), scanning electron micrographs. **A**. Entire specimen, ventral view. **B**. Entire specimen, dorsal view. **C**. Close-up of parapodium, segment III, lateral view. **D**. Close-up of prostomium and segment I, dorsal view. **E**. Segments VII–VII and pygidium, close-up of spermioduct openings, ventral view. **F**. Segments II–III, ventral view. **G**. Compound chaetae of segments II–III. Abbreviations: acf = anterior field of sensory cilia; cb = chaetal blade; cc = compound chaetae; cj = chaetal joint; cs = chaetal shaft; las = lateral antennae scar; lrc = lateral row of cilia; mas = median antennae scar; mo = mouth opening; no = nuchal organ; pa = palp; pvc = palp ventral ciliary row; pp3 = parapodium segment III; pcf = posterior field of sensory cilia; pcs = parapodial cirrus scar; pf = palp furrow; pr = prostomium; py = pygidium; so = spermioduct opening; ss/ba? = sensory cilium or bacterium; tdc = transverse dorsal row of cilia; tvc = transverse ventral row of cilia; vc = midventral ciliary band; I–VIII = segments I–VIII.

**Table 3.** Selected character comparison of *Cirrinerilla sulcipalpata* gen. et sp. nov. with species of closely related genera from the phylogenetic analysis (Fig. 2). Asterisk (*), measurements obtained from illustrations in references 5–6; two asterisks (**), measurements estimated from photos of live specimens, relative to known body length of fixed specimen. Measurements of new species are based on all available specimens, including type material and live observations. Abbreviations: A = absent; ant = antenna; C = compound chaetae; excl. = excluding; G = gonochoristic; H = hermaphroditic; L = length; Lat = lateral; max = maximum; med = median; no. = number; P = present; para. = parapodia; S = simple chaetae; Segm = segment; W = width; ? = unknown. References: 1 = Müller 2002; 2 = Worsaae & Müller 2004; 3 = Swedmark 1959; 4 = Saphonov & Tzetlin 1997; 5 = Müller & Worsaae 2006; 6 = Tzetlin & Saphonov 1992.

| **Species** | **Body** | | | **Antennae** | | | **Palps** | **Eyes** | **Parapodial cirri** | | | **Chaetae** | | | | | **Reproduction** |
|---|---|---|---|---|---|---|---|---|---|---|---|---|---|---|---|---|---|
| | No. segm | Max L | Max W excl. para. | Wrinkled | Med ant, max L | Lat ant, max L | Max L | | Segm I | Max L | Double | Type | Segm I, max no. | Segm I, max L | Segm II–VIII, max no. | Segm II–VIII, max L | |
| ***Cirrinerilla sulcipalpata*** gen. et sp. nov. | 8 | 684 | 127 | A | ? | 400** | 121 | A | A | 310** | A | C | 10 | 149 | 12 | 138 | H |
| *Aristonerilla brevis*[1, 2] | 7 | 670 | 100 | A/P | 330 | 320 | 60 | A/P | A | 175 | A | C | 12 | 200 | 16 | 190 | G |
| *Micronerilla minuta*[1, 2, 3, 4] | 8 | 600 | 90 | P | 150 | 175 | 80 | P | A/P | 150 | A/P | C | ? | ? | ? | ? | G |
| *Trochonerilla mobilis*[2, 5, 6] | 8 | 620 | 150 | A | 5 | 5 | 50*[5] | P | A | 110*[6] | A | S | 15 | 100*[6] | 9 | 105*[6] | G |

anterior ciliated 'funnel' and separate ventral openings (Figs 3H, 4E). Mature egg and many oocytes observed in a single specimen in segments IV–VI (Fig. 3B).

**Distribution and habitat**

'Unnamed Cave (or 'Sho-doukutsu')', northeastern reef of Ie Island, Okinawa Prefecture, Ryukyu Islands, Japan. Marine anchialine cave with entrance from the reef slope at 17 meters depth and main tube penetrating about 50 meters under land (see Osawa & Fujita 2019 for the description of the cave). Specimens collected at 5–17 meters depth from plankton tow and sediment samples from the main tube and the anchialine right hall of the cave. Associated nerillids from the cave include *Leptonerilla* sp. 3, *Mesonerilla gamaglandulata* sp. nov. and *Trochonerilla* sp. 1.

**Molecular information**

*Cirrinerilla sulcipalpata* gen. et sp. nov. is nested within a fully supported larger clade comprising the seven- to eight-segmented genera *Trochonerilla*, *Micronerilla*, and *Aristonerilla* (Fig. 2). Within this clade, *Cirrinerilla* gen. nov. is sister group to *Aristonerilla* (PP/BS: 1/92), together with *Micronerilla* constituting a fully supported subclade, sister to *Trochonerilla*. The phylogenetic analyses (Fig. 2) include two terminals of *C. sulcipalpata* found to represent identical haplotypes.

Pairwise comparison of *C. sulcipalpata* gen. et sp. nov. sequence similarity to phylogenetic closely related species: 18S rRNA – 100% intraspecific similarity between the two *C. sulcipalpata* sequences – 89.28–93.59% similar to its sister group (*Aristonerilla brevis* (Saphonov & Tzetlin, 1997) and *A.* sp. 1); 28S rRNA – 100% intraspecific similarity – 66.21–66.38% similar to its sister group; COI – 100% intraspecific similarity – 74.67–80.44% similar to its sister group; H3 – 100% intraspecific similarity – 96.65% similar to its sister group.

**Remarks** (see also Table 3 for genus comparisons)

*Cirrinerilla sulcipalpata* gen. et sp. nov. shows closest morphological and molecular similarity to species of *Aristonerilla* and *Micronerilla*, and to a lesser degree to species of *Trochonerilla.* Species of all four genera have less than nine segments, three antennae, relatively long parapodial cirri, and are of similar small size. However, *Cirrinerilla sulcipalpata* differs from all species of these closely related genera by being hermaphroditic, having a cigar-shaped body narrowing in width anteriorly and posteriorly, and by having significantly longer and straighter palps with a dorsal longitudinal furrow. Moreover, it differs from species of *Trochonerilla* by having compound rather than capillary chaetae and by lacking dense transverse segmental ciliary bands. It also differs from species of *Aristonerilla* by having eight rather than seven segments and from species of *Micronerilla* by having only single rather than double parapodial cirri on each parapodium as well as only a single rather than two pairs of spermioducts. Therefore, we choose to erect the new genus *Cirrinerilla* gen. nov., since a designation of the new species to *Aristonerilla*, *Micronerilla* or *Trochonerilla* would otherwise result in a considerable ambiguity of their diagnostic genus characters (e.g., reproductive mode, segment number, chaetal type), generally assumed to be constant within the genera of Nerillidae (Jouin 1971; Tzetlin & Larionov 1988; Worsaae 2021; Worsaae *et al.* 2021a).

Additionally, *Cirrinerilla sulcipalpata* gen. et sp. nov. differs from the closely related species of *Aristonerilla* and *Micronerilla* by having longer and straight (rather than wrinkled) antennae, lacking eyes, and having relatively longer parapodial cirri, especially on segment V. Noticeably, *A. brevis* is reported to sometimes possess comparatively much longer parapodial cirri on segment VII (Müller 2002).

Genus *Leptonerilla* Westheide & Purschke, 1996

***Leptonerilla purschkei*** sp. nov.
urn:lsid:zoobank.org:act:CAD96362-1FDA-4243-813E-4F2FBE68AA5E
Figs 5–6; Table 4

**Diagnosis**

A nine-segmented *Leptonerilla* diagnosed by a combination of following characteristics: three long antennae all distally wrinkled, median antenna shorter than lateral antennae. Segment I with cirriform, relatively short cirri and chaetae. Trunk segments with long, double parapodial cirri and long pygidial cirri, exceeding half of body length. Gonochoristic with one pair of oviducts in segment VIII, males not observed.

**Etymology**

The species is named in recognition of the annelid researcher Günter Purschke, who erected the genus *Leptonerilla* and described the morphologically highly similar *L. diplocirrata* Westheide & Purschke, 1996. The Japanese name for this new species is given here as 'Shimoji-doukutsu-usamimi-gokai' (meaning 'Shimoji Island-cave dwelling-rabbit ear-bristle worm' in English).

**Type material**

**Holotype**

JAPAN • ♀ adult; Miyako Islands, Shimoji Island, 'Akuma-no-yakata' (Devil's Hole); 24.82291° N, 125.13551° E; rubble at 22 meters depth; 26 Oct. 2018; Y. Fujita, M. Mizuyama, P.R. Møller and K. Worsaae leg.; NHMD 1842016 mounted on SEM stub.

**Paratype**

JAPAN • 1 ♀ adult; same data as for holotype; NHMD 1842017 as permanent whole mount.

**Representative DNA sequences**

GenBank accession numbers PQ149839 (nuclear 18S rRNA), PQ149820 (nuclear 28S rRNA), PQ570589 (nuclear H3) and PQ421135 (mitochondrial COI); from specimen with same collection data as holotype (Table 1).

**Description**

Measurements are based on LM of holotype, counts and ciliation from SEM; values for paratype are given in parentheses. Body with nine chaetigerous segments (Fig. 5A), total length about 940 µm (745 µm, n = 1). Segment lengths of holotype 97, 90, 104, 123, 115, 103, 101, 77, 68 µm, pygidium 37 µm long. Maximum width about 195 µm including parapodia (165 µm, n = 1), about 145 µm excluding parapodia (115 µm, n = 1). Max length of parapodium on segment I, 41 µm (38, n = 1), on segments II–IX, 45 µm (53 µm, n = 1).

Prostomium with three long antennae wrinkled distally (Fig. 5C), often lost during fixation. Lateral antenna estimated length up to 485 µm (n = 1) (la, Fig. 5A, C), median antenna shorter than lateral antennae (ma, Fig. 5C) with estimated length up to 370 µm from photos of live specimen (n = 1). Prostomium with two club-shaped palps up to 78 µm long (65 µm, n = 1) and 31 µm wide (20 µm, n = 1), inserted ventrally on prostomium (pa, Figs 5A, C, 6A–B) with distinct ventral and frontal ciliation. Two dorsal eyes. Paired nuchal organs laterally between prostomium and peristomium (no, Fig. 6B).

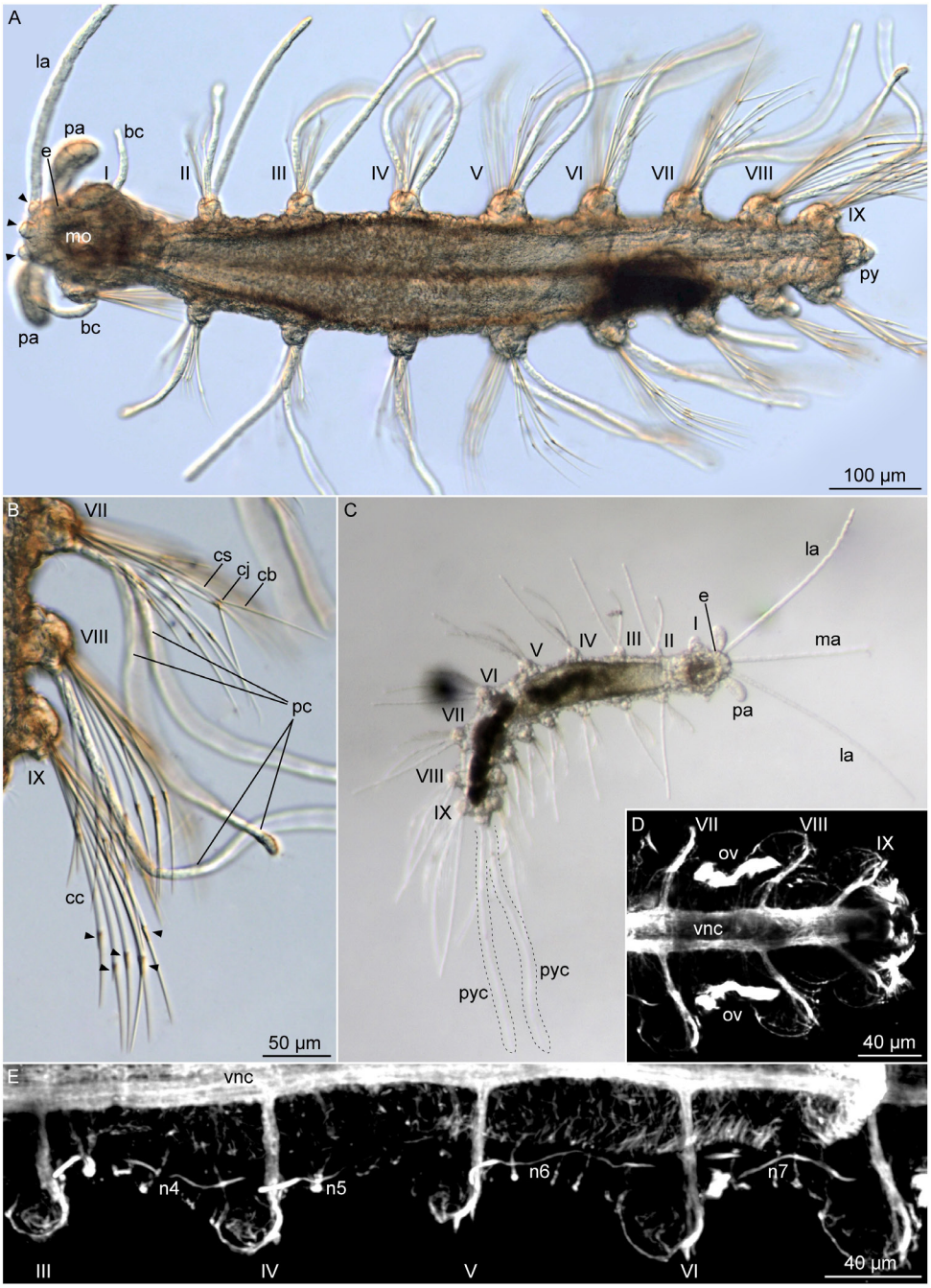


**Fig. 5.** *Leptonerilla purschkei* sp. nov. **A–B**. Holotype, ♀ (NHMD 1842016), light microscopy (LM), dorsal view. **A**. Overview showing one lateral antenna and antennae scars (indicated by arrowheads). **B**. Parapodia on one side of the posterior segments showing compound chaetae and joints (indicated by arrowheads), along with cylindrical double interramal cirri. **C**. Live animal dissecting scope image, showing intact antennae and pygidial cirri (indicated by a dashed line), dorsal view. **D–E**. Paratype, ♀ (NHMD 1842017), confocal laser microscopy (CLSM) labeled with anti-acetylated α-tubulin, maximum intensity projections of z-stack, ventral view. **D**. Posterior end, oviducts opening in segment VIII. **E**. Right side of specimen showing four segmental nephridia opening in segments IV–VII. Abbreviations: bc = buccal cirrus; ch = chaetae; e = eye; la = lateral antenna; ma = median antenna; mo = mouth opening; n4–7 = nephridia in segments IV–VII; ov = oviduct; pa = palp; py = pygidium; pyc = pygidial cirrus; vnc = ventral nerve cord; I–IX = segments I–IX.

Segment I with a single, up to 73 µm long, cylindrical (cirriform) cirrus per parapodium (Figs 5A, 6B). Segments II–IX carrying double, cylindrical interramal parapodial cirri (pc, Figs 5B, 6A), up to 336 µm long, lengths seemingly increasing in posterior segments. Cylindrical pygidial cirri up to 590 µm long (pyc, Fig. 5C), estimated relative to body length from live specimen images.

Compound chaetae in all segments (cc, Fig. 5B). Segment I with one bundle of up to 18 posteriorly pointing chaetae (up to 148 µm long) per parapodium (Fig. 6A–B). Following segments with dorsal and ventral bundles of chaetae; up to 20 chaetae per parapodia (up to 236 µm long) (Fig. 6A). Shaft up to 169 µm long, blade up to 82 µm long, distal extension on shaft at joint up to 15 µm long (Fig. 6C–D).

Prostomium with anterior and posterior fields of presumed sensory cilia and lateral rows of cilia extending between lateral antenna and palp insertion (Fig. 6B). Paired, densely ciliated nuchal organs on lateral border between prostomium and segment I. Palps with ventral longitudinal dense ciliary row from insertion point to tip of palps, dorsal row of minimum 4 ciliary tufts on distal half of palp (each tuft with > 15 cilia), and lateral row of indistinct small tufts of cilia (Fig. 6B). Segment I with paired dorsolateral transverse rows of each two ciliary tufts (each tuft with > 20 cilia) at the level of parapodia. Following trunk segments with dorsal transverse continuous row of up to 14 ciliary tufts at level of parapodia (tdc, Fig. 6A–B); tufts increasing in numbers, ciliary length and showing remarkable density in posterior segments. Segment II with an additional lateral pair of longitudinal ciliary bandlets (ldc, Fig. 6B). Ventral ciliation could not be observed.

Four pairs of segmental nephridia positioned laterally, parallel to ventral nerve cord, opening in segments IV, V, VI and VII (n4–n7, Fig. 5E). Enteronephridia not distinguished. Gonochoristic reproduction; females with one pair of straight oviducts opening latero-ventrally just anterior to the segmental nerve in segment VIII (ov, Fig. 5D). Spermioducts unknown. A single mature egg (about 80 µm long) observed in segments VI–VII (n = 2).

**Distribution and habitat**

Devil's Hole 'Akuma-no-yakata', northwestern coast of Shimoji Island, Ryukyu Islands, Miyako Islands, Japan. Anchialine cave located on coral reef slope. Specimen collected from rubble patches in middle zone of cave at about 22 meters depth (see Osawa & Fujita 2019 for the description of the cave). Associated nerillids from the cave include *Mesonerilla* sp. (Worsaae, unpubl. record and not sequenced), *N. irabuensis* and *Leptonerilla* sp. 2.

**Molecular information**

*Leptonerilla purschkei* sp. nov. constitutes a fully supported clade with *L. westheidei* sp. nov. and *Leptonerilla* sp. 1 (Fig. 2). The clade is sister to a larger clade comprising the remaining *Leptonerilla* spp.

Pairwise comparison of *L. purschkei* sp. nov. sequence similarity to other *Leptonerilla* spp.: 18S rRNA – 99.43–99.89% similar to its sister group (clade comprising *L. westheidei* sp. nov and *L.* sp. 1) – 97.13–98.24% similar to the remaining *Leptonerilla* spp.; 28S rRNA – 96.16% similar to its sister group – 79.30–82.72% similar to the remaining *Leptonerilla* spp.; COI – 88.62–89.57% similar to its sister group – 79.12–80.40% similar to the remaining *Leptonerilla* spp.; H3 – 96.59% similar to its sister group – 88.09–89.31% similar to the remaining *Leptonerilla* spp.

**Remarks** (see also Table 4 for *Leptonerilla* spp. comparisons)

*Leptonerilla purschkei* sp. nov. shows the greatest morphological and molecular similarity to *L. westheidei* sp. nov., but differs from it by a larger body size, segment I with much shorter cirri, and double as many chaetae. Both species share a small body size compared to *L. diatomeophaga* (Núñez in Núñez, Ocaña & Brito, 1997) and especially *L. prospera* Sterrer & Iliffe, 1982 (Sterrer & Iliffe 1982;

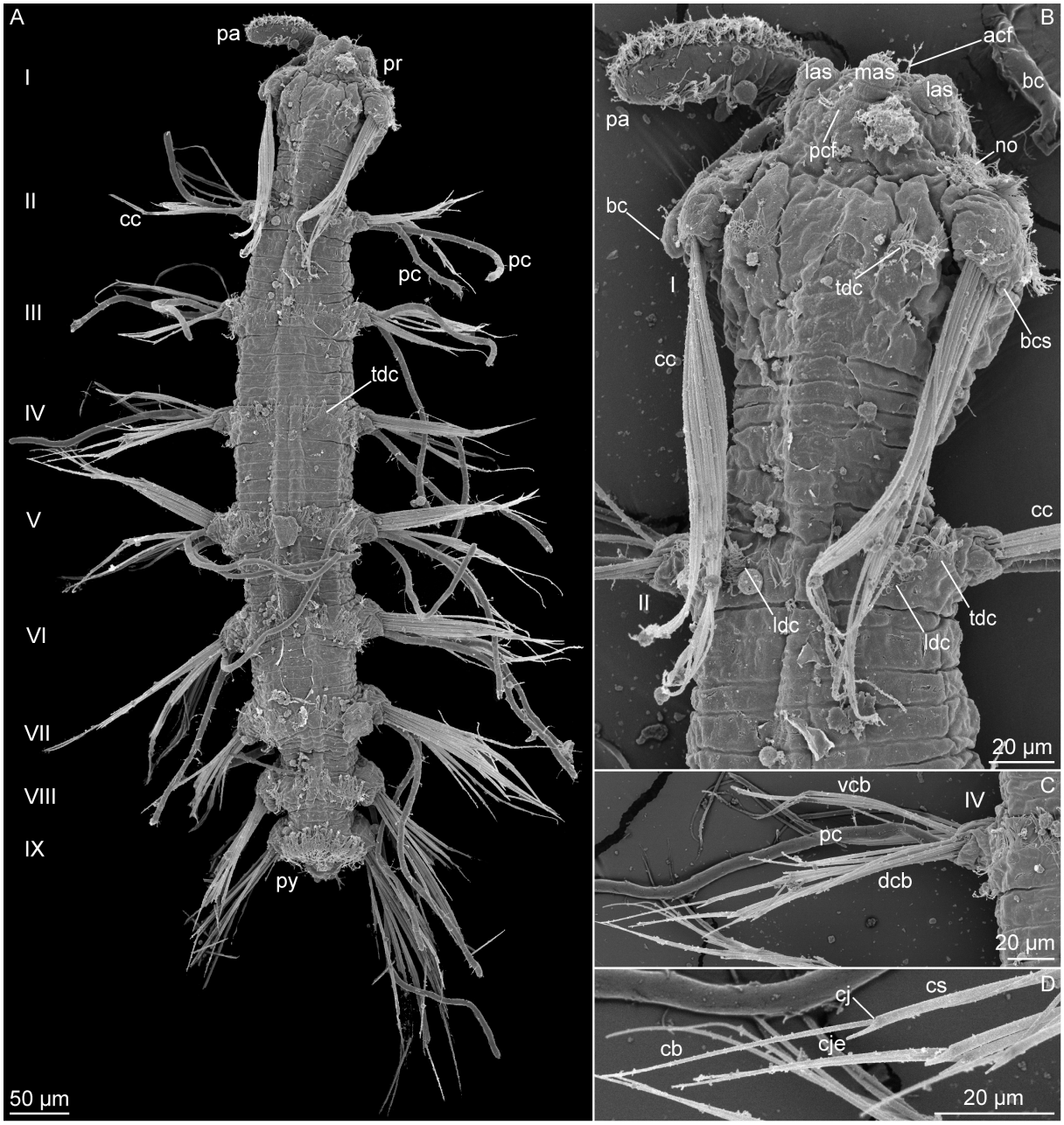


**Fig. 6.** *Leptonerilla purschkei* sp. nov., holotype, ♀ (NHMD 1842016), scanning electron micrographs. **A**. Overview of entire specimen, dorsal view. **B**. Close-up of prostomium and two anterior segments, showing one left palp and antennae scars. **C**. Close-up of segment IV, left side, showing interramal parapodial cirrus. **D**. Close-up of dorsal compound chaetae of segment IV. Abbreviations: acf = anterior ciliary field; bc = buccal cirrus; bcs = buccal cirrus scar; cb = chaetal blade; cc = compound chaetae; cj = chaetal joint; cje = chaetal joint extension; cs = chaetal shaft; dcb = dorsal chaetal bundle; las = lateral antenna scar; ldc = longitudinal dorsal bandlet of cilia; mas = median antenna scar; no = nuchal organ; pa = palp; pc = parapodial cirrus; pcf = posterior ciliary field; pr = prostomium; py = pygidium; tdc = transverse dorsal row of cilia; vcb = ventral chaetal bundle; I–IX = segments I–IX.

**Table 4.** Selected morphological characters comparison in species of *Leptonerilla* Westheide & Purschke, 1996. All measurements in µm. Asterisk (*), measurements estimated from photos of live specimens, relative to known body length of fixed specimen. Measurements of new species are based on all available specimens, including type material and live observations. Abbreviations: ant = antenna; excl. = excluding; L = length; Lat = lateral; max = maximum; med = median; para = parapodia; segm = segment; W = width; ? = unknown. References: 1 = Núñez *et al*. 1997; 2 = Westheide & Purschke 1996; 3 = Sterrer & Iliffe 1982; Worsaae *et al*. 2009.

| Species | Body | | Antennae | | Palps | Parapodial cirri | | | Pygidial cirri | Chaetae | | | |
|---|---|---|---|---|---|---|---|---|---|---|---|---|---|
| | Max L | Max W excl. para | Med ant, max L | Lat ant, max L | Max L | Segm I, max L | Segm I, shape | Segm II–IX (double), max L | Max L | Segm I, max no. | Segm I, max L | Segm II–VIII, max no. | Segm II–VIII, max L |
| ***Leptonerilla purschkei*** sp. nov. | 940 | 145 | 370* | 485 | 78 | 73 | Cirriform | 336 | 590* | 18 | 148 | 20 | 236 |
| ***L. westheidei*** sp. nov. | 705 | 130 | ? | ? | 48 | 123 | Cirriform | 263 | ? | 9 | 135 | 18 | 195 |
| *L. diatomeophaga*[1] | 1200 | 210 | 200 | 250 | 27 | 30 | Short | 260 | 262 | 12 | 260 | 24 | 250 |
| *L. diplocirrata*[2] | 690 | 90 | 250 | 215 | 56 | 50 | Cirriform | 215 | 270 | 20 (in 2 bundles) | ? | 20 | ? |
| *L. prospera*[3] | 2050 | 420 | 650 | 600 | 230 | 30 | Short | 550 | 120 | 20 | 215 | 20 | 310 |

Núñez *et al*. 1997; Worsaae *et al*. 2009). *Leptonerilla purschkei* differs from these latter two species by having longer cirriform, cylindrical parapodial cirri on segment I, although these are similar in shape and relative length to those of *L. diplocirrata*. *Leptonerilla purschkei* differs from all other species of *Leptonerilla* by the very long pygidial cirri and by the very long antennae, more than half the body length, with a wrinkled appearance, otherwise only described for the distantly related *Micronerilla* and *Aristonerilla* (Swedmark 1959; Saphonov & Tzetlin 1997; Müller 2002). It thereby also differs from the only other described species of *Leptonerilla* from the West pacific region, *L. diplocirrata* found more than 1000 kilometres away, near Hainan, China. *Leptonerilla purschkei* also differs molecularly from both *L*. sp. 2 found within the same cave and *L.* sp. 3 found further North off Okinawa in 'unnamed cave' of Ie Island. Both two latter potential new cave species were only found as single specimens with very limited morphological information obtainable prior to DNA extraction of all their tissue.

***Leptonerilla westheidei*** sp. nov.
urn:lsid:zoobank.org:act:756B9FFA-2D1E-49B3-AF75-7558EF2FA291
Fig. 7; Table 4

**Diagnosis**

A *Leptonerilla* diagnosed by a combination of following characteristics: three antennae, two club-shaped palps. Segment I with relatively long, unpaired, cylindrical cirri and few chaetae. Following trunk segments with long, double parapodial cirri. Gonochoristic; females with one pair of oviducts in segment VIII, males not observed.

**Etymology**

The species is named in recognition of the annelid researcher Wilfried Westheide, who erected the genus *Leptonerilla* and described the morphologically highly similar *L. diplocirrata*.

**Type material**

**Holotype**

SOUTH KOREA • adult; Jeju Island, Munseom Islet; 33.22772° N, 126.56330° E; sand and shell gravel around 25 meters depth; 21 Oct. 2015; K. Worsaae and T. Park leg.; NIBRIV0000927415 mounted on SEM stub.

**Paratype**

SOUTH KOREA • 1 adult; same data as for holotype; NIBRIV0000927416 mounted on SEM stub.

**Representative DNA sequences**

GenBank accession numbers PQ149836 (nuclear 18S rRNA), PQ570586 (nuclear H3) and PQ421134 (mitochondrial COI); from specimen collected near type locality: SOUTH KOREA • Jeju Island, Beomseom Islet; 33.22115° N, 126.51809° E; sand and shell gravel at around 20 meters depth; 23 Oct. 2015 (Table 1).

**Description**

Measurements are based on LM of holotype, counts and ciliation from SEM; values for paratype are given in parentheses. Body with nine chaetigerous segments (Fig. 7A–B), total length about 705 µm (565–640 µm, n = 2). Segment lengths 54, 75, 91, 83, 81, 78, 74, 65, 63 µm. Maximum width about 180 µm including parapodia (140–145 µm, n = 2), about 130 µm excluding parapodia (90–95 µm, n = 2).

Prostomium with median and two lateral antennae (only scars visible) and two, ventrally inserted, short, club-shaped palps (47–50 µm long and 35–36 µm wide, n = 2) (las, mas, pa, Fig. 7A, D, F). Presence of eyes difficult to discern in fixed material.

Parapodium of segment I uniramous with long, single, cylindrical (cirriform) cirrus, up to 120 µm long (85 µm, n = 1) and inserted ventral to the chaetal bundle (bc, Fig. 7B, D, F). All trunk segments with long, cylindrical, double, interramal cirri (Fig. 7A), up to 263 µm long (186–192 µm, n = 2). Parapodial cirri with few evenly scattered cilia. Pygidium with scars from two lost cirri and midterminal short, cirriform lobe (pyl, Fig. 7A).

Compound chaetae in segments I–IX plus 1–2 short, dorsal, bent, simple chaetae in most trunk segments (n = 2). Up to nine posteriorly pointing compound chaetae in segment I (n = 3), maximum 135 µm long (Fig. 7A, D, F); up to 18 compound chaetae in segments II–IX (n = 3), maximum 195 µm long (blade up to 150 µm, shaft up to 54 µm, extension of shaft at chaetal joint up to 8 µm) (Fig. 7A); length of chaetae increasing posteriorly.

Prostomium with anterior and posterior fields of presumed sensory cilia, lateral rows of cilia between lateral antenna and palp insertion, paired densely ciliated nuchal organs on lateral border between prostomium and segment I (Fig. 7D, F). Palps with ventral longitudinal dense ciliary row from insertion point to tip of palps (pvc, Fig. 7F), dorsal row of minimum 3 ciliary tufts on distal half of palp (each tuft with > 15 cilia) (ct, Fig. 7F), and lateral row of small tufts of cilia (sct, Fig. 7F). Segment I with paired dorsolateral transverse rows of each two ciliary tufts at the level of parapodia. Following trunk segments with dorsal transverse continuous row of up to 12 ciliary tufts at level of parapodia (tdc, Fig. 7A, C, E); tufts increasing in numbers, ciliary length, and density in posterior segments. Segment II with an additional lateral pair of longitudinal ciliary bandlets (ldc, Fig. 7E). Ventral ciliation not examined.

Gonochoristic. Females with mature eggs (up to 110 µm long) and oocytes in segments VI–VIII (eg, Fig. 6B). Nephridia and gonoducts not examined.

**Distribution and habitat**

Western coast of Munseom Islet and northern coast of Beomseom Islet, south of Jeju Island, South Korea. Collected between 20–25 meters depth from sediment consisting of sand and shell gravel. Associated nerillids from the Munseom and Beomseom islets include *Meganerilla* sp. 2, *Mesonerilla dannyi* sp. nov. and *Nerillidium* sp. 1.

**Molecular information**

*Leptonerilla westheidei* sp. nov. always groups together with *L. purschkei* sp. nov. and *L.* sp. 1 in all phylogenetic analyses.

Pairwise comparison of *L. westheidei* sp. nov. sequence similarity to other *Leptonerilla* spp.: 18S rRNA – 99.66% similar to its sister group (*L.* sp. 1) – 97.25–99.89% similar to the remaining *Leptonerilla* spp.; COI – 96.53% similar to its sister group (*L.* sp. 1) – 81.29–89.57% similar to the remaining *Leptonerilla* spp.; H3 – 98.66% similar to its sister group – 89.69–96.59% similar to the remaining *Leptonerilla* spp.

Remarks (see also Table 4 for *Leptonerilla* spp. comparisons). The small sized *Leptonerilla westheidei* sp. nov. shows the greatest morphological and molecular similarity to the two geographically closest species *L. purschkei* sp. nov. from Japan and *L. diplocirrata* from Hainan, China. It differs, however, from both by its half number of chaetae in segment I, and from these and all other species of *Leptonerilla* by having much longer cirri on segment I and molecular differences (see also remarks of *L. purschkei*).

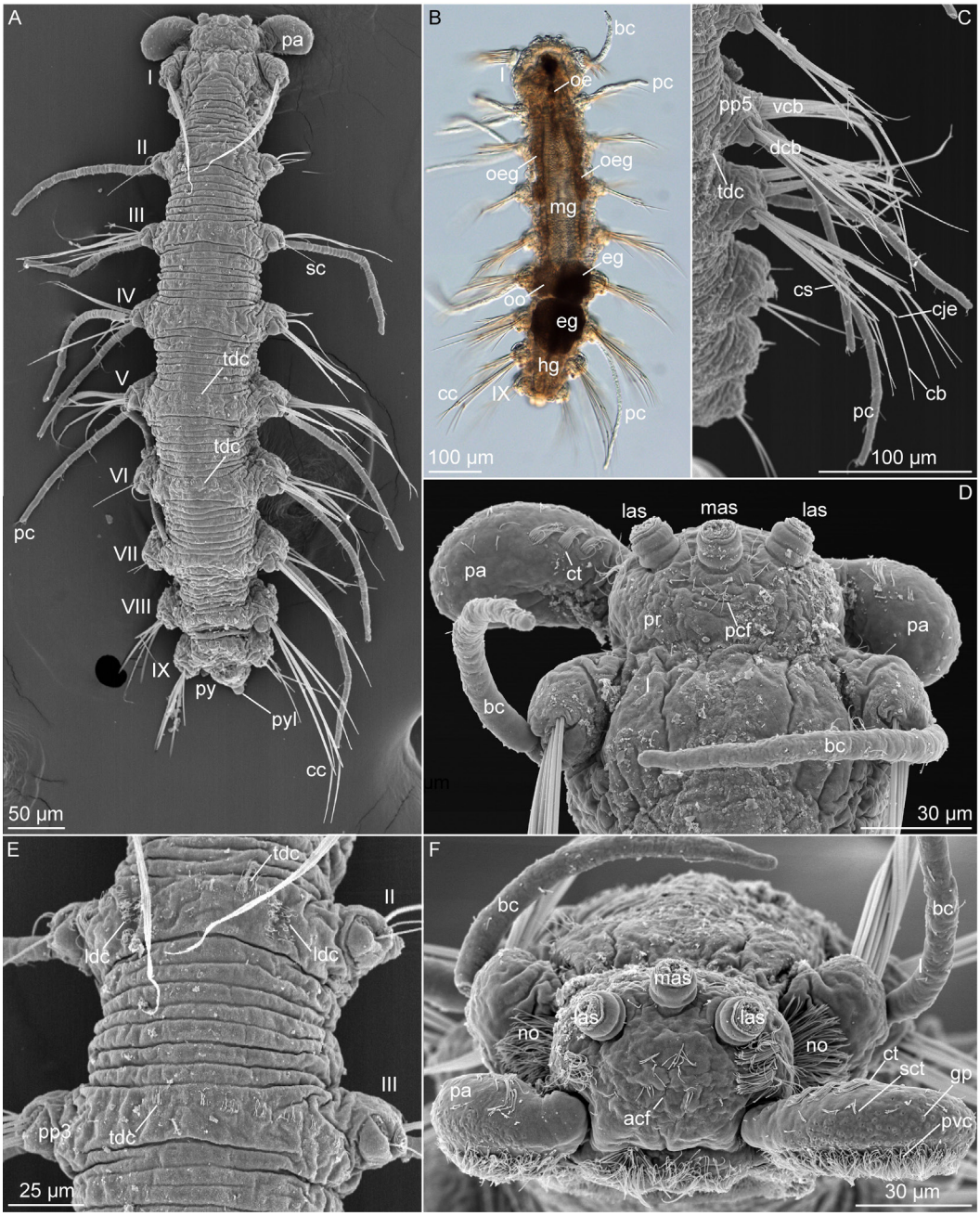


**Fig. 7.** *Leptonerilla westheidei* sp. nov., light (B) and scanning electron micrographs (A, C–F). **A, E**. Holotype (NIBRIV0000927415). **B**. Adult female (lost) with eggs. **C–D, F**. Paratype (NIBRIV0000927416). **A**. Overview of entire specimen, dorsal view. **B**. Dorsal view. **C**. Dorsal view of parapodia and chaetae of right side. **D**. Dorsal view of prostomium and first (buccal) segment. **E**. Close up of segments V–VI. **F**. Frontal view of prostomium. Abbreviations: acf = anterior ciliary field; bc = buccal cirrus; cb = chaetal blade; cc = compound chaetae; cje = chaetal joint extension; cs = chaetal shaft; ct = ciliary tuft; dcb = dorsal chaetal bundle; eg = egg; gp = glandular pore; hg = hindgut; las = lateral antenna scar; ldc = longitudinal dorsal bandlet of cilia; mas = median antenna scar; mg = midgut; no = nuchal organ; oo = oocyte; pa = palp; pc = parapodial cirrus; pcf = posterior ciliary field; pp3,5 = parapodium segment III, V; pr = prostomium; py = pygidium; pyl = pygidial median lobe; pvc = palp ventral ciliary row; sc = simple chaeta; sct = small ciliary tuft; tdc = transverse dorsal row of cilia; vcb = ventral chaetal bundle; I–IX = segments I–IX.

Specimens of *L. westheidei* sp. nov. used for morphological examination were collected from Munseom Islet, while the specimen used for DNA analysis was obtained from Beomseom Islet and identified in the field prior to DNA extraction.

Genus *Meganerilla* Boaden, 1961

***Meganerilla iensis*** sp. nov.
urn:lsid:zoobank.org:act:4A0AF43F-DC06-4522-BA89-CDBD236CE3EF
Figs 8–9; Table 5

**Diagnosis**

*Meganerilla* without a median antenna. Small body length, less than 450 µm. No eyes present. Short cirri in segment I. Parapodial cirri increasing in length posteriorly; glandular pigmentation in parapodial cirri of segments VI–VII and distally in pygidial cirri. Chaetae only lacking in segment I.

**Etymology**

Named after the type locality at 'Ie Island', and the Latin root '*-ensis*' ('of'). The Japanese name for this new species is given here as 'Sango-usamimi-gokai' (meaning 'Coral reef-rabbit ear-bristle worm' in English).

**Type material**

**Holotype**

JAPAN • late juvenile; Ryukyu Islands, Okinawa Prefecture, Ie Island; 26.72518° N, 127.83107° E; coarse coral sand at 13–15 meters depth; 3 Jun. 2019; Y. Fujita, M.J. Hansen, M.C. Allentoft-Larsen and K. Worsaae leg.; NHMD 1842018 mounted on SEM stub.

**Representative DNA sequences**

GenBank accession numbers PQ149840 (nuclear 18S rRNA), PQ149821 (nuclear 28S rRNA), PQ570590 (nuclear H3) and PQ421132 (mitochondrial COI); from specimen with same collection data as holotype (Table 1).

**Description**

Measurements are based on LM of holotype, counts and ciliation from SEM (no measurements from SEM pictures where the specimen seemingly shrank to about 60% of live length). Body about 405 µm long with nine segments (Figs 8A, 9C). Segment lengths of 43, 44, 40, 47, 47, 45, 54, 31, 27 µm. Trunk segments about 90 µm wide including parapodia, about 55 µm excluding parapodia. Segments II–VII similar in length and width, segments VIII and IX shorter and less wide, possibly because not fully grown (Figs 8A–B, 9B).

Prostomium round with straight palps, increasing slightly in width distally (pa, Figs 8C, 9A). Palp 92 µm long and 29 µm wide. Prostomial lateral ciliary band next to palp insertion. Antennae and indicative scars thereof absent. Eyes absent. Nuchal organs laterally in groove between prostomium and segment I (no, Figs 8C, 9A, E).

Cirri on segment I short, 13 µm long and with several cilia on and/or next to cirri (Fig. 9F). Lanceolate parapodial cirri on segments III–VIII, increasing in length and width posteriorly until segment VII (pc, Figs 8B, D, 9B–C), maximum length 38 µm. Parapodial cirri on segments VI–VII with brown pigmented glands (Fig. 8D). Short pygidium with cylindrical pygidial cirrus, 73 µm long, and a shorter regenerating cirrus, 41 µm long (pyc, Figs 8A–B, 9B–C). Pygidial cirri with brown pigmentation at distal tip.

Capillary chaetae in all trunk segments, increasing in length posteriorly until segment VIII, maximum 72 µm long. Maximum six chaetae in each parapodium of segments II–IX; many chaetae lost.

Prostomium with anterior and posterior fields of presumed sensory cilia and lateral rows of cilia next to palp insertion. Paired, densely ciliated nuchal organs on lateral border between prostomium

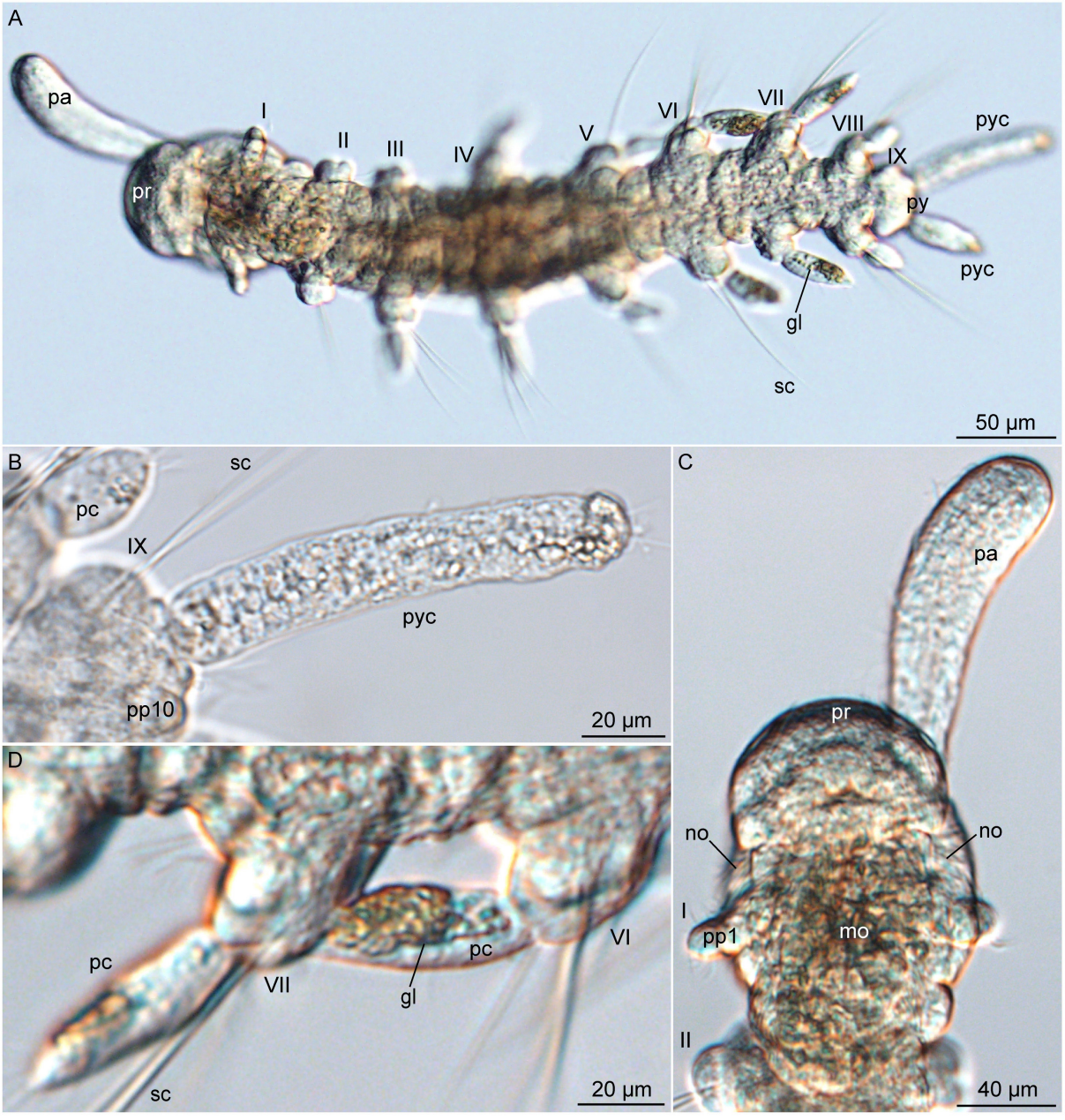


**Fig. 8.** *Meganerilla iensis* sp. nov., holotype (NHMD 1842018), light microscopy (LM), dorsal view; **A**. Overview of entire specimen. **B**. Pygidial cirri on an adult specimen **C**. Peristomium, prostomium and palp of an adult specimen. **D**. Posterior parapodial cirri with brown pigmentation, dorsal view of an adult specimen. Abbreviations: bc = buccal cirrus; no = nuchal organ; pa = palp; pc = parapodial cirrus; pp = pygidial prolongation; pr = prostomium; py = pygidium; pyc = pygidial cirrus; sc = simple chaetae; I–IX = segments I–IX.

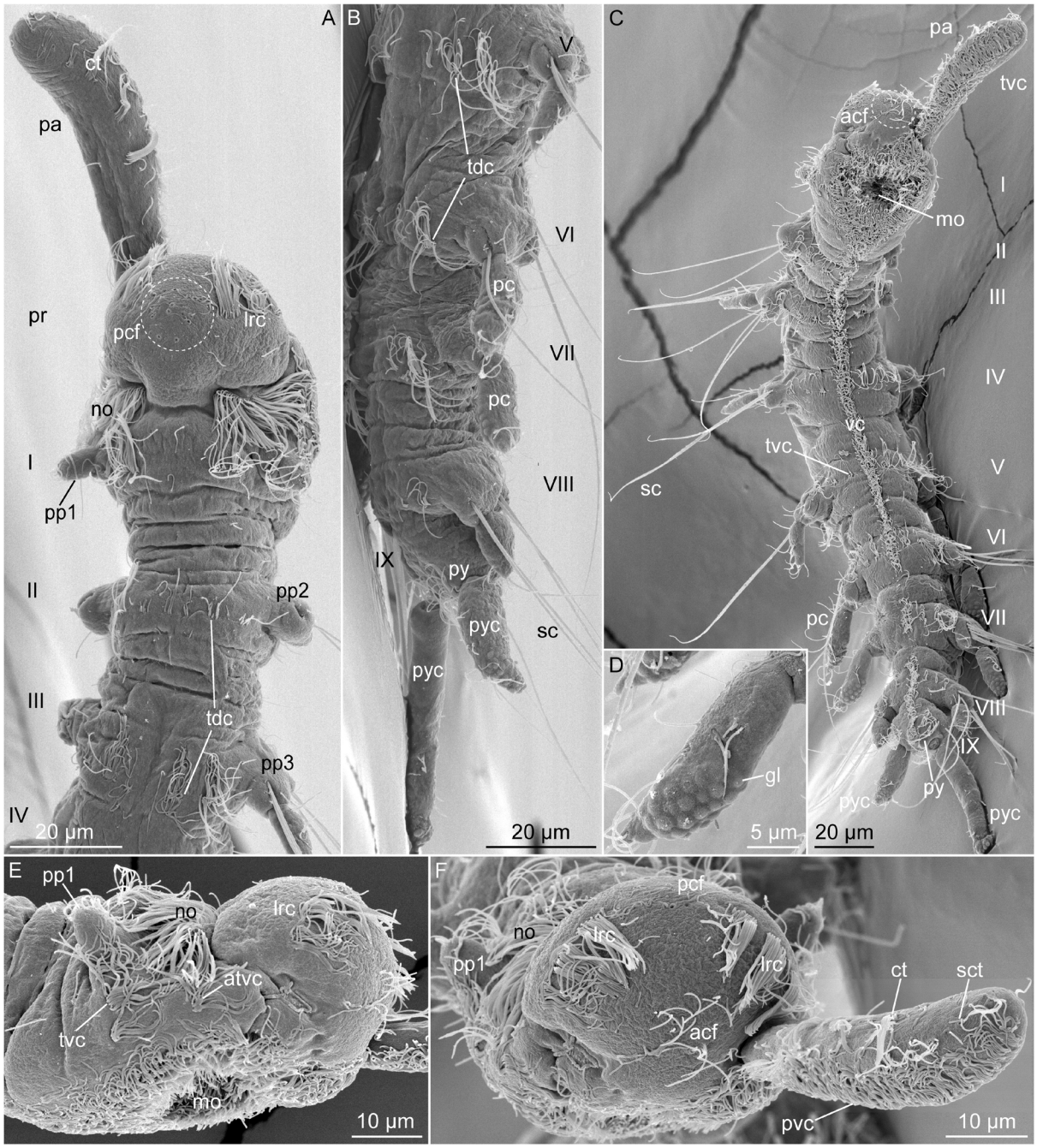


**Fig. 9.** *Meganerilla iensis* sp. nov., holotype (NHMD 1842018), scanning electron micrographs (SEM). **A**. Close-up of prostomium and three anterior segments showing the palp, dorsal view. **B**. Close-up of segments V–IX with segment IX carrying pygidium, lateral view. **C**. Overview of entire specimen, ventral view. **D**. Close-up of parapodial cirrus carrying glands from C, segment VII, ventral view. **E**. Close-up of prostomium carrying the mouth opening, lateral view. **F**. Frontal view of prostomium. Abbreviations: acf = anterior ciliary field; atvc = anterior transverse dorsal row of cilia; ct = ciliary tuft; gl = gland; lrc = lateral row of cilia; mo = mouth opening; no = nuchal organ; pa = palp; pc = parapodial cirrus; pcf = posterior field of sensory cilia; pp1–3 = parapodium segment I–III; pr = prostomium; pvc = palp ventral ciliary row; py = pygidium; pyc = pygidial cirrus; sc = simple chaeta; sct = small ciliary tuft; tdc = transverse dorsal row of cilia; tvc = transverse ventral row of cilia; vc = midventral ciliary band; I–IX = segments I–IX.

and segment I (acf, lrc, pcf, Fig. 9A, C, E–F). Palp with ventral longitudinal dense ciliary row from insertion to tip of palp, and lateral rows of small tufts of cilia (ct, sct, pcf, Fig 9F). Segment I with paired dorsolateral transverse rows of ciliary tufts at level of parapodia. Following trunk segments with dorsal transverse continuous rows of cilia in all segments at level of parapodia (tdc, Fig. 9A–B). Ventral ciliation consisting of i) densely ciliated mouth (mo, Fig. 9C, E), ii) midventral longitudinal ciliary band extending from mouth to pygidium and iii) transverse ventral rows of cilia of up to 6 ciliary tufts in all segments at level of parapodia (tvc, vc, Fig. 9C). Multiple single cilia scattered on dorsal, lateral, and ventral sides of body.

Reproduction unknown. Nephridia and gonoducts not investigated.

**Distribution and habitat**

Reef slope in front of and near Unnamed Cave, northern part of eastern reef of Ie Island, Okinawa Prefecture, Ryukyu Islands, Japan. Patches of coarse coral sand with shells and small coral fragments at 13–15 meters of depth between corals. Associated nerillids from the same locality include *Nerillidium* sp. 2 and *Mesonerilla* sp. 4.

**Molecular information**

*Meganerilla iensis* sp. nov. nests within a fully supported clade of *Meganerilla* spp., next to *Meganerilla* sp. 1 from Miyako Islands, Japan (with no morphological information available).

Pairwise comparison of *Meganerilla iensis* sp. nov. sequence similarity to other *Meganerilla* spp.: 18S rRNA – 99.77% similar to its sister taxon (*M*. sp. 1) – 97.89–99.54% similar to the remaining *Meganerilla* spp.; 28S rRNA – 99.80% similar to *M*. sp. 1 – 88.35–97.83% similar to the remaining *Meganerilla* spp.; COI – 94.56% similar to *M*. sp. 1 – 94.07% similar to the remaining *Meganerilla* spp.; H3 – 100% similarity *M*. sp. 1 – 90.52–96.27% similar to the remaining *Meganerilla* spp.

**Remarks** (see also Table 5 for *Meganerilla* spp. comparisons)

Like its five congeneric described relatives, *M. iensis* sp. nov. has nine segments, simple chaetae, lanceolate or leaf-shaped parapodial cirri (not found in *Meganerilla bactericola* (Müller, Bernhard & Jouin-Toulmond, 2001)) and relatively large palps (Boaden 1961; Magagnini 1966; Riser 1988; Müller *et al*. 2001; Westheide 2008; Worsaae *et al*. 2009; Worsaae 2021).

*Meganerilla iensis* sp. nov. is smaller in size compared to other species of *Meganerilla* (Boaden 1961; Núñez *et al*. 1997; Worsaae *et al*. 2009); however, the holotype may not be fully grown. *Meganerilla iensis* does not possess any median antenna, as in *M. cesari* and *M. bactericola*, and lacks chaetae in the first segment but not in the following trunk segment. Moreover, *M. iensis* possesses apomorphic pigmented glands in the parapodial and pygidial cirri.

*Meganerilla* sp. 1 and *M. iensis* sp. nov. were collected from two Japanese islands about 350 km apart. Neither species was found in isolated caves, as *Meganerilla* sp. 1 was collected from subtidal sand at Irabu Island. The two taxa show a high molecular affinity (99.77% for 18S rRNA; 99.80% for 28S rRNA; 98.56% for COI; 100% for H3), but no morphological information is available for *Meganerilla* sp. 1. Out of caution, they are so far treated as separate species mainly due to dissimilarities in COI. Additional morphological and molecular data are necessary to assess the taxonomic status of *Meganerilla* sp. 1.

**Table 5.** Selected morphological characters comparison of *Meganerilla* Boaden 1961. All measurements in µm. Asterisk (*), measurements estimated from photos of live specimens, relative to known body length of fixed specimen. Measurements of new species are based on holotype. Abbreviations: ant = antenna; excl. = excluding; L = length; max = maximum; med = median; para = parapodia; segm = segment; W = width; ? = unknown. References: 1 = Boaden 1961; 2 = Magagnini 1966; 3 = Müller *et al*. 2001; 4 = Riser 1988; 5 = Worsaae *et al*. 2009, 2019a.

| Species | Body | | Antennae | Palps | Eyes | Parapodial cirri | | Pygidial cirri | | Chaetae | | | | Reproduction |
|---|---|---|---|---|---|---|---|---|---|---|---|---|---|---|
| | Max L | Max W excl. para | Med ant, max L | Max L | | Segm I, max L | Segm II–IX, max L | Max L | Shape | Segm I, max no. | Segm I, max L | Segm II–VIII, max no. | Segm II–VIII, max L | Spermioducts |
| ***Meganerilla iensis*** sp. nov. | 405 | 55 | A | 92 | A | 13 | 38 | 73 | Cylindrical | A | A | 6 | 72 | ? |
| *M. bactericola*[3] | 1100 | 90 | A | 118 | A | A | 55 | ca 55 | Leaf shaped | A | A | Few | 165 | Fused |
| *M. cesari*[5] | 1005 | 129 | A | 288 | A | 28 | 95 | ? | ? | 5 | 30 | 17 | 110 | ? |
| *M. clavata*[2] | 1500 | 190 | 115 | 400 | A | 20 | 116 | 290 | Cylindrical | 6 | 25* | 20 | 130* | Paired |
| *M. penicillicauda*[4] | 2000 | 250 | 100 | 300 | A | 30 | 100 | 140 | Leaf shaped | 4 | 140* | 16 | 270 | Paired |
| *M. swedmarki*[1] | 2100 | 250 | A | 520 | P | 30 | 152 | 350 | Cylindrical | 5 | 110 | 23 | 220 | Paired |

Genus *Mesonerilla* Remane, 1949

***Mesonerilla gamaglandulata*** sp. nov.
urn:lsid:zoobank.org:act:E06FA3A6-4975-48AB-977B-232B72E7CE8C
Figs 10–11; Table 6

**Diagnosis**

*Mesonerilla* with similar-sized cylindrical parapodial cirri on segments II–I, and longer cylindrical pygidial cirri. Three antennae, median short and slightly swollen. Segment I with chaetae and short cirri. Three pairs of pigmented glands in segments I and II. Ventral transverse rows of ciliary tufts between parapodia and intersegmentally. About 14 enteronephridia spanning the hindgut; pairs of nephridia opening in segments III, IV, V. Hermaphroditic with spermioducts opening in segments VI and VII and gonoducts in segment VIII.

**Etymology**

'Gama', means 'cave' in Okinawan dialect and 'glandulata' refers to the relatively many glands associated with palps, peristomium and oesophagus. The Japanese name for this new species is given here as 'Gama-usamimi-gokai' (meaning 'Cave dwelling-rabbit ear-bristle worm' in English).

**Type material**

**Holotype**

JAPAN • adult; Okinawa Prefecture, Ie Island, 'Unnamed Cave' (or 'Sho-doukutsu'); 26.72518° N, 127.83107° E; 5–12 meters depth; 9 Jun. 2019; Y. Fujita, M.J. Hansen, M.C. Allentoft-Larsen and K. Worsaae leg.; NHMD 1842019 mounted on SEM stub.

**Paratypes**

JAPAN • 3 adults; same data as for holotype; 3 Jun. 2019; NHMD 1842021 to NHMD 1842023 (mounted on SEM stubs) • 1 adult; same data as for holotype; 10–17 meters depth; 3 Jun. 2019; NHMD 1842020 as permanent whole mount.

**Representative DNA sequences**

GenBank accession numbers PQ149843 (nuclear 18S rRNA), PQ149824 (nuclear 28S rRNA), PQ570593 (nuclear H3) and PQ421136 (mitochondrial COI); from specimen with same collection data as holotype (Table 1).

**Description**

Measurements are based on LM of holotype, counts and ciliation from SEM, and values for paratypes are given in parentheses. Hyaline body, about 785 µm long (670–785 µm, n = 4) with nine segments (Figs 10A, 11A). Segment lengths of holotype 93, 91, 92, 94, 101, 83, 78, 67, 60 µm. Trunk segments about maximum 135 µm wide, including parapodia (135–150 µm, n = 3), about 105 µm excluding parapodia (100–110 µm, n = 3).

Prostomium with club-shaped palps, 81 µm long (64–82 µm, n = 3) and 41 µm wide (36–40, n = 3) (pa, Figs 10A, D, 11B, F–G) with unique lateral row of 4–6 glandular papillae interspersed by tufts of cilia (ppl, Fig. 11C). Median antenna cylindrical and slightly swollen distally (ma, Figs 10C, 11B, F), 84 µm long (75–80 µm, n = 3). Only scars from lateral antennae left but presence further documented by CLSM of lateral antennae muscles in prostomium (lam, mam, Fig. 10E). Eyes absent. Paired nuchal organ between prostomium and segment I. Three groups of dark, paired glands: i) small, dorso-anterior

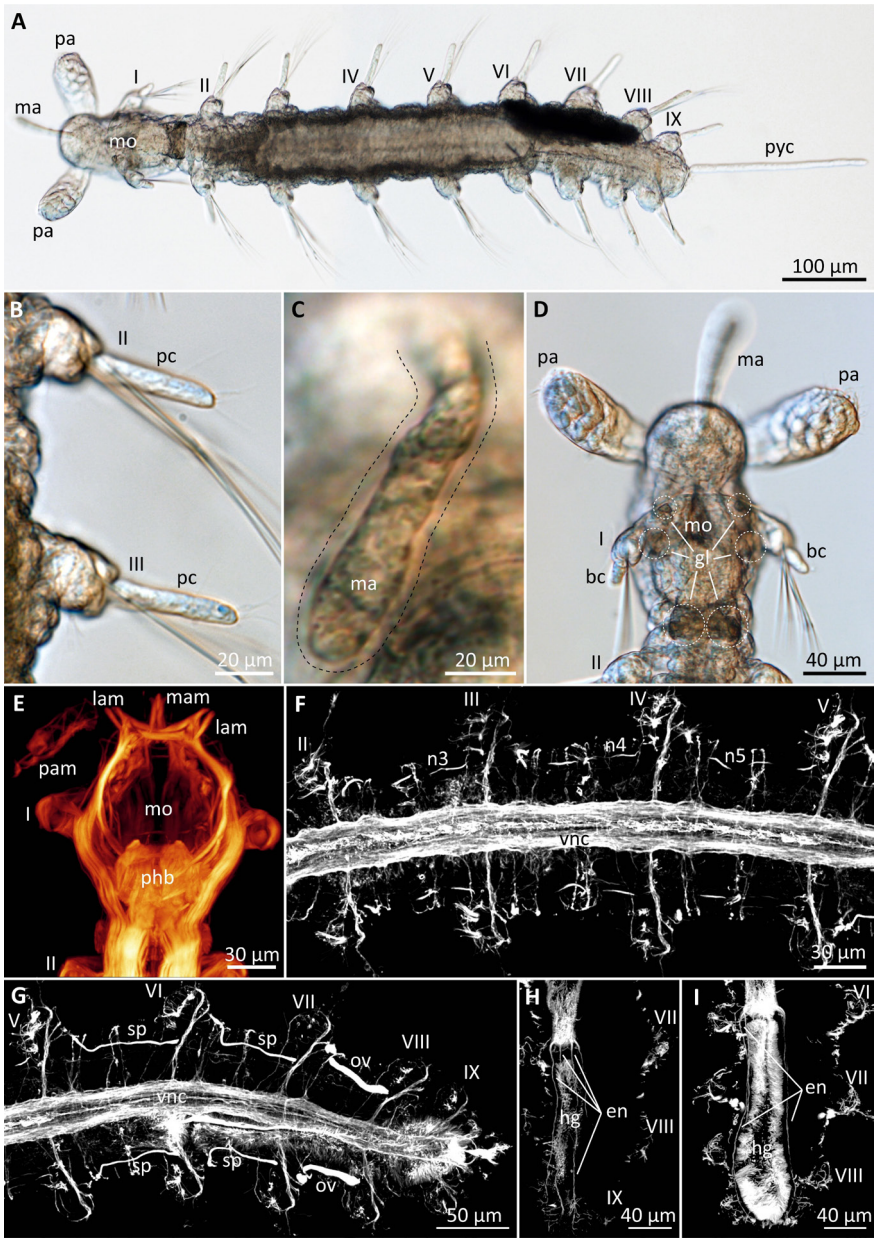


**Fig. 10.** *Mesonerilla gamaglandulata* sp. nov., paratypes, adult specimens. **A–B, D**. NHMD 1842021. **C**. NHMD 1842023. **E–I**. NHMD 1842020. **A–D**. Light microscopy (LM). **E–I**. Confocal laser scanning micrographs. **A**. LM of a specimen with long pygidial cirrus, dorsal view. **B**. LM of parapodial cirri, dorsal view. **C**. LM of dorsal view of median antenna. **D**. LM of head with palps and three groups of glands (indicated by dashed circles), dorsal view. **E**. Maximum intensity projection of z-stack of phalloidin of the head of specimen labelled with phalloidin, ventral view. **F**. Anti-acetylated α-tubulin immunoreactivity showing pairs of nephridia in segment III–V, ventral view. **G**. Maximum intensity projection of z-stack of specimen labelled with anti-acetylated α-tubulin, focusing on posterior segments in adult specimen with gonoducts. **H**. Acetylated α-tubulin immunoreactivity of dorsal enteronephridia. **I**. Acetylated α-tubulin immunoreactivity of lateral enteronephridia. Abbreviations: bc = buccal cirrus; en = enteronephridia; gl = gland; hg = hindgut; lam = lateral antenna muscle; ma = median antenna; mam = median antenna muscle; mo = mouth opening; n3–5 = nephridia in segments III–V; ov = oviduct; pa = palp; pam = palp muscle; pc = parapodial cirrus; phb = pharyngeal bulbous; pyc = pygidial cirrus; sp = spermioduct; vnc = ventral nerve cord; I–IX, segments I–IX.

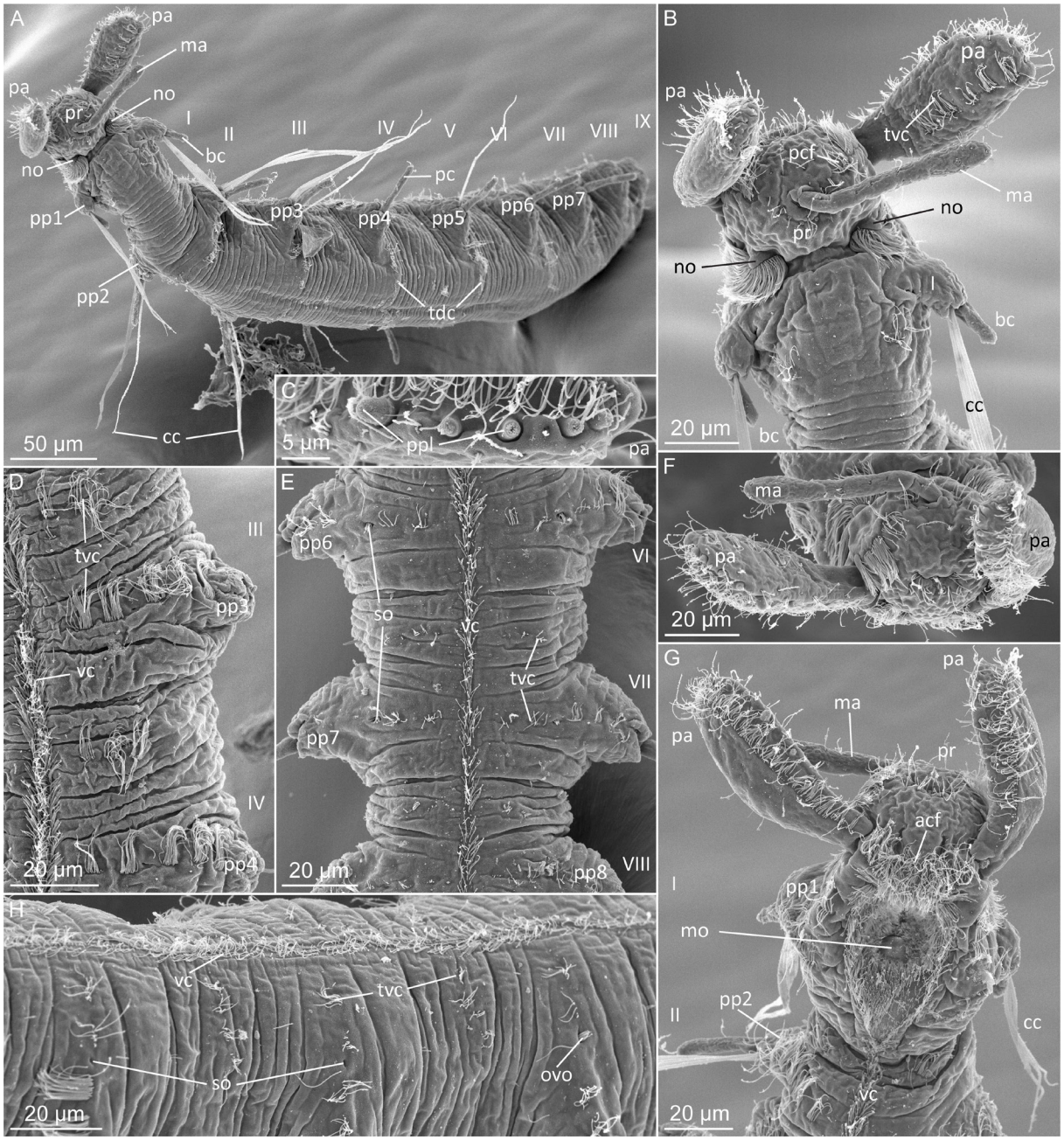


**Fig. 11.** *Mesonerilla gamaglandulata* sp. nov., scanning electron micrographs (SEM), adult specimens. **A–C, E–H**. Holotype (NHMH 1842019). **D**. Paratype (NHMH 1842023). **A**. Overview of entire specimen, dorsolateral view. **B**. Peristomium and prostomium carrying palps and medium antenna, dorsal view. **C**. Lateral row of 4–6 glandular papillae interrupted by tufts of cilia, lateral view. **D**. Close-up of the midventral ciliary band and transverse rows of cilia, ventral view. **E**. Close-up of segments VI–VII from A, carrying the gonoducts opening, ventral view. **F**. Frontal view of prostomium. **G**. Peristomium and prostomium carrying the mouth, ventral view. **H**. Close-up of the gonoducts opening on segments VI–VII, lateral view. Abbreviations: acf = anterior field of sensory cilia; bc = buccal cirrus; cc = compound chaetae; ma = median antenna; no = nuchal organ; ovo = oviducts opening; pa = palp; pcf = posterior field of sensory cilia; pp1–8 = parapodium segment I–VIII; ppl = glandular papillae; pr = prostomium; so = spermioduct opening; tdc = transverse dorsal row of cilia; tvc = transverse ventral row of cilia; vc = midventral ciliary band; I–IX = segments I–IX.

on segment I and extending ventrally, ii) large, rounded, opening into mouth cavity, and iii) large group, dorsally in segment II (oesophageal?) (gl, Fig. 10D).

Parapodial cirri in segment I short (bc, Figs 10D, 11A–B), 15–20 µm long (16–22 µm, n = 3). Trunk segments with cylindrical cirri of similar length (pc, Figs 10A–B, 11A), maximum 55 µm (49–59 µm, n = 3). Pygidium with 216 µm long cylindrical cirrus (pyc, Fig. 10A).

Straight to slightly curved compound chaetae in all segments. Parapodia with up to eight chaetae, maximum 75 µm long in segment I and maximum 120 µm long in trunk segments.

Prostomium with anterior and posterior fields of sensory cilia extending between lateral antennae scars and palp insertions (acf, pcf, Fig. 11B, G). Paired densely ciliated nuchal organs on dorsolateral border between prostomium and segment I. Palps with ventral longitudinal dense ciliary row from insertion points to tip of palps, lined by dorsolateral row of five ciliary tufts present posteriorly (each tuft with up to 15 cilia). Segment I with paired dorsolateral transverse rows of each two ciliary tufts (each tuft with > 10 cilia) at the level of parapodia. Continuous transverse dorsolateral row with numerous cilia on all trunk segments, extending from basis of parapodia to about halfway to mid-dorsal line (tdc, Fig. 11A–B). Ventral ciliation consisting of i) densely ciliated mouth (mo, Fig. 11G), ii) midventral longitudinal ciliary band extending from mouth to pygidium (vc, Fig. 11E) and iii) transverse rows of up to five tufts of cilia on each parapodia (tvc, Fig. 11D, H). Additional ventral row intersegmentally with 2–6 tufts between segments I–VIII.

Three pairs of discontinuous ciliated nephridia extending along segments and opening latero-ventrally in segments III, IV, V (n3–n5, Fig. 10F). About 14 enteronephridia extending along the hindgut (en, Fig. 10H–I), on the dorsal (4), lateral (6) and ventral (4) sides. Hermaphroditic with two pairs of slightly curved dorsoventrally extending spermioducts opening separately in segments VI and VII (sp, Figs 10G, 11E, H) and one pair of relatively straight oviducts opening in segment VIII (ov, Figs 10G, 11H).

**Distribution and habitat**

Unnamed Cave 'Sho-doukutsu', eastern reef of Ie Island, Okinawa Prefecture, Ryukyu Islands, Japan. Submarine cave located on the reef slope. Specimens collected from plankton tow and sediment samples from the anchialine right hall of the cave, at 5–17 meters of depth; see Osawa & Fujita (2019) for the description of the cave. Associated nerillids from the cave include *Cirrinerilla sulcipalpata* gen. et sp. nov., *Leptonerilla* sp. 3 and *Trochonerilla* sp. 1.

**Molecular information**

*Mesonerilla gamaglandulata* sp. nov. is found in both analyses (Fig. 2) as a sister taxon to *M. armoricana* Swedmark, 1954 and *M. roscovita* Levi, 1953, albeit with low support (PP/BS: 0.51/69). Together, this clade has a sister relationship to *M. dannyi* sp. nov. (PP/BS: 1/99). The hermaphroditic *Mesonerilla* spp. within clade C does not form a monophyletic sub-clade, as *Nipponerilla irabuensis* groups with the previously mentioned species of *Mesonerilla*, although with low support (PP/BS: 0.68/79), and this clade is itself sister to the hermaphroditic *Mesonerilla fagei* Swedmark, 1959 (PP/BS: 1/96). Morphologically, *M. gamaglandulata* sp. nov. has a strong resemblance to the three hermaphroditic *Mesonerilla* spp. and exhibits a high degree of similarity in 18S rRNA and 28S rRNA sequences.

Pairwise comparison of *M. gamaglandulata* sp. nov. sequence similarity to other hermaphroditic *Mesonerilla* spp. and *Nipponerilla irabuensis*: 18S rRNA – 98.83–98.89% similar to its sister group (clade comprising *M. armoricana* and *M. roscovita*) – 98.88–99.14% similar to remaining hermaphroditic *Mesonerilla* spp. – 96.92% similar to *N. irabuensis*; 28S rRNA – 90.52% similar to its sister group – 89.42–91.37% similar to the remaining hermaphroditic *Mesonerilla* spp. – 84.89% similar

**Table 6** (continued on next page). Selected morphological characters comparison of *Mesonerilla* Remane, 1949 with brooding hood, hermaphroditic *Mesonerilla* and *Nipponerilla irabuensis* Worsaae, Hansen & Fujita, 2021. All measurements are in µm. Asterisk (*) indicates measurements of species obtained from scanning electron microscopy (SEM). Measurements of new species are based on available specimens, including type material and live observations. Abbreviations: A = absent; ant = antenna; G = gonochoristic; H = hermaphroditic; L = length; max = maximum; med = median; segm = segment; P = present; para = parapodial; I–IX = segments I–IX; ? = unknown. References: 1 = Lévi 1953; 2 = Swedmark 1959; 3 = Westheide 2008; 4 = Wilke 1953; 5 = Worsaae *et al*. 2019a; 6 = Worsaae *et al*. 2021b.

| Species | Body | | Antennae | | Palps | Parapodial cirri | | | Pygidial cirri |
|---|---|---|---|---|---|---|---|---|---|
| | Max L | Trunk segm, relative size | Shape | Distinctly shorter med ant | Max L | Size along body | Max L | Shape | Max L |
| ***M. harubangi*** sp. nov.* | 725 | Equal | Cylindrical | ? | 56 | Increasing | 152 | Cylindrical; tapering | 70 |
| *M. intermedia*[3,4] | 1645 | Equal | Cylindrical; tapering | Yes | 210 | Increasing | 360 | Bottle-shaped | 330 |
| *M. laerkae*[6] | 1170 | Equal | Bottle-shaped; tapering | No | 70 | Equal | 90 | Bottle-shaped | 170 |
| ***M. gamaglandulata*** sp. nov. | 785 | Segment VII–IX smaller | Cylindrical; slightly swollen | ? | 82 | Equal | 59 | Cylindrical; tapering | 216 |
| ***M. dannyi*** sp. nov. | 875 | Equal | Cylindrical; slightly swollen | ? | ? | Equal | 65 | Cylindrical; tapering | ? |
| *M. armoricana*[2,3] | 1100 | Equal | Cylindrical; slightly swollen | Yes | 80 | Equal | 50 | Cylindrical | 225 |
| *M. fagei*[2,3] | 1000 | Equal | Cylindrical | Yes | 175 | Equal | 100 | Cylindrical | 240 |
| *M. roscovita*[1,3] | 800 | Equal | Cylindrical | Yes | 100 | Equal in segm II–VIII; longer in segm IX | 45 | Cylindrical | 200 |
| *Nipponerilla irabuensis*[5] | 616 | Segment IV–V widest | Cylindrical | No | 117 | Slightly increasing | 85 | Cylindrical | 28 (broken) |

**Table 6** (continued). Selected morphological characters comparison of *Mesonerilla* Remane, 1949 with brooding hood, hermaphroditic *Mesonerilla* and *Nipponerilla irabuensis* Worsaae, Hansen & Fujita, 2021. All measurements are in µm. Asterisk (*) indicates measurements of species obtained from scanning electron microscopy (SEM). Measurements of new species are based on available specimens, including type material and live observations. Abbreviations: A = absent; ant = antenna; G = gonochoristic; H = hermaphroditic; L = length; max = maximum; med = median; segm = segment; P = present; para = parapodial; I–IX = segments I–IX; ? = unknown. References: 1 = Lévi 1953; 2 = Swedmark 1959; 3 = Westheide 2008; 4 = Wilke 1953; 5 = Worsaae *et al*. 2019a; 6 = Worsaae *et al*. 2021b.

| Species | Chaetae | | | | | Reproduction | | | |
|---|---|---|---|---|---|---|---|---|---|
| | Segm lacking chaetae | Segm I, max no. | Segm I, max L | Segm II–IX, max no. | Segm II–IX, max L | | Brooding hood | Max no. embryos | Spermioducs opening |
| ***M. harubangi*** sp. nov. * | – | 12 | 109 | 26 | 191 | G | P | 2 | ? |
| *M. intermedia*[3,4] | – | 13 | 195 | 16 | 345 | G | P | 4 | V + VI (fused) |
| *M. laerkae*[6] | – | 4 | 80 | 15 | 180 | G | P | 6 | ? |
| ***M. gamaglandulata*** sp. nov. | – | 8 | 75* | 8 | 120* | H | A | ? | VI + VII |
| ***M. dannyi*** sp. nov. | I | – | – | 12 | 180 | H | A | ? | VI + VII |
| *M. armoricana*[2,3] | I | – | – | 9 | 80 | H | A | ? | VI + VII |
| *M. fagei*[2,3] | – | 9 | 100 | 10 | 160 | H | A | ? | VI + VII |
| *M. roscovita*[1,3] | I | – | – | 17 | 140 | H | A | ? | VI + VII |
| *Nipponerilla irabuensis*[5] | – | 10 | ? | 12 | 141 | H | A | ? | VII + VIII |

to *N. irabuensis*; COI – 72.86% similar to the remaining hermaphroditic *Mesonerilla* spp. – 70.36% similar to *N. irabuensis*; H3 – 90.76–92.32% similar to its sister group – 86.72% similar to the remaining hermaphroditic *Mesonerilla* spp. – 91.97% similar to *N. irabuensis*.

**Remarks** (see also Table 6 for comparisons of morphologically similar nerillids)

With its nine segments, compound chaetae, spoon-shaped palps, three antennae, equally long parapodial cirri and configuration of gonoducts *M. gamaglandulata* sp. nov. bears most resemblance to the three hermaphroditic species of *Mesonerilla* (*M. roscovita*, *M. fagei* and *M. armoricana*) and *Mesonerilla dannyi* sp. nov. (Levi 1953; Swedmark 1959; Westheide 2008; Worsaae *et al*. 2019a, 2021a; Worsaae 2021). *Mesonerilla gamaglandulata* shares different characteristics with the three hermaphroditic *Mesonerilla* including the presence of chaetae and shorter cirri in segment I (also seen in *M. fagei*), ventrolateral rows of cilia, oesophageal glands and cylindrical pygidial cirri (also seen in *M. roscovita* and *M. fagei*) and a swollen median antenna and spoon-shaped palps (also seen in *M. armoricana*) (Levi 1953; Swedmark 1959; Westheide 2008; Worsaae *et al*. 2019a). The main difference between *M. gamaglandulata* and *Mesonerilla dannyi* is the presence or absence of chaetae in segment I, respectively. *Mesonerilla gamaglandulata*, *Mesonerilla dannyi* and *N. irabuensis* were monophyletic in the Bayesian and maximum likelihood analyses and they all have compound chaetae, nine segments and three antennae. *Nipponerilla irabuensis* differs from the two others by having a cigar-shaped body, spermioducts in segments VII and VIII and being gonochoristic. In contrast to *M. gamaglandulata*, *N. irabuensis* also has long palps and a relatively long median antenna (Worsaae *et al*. 2021b), traits that could not be determined from *Mesonerilla dannyi*.

Apart from *M. gamaglandulata* sp. nov., oesophageal glands have also been recorded in *M. laerkae*, *Mesonerilla katharinae* Worsaae, Mikkelsen & Martínez, 2019, *M. roscovita*, *M. fagei* and *M. xurxoi* Worsaae, Mikkelsen & Martínez, 2019, with two lateral glands also being observed in segment I of the latter species (Worsaae *et al*. 2019a). Furthermore, *M. minuta* Jouin, 1970 has about 10 yellowish dorsal epidermal glands on each side of segment I (Swedmark 1959). Three independent groups of glands in the head region, as seen in *M. gamaglandulata*, have, to our knowledge, not been recorded previously in Nerillidae and the anteriormost pair of small glands seems unique to the species.

***Mesonerilla harubangi*** sp. nov.
urn:lsid:zoobank.org:act:32DE4DE5-C0FB-4AE8-BAE5-D108C2E8114C
Fig. 12; Table 6

**Diagnosis**

*Mesonerilla* with three antennae. Segment I uniramous, with oval cirri; trunk segments biramous with cylindrical parapodial cirri. Pygidial cirri cylindrical. Row of seven dorsolateral ciliary tufts on palps. Trunk segments with short continuous ventrolateral band of cilia at each parapodia. Paired dorsolateral rows of cilia at basis of parapodia, not medially connecting. Dorsolateral ciliary tufts next to chaetae in segments II–VII. Gonochoristic. Females with rounded brooding hood extruding from the dorsal epidermis of segment VIII.

**Etymology**

The species name refers to the characteristic stone statues and deities (Dol-Hareubang, which means ‘Stone Grandfather’) of Jeju Island in South Korea, a large island geographically close to the islets where the species was collected.

**Type material**

**Holotype**

SOUTH KOREA • ♀; Jeju Island, Munseom Islet; 33.22772° N, 126.56330° E; sand and shell gravel at around 28 meters depth; 21 Oct. 2015; K. Worsaae and T. Park leg.; NIBRIV0000924478 mounted on SEM stub.

**Paratypes**

SOUTH KOREA • 4 ♀♀ adults; same data as for holotype; NIBRIV0000924479 to NIBRIV0000924482 mounted on SEM stub • 3 adults; same data as for holotype; NIBRIV0000924483 to NIBRIV0000924485 mounted on SEM stub.

**Representative DNA sequences**

GenBank accession numbers PQ149844 (nuclear 18S rRNA) and PQ570594 (nuclear H3); from specimen collected near type locality: SOUTH KOREA • Jeju Island, Seopseom Islet; 33.2294° N, 126.6027° E; shell gravel at around 33 meters depth, 19 October 2015, same collectors as holotype (Table 1).

**Description**

Measurements are based on holotype and values for paratypes are given in parentheses, all measurements obtained from SEM. Body with nine chaetigerous segments (Fig. 12A), total length about 590 µm excluding appendages (455–725 µm, n = 7). Trunk segments similar in size and up to about 130 µm wide including parapodia (120–125 µm, n = 2), about 80 µm excluding parapodia (75–80 µm, n = 2).

Prostomium with club-shaped palps, 56 µm long (50–52 µm, n = 2) and 23 µm wide (26–28 µm, n = 2) (pa, Fig. 12A, C–D), and three antennae (las, mas, Fig. 12B–D). Lateral antennae lost in holotype and in all but one paratype (148 µm long) (la, Fig. 12B). Median antenna, 30 µm and possibly broken (ma, Fig. 12B). Eyes absent. Paired nuchal organs dorsolaterally between prostomium and segment I (no, Fig. 12B).

Parapodia uniramous in segment I (Fig. 12B, D), with short oval cirrus in paratype (36 µm long) (bc, Fig. 12D). Parapodia biramous in segments II–IX, with cylindrical and tapering interramal cirrus (pc, Fig. 12A, F); increasing in length posteriorly up to 123 µm (56–152 µm, n = 7). Pygidium with 70 µm long cirri similar in shape to parapodial cirri, (pyc, Fig. 12H).

Compound chaetae in all segments. Chaetae with distal extension (es, Fig. 12G) and increasing in length towards pygidium. Parapodia with up to 10 chaetae in segment I, maximum 109 µm long (42–98 µm, n = 7). Up to 13 neuro- and 13 notochaetae in segments II–IX, maximum 184 µm long (127–191 µm, n = 7).

Prostomium with anterior and posterior fields of cilia and paired lateral ciliary bands extending between lateral antenna and palps insertion (an, Fig. 12D). Palps ciliated continuously on frontal side from insertion point to tip of palps (ct, Fig. 12C), lined by dorsolateral row of ciliary tufts present posteriorly (each tuft with up to seven cilia). Ventral ciliation consisting of i) densely ciliated mouth (mo, Fig. 12D), ii) midventral longitudinal ciliary band extending from mouth to pygidium (vb, Fig. 12F) and iii) short transverse ventrolateral band of at least 20 cilia on each parapodia (vt, Fig. 12F–G). Continuous transverse dorsolateral row with numerous cilia on all trunk segments, extending from basis of parapodia to about halfway to mid-dorsal line (dt1, Fig. 12E). Dense dorsolateral tuft of more than 20 cilia on each parapodium next to notochaetae insertion and cirrus in segments II–VII (dt2, Fig. 12E). Dorsal ciliation patterns of last two segments not observable. Few individual cilia scattered on ventral and dorsal surfaces. Sixteen ciliary tufts observed on ridge of the brooding hood (ct, Fig. 12H).

Gonochoristic. Females with round brooding hood, 103 µm long and 126 µm wide, in segment VII at parapodia level (bh, Fig. 12A, H), partially covering up to two embryos attached dorsally. One embryo

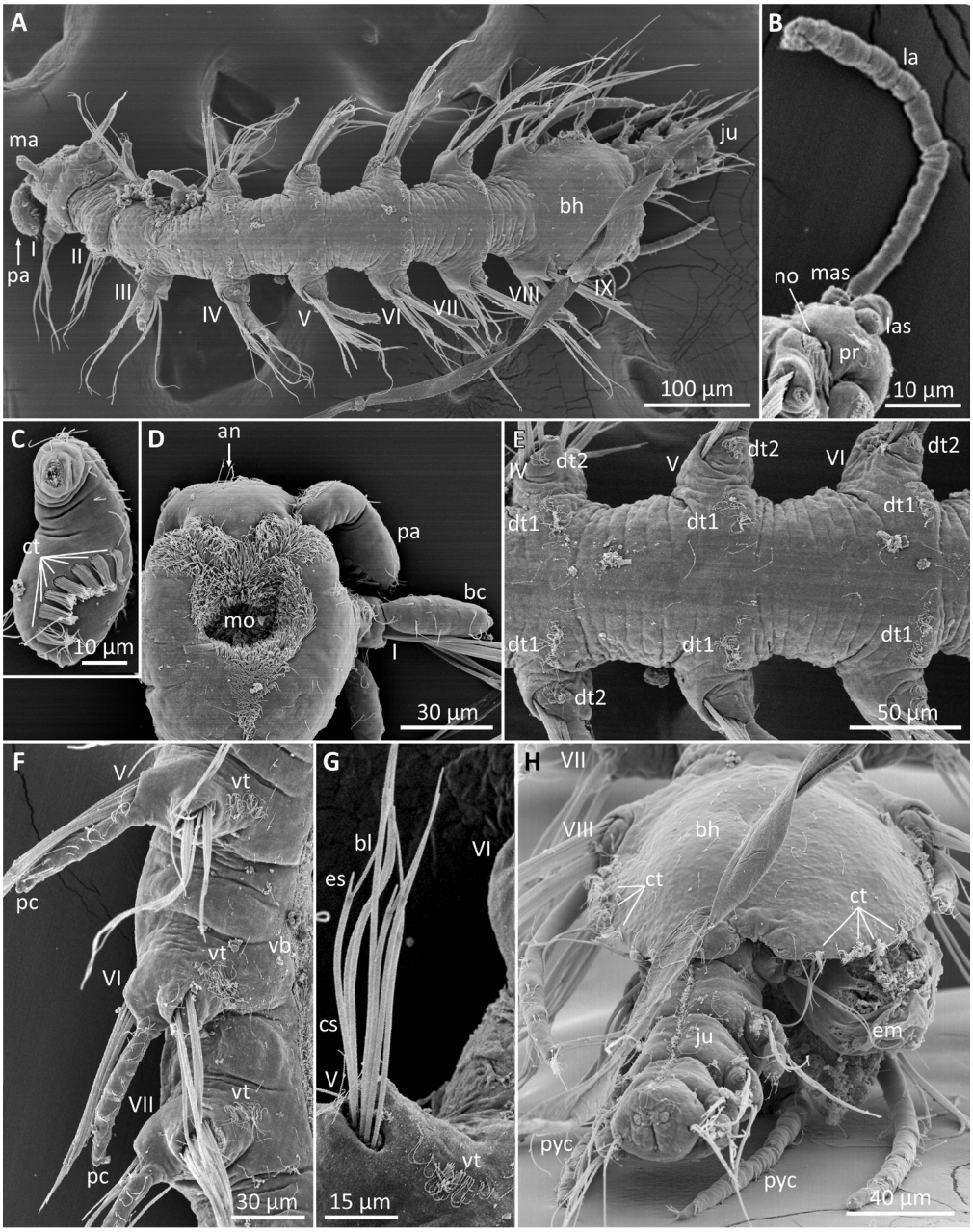


**Fig. 12.** *Mesonerilla harubangi* sp. nov., scanning electron micrographs (SEM). **A, E, H**. Holotype, ♀ (NIBRIV0000924478). **B**. Paratype, ♀ (NIBRIV0000924479). **C–D**. Paratype, ♀ (NIBRIV0000924482). **F**. Paratype (NIBRIV0000924484). **G**. Paratype, ♀ (NIBRIV0000924480). **A**. Overview of entire adult with brooding hood, dorsal view. **B**. Prostomium and intact lateral antenna of adult, lateral view. **C**. Palp broken off from adult, ventral view. **D**. Peristomium and prostomium of adult, ventral view. **E**. Close-up of segment IV–VI showing ciliation of adult, dorsal view. **F**. Close-up of segment V–VII showing ciliation and biramous parapodia of adult, ventrolateral view. **G**. Chaetae in adult, ventrolateral view. **H**. Brooding hood covering juvenile and embryo, posterolateral view. Abbreviations: an = anterior field of cilia; bc = buccal cirrus; bh = brooding hood; bl = chaetal blade; cs = chaetal shaft; ct = ciliary tuft; dt1–2 = dorsal ciliary tuft; em = embryo; es = extension of the shaft; ju = juvenile; la = lateral antenna; las = lateral antenna scar; ma = median antenna; mas = median antenna scar; mo = mouth opening; no = nuchal organ; pa = palp; pc = parapodial cirrus; pr = prostomium; pyc = pygidial cirrus; vb = midventrally ciliary band; vt = ventrolateral ciliary tuft; I–IX = segments I–IX.

typically more developed. Juveniles attached to female with six chaetigers maximum and conspicuous parapodia. Male gonopores not found. Nephridia and gonoducts not studied.

**Distribution and habitat**

Eastern coast of Seopseom Islet and the western coast of Munseom Islet, south of Jeju Island, South Korea. Collected from 22–33 meters depth from sediment consisting of sand and shell gravel. Associated nerillids from the Seopseom and Munseom Islets include *Leptonerilla westheidei* sp. nov., *Mesonerilla dannyi* sp. nov. and *Nerillidium* sp. 1.

**Molecular information**

Only the maximum likelihood analysis resolved *M. harubangi* sp. nov. as a sister group to *Mesonerilla* sp. 2 and *M. laerkae* (albeit poorly supported, BS: 78) within the large clade of gonochoristic *Mesonerilla* spp.

Pairwise comparison of *M. harubangi* sp. nov. sequence similarity to other gonochoristic *Mesonerilla* spp.: 18S rRNA – 96.28–97.42% similar to its sister group (clade comprising *M. laerkae* and *M.* sp. 2) – 96.22–97.38% similar to the remaining gonochoristic *Mesonerilla* spp.; COI – 65.28–65.86% similar to its sister group – 56.57–71.65% similar to the remaining gonochoristic *Mesonerilla* spp.

**Remarks** (see also Table 6 for comparisons of morphologically similar nerillids)

*Mesonerilla harubangi* sp. nov. has nine segments, compound chaetae and club-shaped palps, and thereby conforms to the main characteristics of *Mesonerilla*. Furthermore, it resembles *M. intermedia* and *M. laerkae* by possessing a brooding hood and being gonochoristic (Worsaae 2005a, 2021; Worsaae *et al*. 2019a). *Mesonerilla laerkae* has a pointed tip on the brooding hood and equally long parapodial cirri in the trunk segments, which is not seen in either *M. harubangi* or *M. intermedia*. *Mesonerilla harubangi* differs from both species by being smaller in size and by not possessing continuous dorsolateral transverse ciliary rows (found in *M. intermedia*). The dorsal and ventral ciliation patterns of *M. harubangi* are most comparable to those of *M. xurxoi*, but this species does not possess a brooding hood (Worsaae *et al*. 2019a).

Specimens of *M. harubangi* sp. nov. used for morphological examination were collected from Munseom Islet, while the specimen used for DNA analysis was obtained from Seopseom Islet and identified in the field prior to DNA extraction.

The unresolved phylogenetic position of *M. harubangi* sp. nov. among the other gonochoristic *Mesonerilla* could be explained by the absence of two of the four genes, as only 18S rRNA and COI fragments were successfully obtained. Individual maximum likelihood analysis of COI sequences found *M. harubangi* as sister group to *Mesonerilla*, *Meganerilla*, *Speleonerilla*, *N. irabuensis*, *C. sulcipalpata* gen. et sp. nov., *Micronerilla*, *Leptonerilla*, *Trochonerilla* and *Aristonerilla*. This is also reflected in the low pairwise sequence similarity of COI between *M. harubangi* and all other gonochoristic *Mesonerilla* (around 60%). Inclusion of additional sequence data is expected to clarify the phylogenetic position of this species within the clade of gonochoristic *Mesonerilla* spp.

***Mesonerilla dannyi*** sp. nov.
urn:lsid:zoobank.org:act:AF47235F-7D0A-464E-904C-61D83C1E2AA3
Figs 13–14; Table 6

**Diagnosis**

Hermaphroditic *Mesonerilla* with three antennae and equally short parapodial cirri on segments II–VIII. Segment I with short, ovoid cirri and lacking chaetae. Hermaphroditic with two pairs of spermioducts with separate openings in segments VI, VII, and one pair of oviducts opening in segment VIII.

**Etymology**

Named in honour of Danny Eibye-Jacobsen, in recognition of his valuable contributions to annelid taxonomy and systematics, as well as his highly appreciated mentorship of the first author.

**Type material**

**Holotype**

SOUTH KOREA • adult; Jeju Island, Munseom Islet; 33.22779° N, 126.5675° E; shell gravel with mud at 25 meters depth; 24 May 2018; K. Worsaae and T. Park leg.; NIBRIV0000924486 as permanent whole mount.

**Paratypes**

SOUTH KOREA • 2 adults; Jeju Island, Seopseom Islet; 33.2304° N, 126.6015° E; shell gravel at 15 meters depth; 25 May 2018; K. Worsaae and T. Park leg.; NHMD 1842024, NHMD 1842025 mounted on SEM stubs.

**Representative DNA sequences**

GenBank accession numbers PQ149847 (nuclear 18S rRNA), PQ149827 (nuclear 28S rRNA) and PQ570598 (nuclear H3); from specimen with same collection data as holotype (Table 1).

**Description**

Measurements are based on LM of holotype, counts and ciliation from SEM; values for paratypes are given in parentheses. Body with nine segments (Figs 13A, 14A), total length about 875 µm long (810–985 µm, n = 3). Trunk segments up to about 185 µm wide including parapodia (155–185 µm, n = 3), about 120 µm (115–135 µm, n = 3) excluding parapodia. Segment lengths of paratype 72, 69, 86, 102, 92, 112, 88, 77, 49 µm.

Round prostomium with palps and antennae lost in all mounted specimens, but median antennal and lateral antennal scars observed in SEM (las, ma, Fig. 13A–B). Eyes absent. Nuchal organs visible with CLSM and SEM (no, Fig. 14B).

Parapodial cirri in segments I–IX. Segment I with short cylindrical cirri, 35 µm long (33 µm long, n = 1) (bc, Fig. 13B). Segments II–VIII with cylindrical, slightly tapering cirri, up to 65 µm long (54–74 µm long, n = 3), similar in length, slightly shorter cirri on segment VIII (pc, Fig. 13C). Only regenerating pygidial cirri were observed (rpc, Fig. 13D).

Compound chaetae in segments II–IX, with up to 12 chaetae per parapodium and maximum 180 µm long (128–155 µm long, n = 2) (cc, Fig. 14A).

Prostomium with anterior and posterior fields of presumed sensory cilia (acf, Fig. 14B). Paired, densely ciliated nuchal organs on dorsolateral border between prostomium and segment I (no, Fig. 14B). Ventral ciliation consisting of i) densely ciliated mouth (mo, Fig. 14C), ii) midventral longitudinal ciliary band extending from mouth to pygidium (vc, Fig. 14C–D) and iii) transverse rows of up to about 10 small ciliary tufts at level of parapodia (tvc, Fig. 14D). Multiple single cilia scattered on dorsal, lateral, and ventral sides of body. Many cilia lost during preparation.

Three lateral enteronephridia extending from posterior end of stomach along the hindgut until pygidium (Fig. 13F). Spermioducts present in segments VI and VII with posterior ventral opening. Two relatively long and slender oviducts opening ventrally in segment VIII (so, ovo, Figs 13E, 14D).

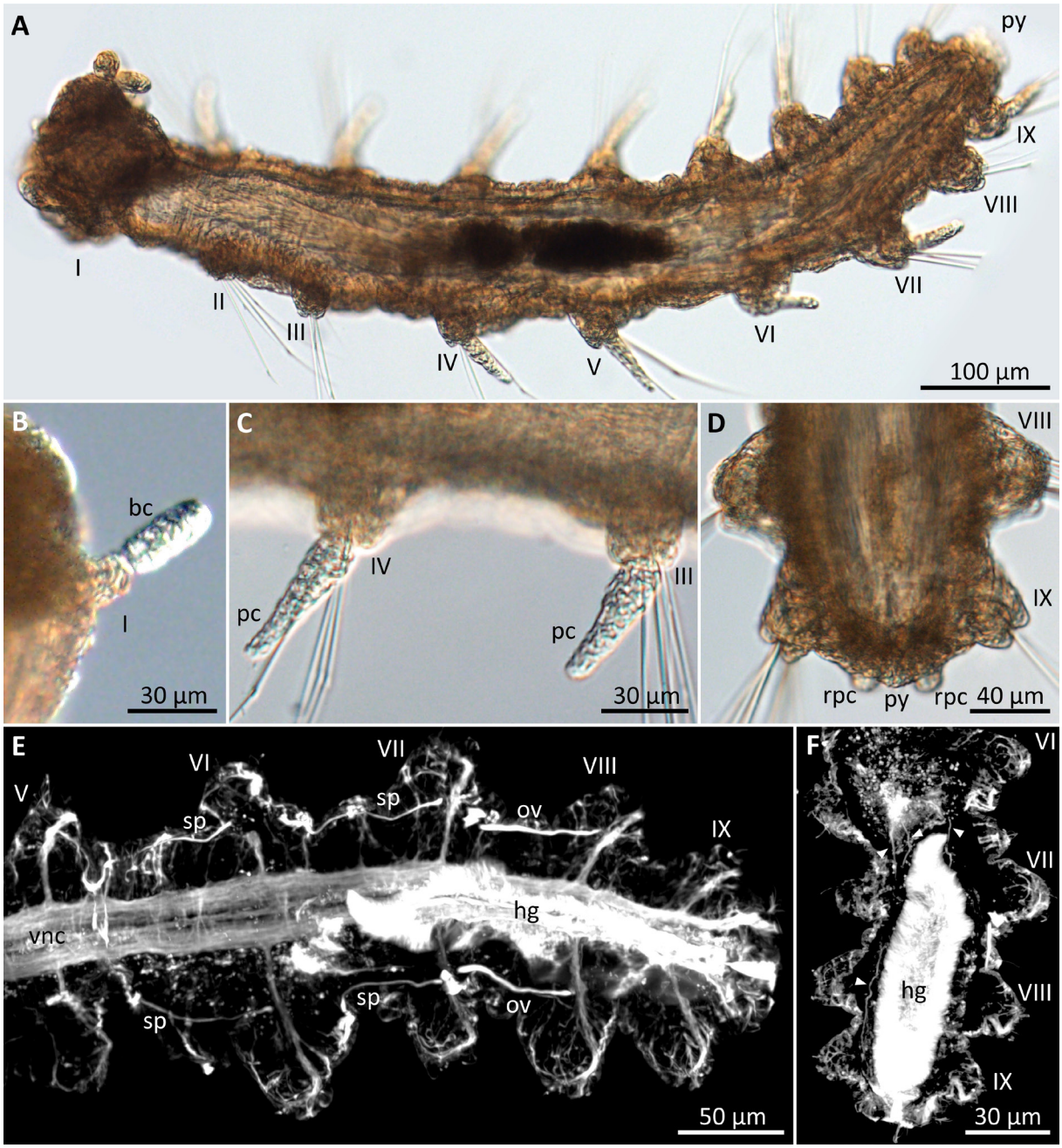


**Fig. 13.** *Mesonerilla dannyi* sp. nov., light (A–D) and confocal laser scanning micrographs (E–F). **A**. Overview of an adult specimen (lost). **B**. Close-up of buccal cirri of an adult specimen (lost). **C**. Close-up of parapodial cirri of A. **D**. Posterior segment and pygidium with regenerating pygidial cirri of B. **E–F**. Holotype (NIBRIV0000924486). **E**. Maximum intensity projection of z-stack of specimen labelled with anti-acetylated α-tubulin showing gonoducts. **F**. Acetylated α-tubulin immunoreactivity of posterior segments, with arrowheads indicating enteronephridia. Abbreviations: bc = buccal cirrus; hg = hindgut; ov = voviduct; pc = parapodial cirrus; py = pygidium; rpc = regenerating pygidial cirrus; sp = spermioduct; vnc = ventral nerve cord; I–IX = segments I–IX.

**Distribution and habitat**

Eastern coast of Seopseom Islet and southern coast of Munseom Islet, south of Jeju Island, South Korea. Collected from 25 meters depth from shell gravel with mud. Associated nerillids from Munseom Islet include *Leptonerilla westheidei* sp. nov., *M. harubangi* sp. nov. and *Nerillidium* sp. 1.

**Molecular information**

*Mesonerilla dannyi* sp. nov. is found as sister group to a clade composed of *M. gamaglandulata* sp. nov., *Mesonerilla roscovita* and *Mesonerilla armoricana* (PP/BS: 1/99).

*Mesonerilla dannyi* sp. nov., like *M. gamaglandulata* sp. nov., has a high sequence similarity of 18S rRNA and 28S rRNA to three hermaphroditic *Mesonerilla*.

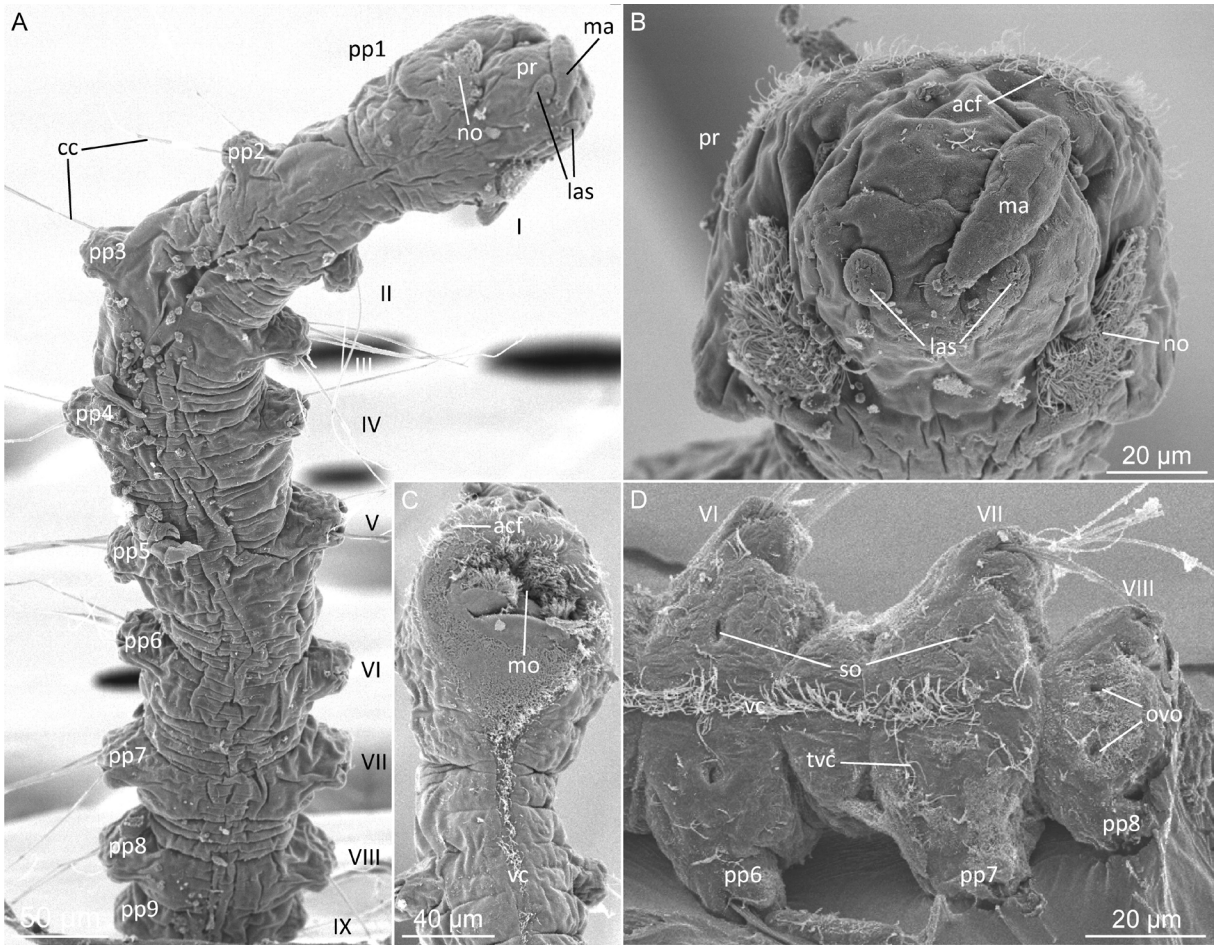


**Fig. 14.** *Mesonerilla dannyi* sp. nov. **A–C**. Paratype (NHMD 1842025), scanning electron micrographs (SEM). **A**. Overview of adult specimen, dorsal view. **B**. Frontal view of prostomium of adult specimen. **C**. Prostomium of adult specimen carrying the mouth, ventral view. **D**. Paratype (NHMD 1842024), close-up of segments VI–VII carrying the spermioducts and oviducts of juvenile, ventral view. Abbreviations: acf = anterior field of sensory cilia; cc = compound chaetae; las = lateral antenna scar; ma = median antenna; mo = mouth opening; no = nuchal organ; ovo = oviducts opening; pcf = posterior field of sensory cilia; pp1–9 = parapodium segment I–XI; pr = prostomium; so = spermioduct opening; tvc = transverse ventral row of cilia; vc = midventral ciliary band; I–IX = segments I–IX.

Pairwise comparison of *M. dannyi* sp. nov. sequence similarity to other hermaphroditic *Mesonerilla* and *Nipponerilla irabuensis*: 18S rRNA – 98.88–99.04% similar to its sister group (clade comprising *M. gamaglandulata* sp. nov., *M. roscovita* and *M. armoricana*) – 99.11% similar to *M. fagei* – 97.52% similar to *N. irabuensis*; 28S rRNA – 89.42% similar to its sister group – 90.85% similar to *M. fagei* – 84.86% similar to *N. irabuensis*; COI – 72.86% similar to its sister group – 68.07% similar to *N. irabuensis*.

**Remarks** (see also Table 6 for comparisons of morphologically similar nerillids)

*Mesonerilla dannyi* sp. nov. is morphologically most similar to the hermaphroditic *Mesonerilla* (Levi 1953; Swedmark 1959; Worsaae *et al*. 2019a), due to its nine-segmented body, compound chaetae, three antennae, equally short and single parapodial cirri in segments II–VIII, and its configuration of gonoducts. It shares the absence of chaetae in segment I with *M. roscovita* and *M. armoricana* as well as the presence of short, ovoid cirri with *M. fagei.* Similar to *M. armoricana*, *M. fagei* and *M. gamaglandulata* sp. nov., cirri on the last segment are similar or nearly equal in length to cirri in the remaining trunk segments (Levi 1953; Swedmark 1959; Worsaae *et al*. 2019a*)*.

## Discussion

This study presents a previously unassessed and high diversity of Nerillidae in the East China Sea, including seven new species described herein and an additional nine potentially new species pending further investigation. Besides the new genus *Cirrinerilla* here described, *Nipponerilla irabuensis* Worsaae, Hansen & Fujita in Worsaae *et al*., 2021 was previously described from the same sampling campaigns (Worsaae *et al.* 2021b). These first two studies on nerillid diversity in the area also revealed two new genera of the family, *Nipponerilla* and *Cirrinerilla*.

Our study also greatly expands the known distribution of *Meganerilla*, *Mesonerilla*, and *Trochonerilla* into the Northwest Pacific Ocean. *Mesonerilla* is the most species-rich nerillid genus, now containing 17 described species (Worsaae *et al*. 2019a, 2021a, 2021b; this study) and represents the highest diversity in the East China Sea with five genetically distinct terminals. Additionally, *Leptonerilla*, *Meganerilla* and *Nerillidium*, previously containing three, five and eight species, respectively (Worsaae 2005a; Worsaae *et al*. 2009), were also well represented.

The phylogenetic analyses yield high support for the monophyly of *Aristonerilla*, *Leptonerilla*, *Meganerilla*, *Micronerilla*, and *Trochonerilla*, albeit low support for *Nerillidium* (BPP = 37, MLB = 0.58). The East Atlantic stygobitic *Speleonerilla isa* Worsaae, Gonzalez, Kerbl, Nielsen, Jørgensen, Armenteros, Iliffe & Martínez, 2018 does not group with the remaining West Atlantic *Speleonerilla* spp. in our analyses. Although *S. isa* also shows a significant morphological distance to the other species of *Speleonerilla*, e.g., with nine versus eight segments, the still limited number of terminals in our analyses may have affected this phylogenetic result. Similar to previous studies (Worsaae 2005a, 2005b; Worsaae *et al*. 2019a) *Mesonerilla* is paraphyletic with two separate clades containing hermaphroditic and gonochoristic terminals, respectively, warranting a revision (Worsaae *et al*. in prep.).

The species of Nerillidae encountered in this study all show a limited distribution. All Japanese species were genetically distinct from the South Korean ones in the phylogenetic analyses, indicating that recent dispersal has not occurred between the two regions. One factor that could play an important role in the connectivity within and between South Korea and Japan is the Kuroshio Current. The northeastern going current, assisted by eddy mixing, could promote inter-island dispersal within the Ryukyu Islands, as seen in the modelling of coral egg and larval dispersal (Odani *et al*. 2017). However, combined with the deep Okinawa Trough, the strong Kuroshio Current might also act as a dispersal barrier (He *et al*. 2015) for shallow water organisms between the northern (e.g., South Korea) and southeastern (e.g., the Ryukyu Islands) areas of the East China Sea. This might be especially true for nerillids that are considered to

have poor dispersal capabilities, as most species have direct development, only produce few offspring, and some genera even display brooding behaviours with juveniles being attached to the mother (i.e., *Mesonerilla*, *Nerillidium* and *Nerillidopsis*) (Westheide 2008; Worsaae *et al*. 2019a; Worsaae 2021).

Dispersal between the Ryukyu Islands may also be affected by the Kerama Gap, located between the Okinawa Islands and the Miyako Islands, which has been shown to limit the inter-island genetic connectivity of, e.g., the tideland snail *Pirenella cingulata* (Gmelin, 1791) (Kojima *et al*. 2006). However, the Kerama Gap does not seem to have been an effective dispersal barrier for nerillids until more recently, since *M. iensis* sp. nov. and *Meganerilla* sp. 1, as well as the two cave species *Leptonerilla* sp. 2 and *L.* sp. 3, constitute genetically separate sister lineages on each side of the gap with high molecular similarity. Nonetheless, it is only among the three geographically close South Korean localities that we find a clear overlap in species distribution: *L. westheidei* sp. nov. and *M. harubangi* sp. nov. have been discovered in samples collected from both Munseom, Seopseom and Beomseom islets off Jeju Island.

Abiotic factors such as salinity, granulometry, and temperature variations may also contribute to the observed distribution patterns but could not be tested with the present sampling efforts (Worsaae *et al*. 2019b, 2021b; Worsaae 2021). Environmental parameters can differ radically across short distances, e.g., within 100 meters inside and outside Unnamed Cave Ie Island, which contains much finer sediment and a different fauna than on the fringing reef. In this way, even open caves can in themselves function as isolation barriers, restricting species dispersal. *Meganerilla iensis* sp. nov. was collected near 'Unnamed Cave' but was absent within the cave itself. In contrast, *C. sulcipalpata* gen. et sp. nov., *L.* sp. 3, *M. gamaglandulata* sp. nov. and *T.* sp. 1 were exclusively found within the cave.

Micro-habitat niches within locations may explain the co-occurrence of three or more nerillid species in many of the sampled localities. Previous studies have found a similar diversity of Nerillidae at localities in the Mediterranean Sea and the Canary Islands (Worsaae *et al*. 2009; Curini-Galletti *et al*. 2012; Martínez *et al*. 2019). The same studies also found a maximum of four to five distinct nerillid species co-occurring and a remarkably high diversity within cave systems, congruent with our results.

In summary, this first insight into the diversity of Nerillidae in the East China Sea revealed an impressively high diversity of novel species, which will contribute significantly to the current regional knowledge on the diversity of meiofaunal annelids and nerillids. The present study furthermore demonstrates the great potential to discover new and important meiofauna in less explored parts of the world and the call for more intensive meiofauna research within the Northwest Pacific and anchialine caves.

## Acknowledgements

We would like to express our deepest gratitude to all who helped with sampling and logistical tasks related to the past 5 years of expeditions to South Korea and Japan. We are indebted to Hyun Soo Rho for his assistance with collecting at Jeju Island in 2015 and to María Herranz and Martin V. Sørensen for their assistance with sorting samples in South Korea in 2018. We greatly acknowledge the assistance: at Iriomote Island 2018 of Shinta Fujimoto, Norio Miyamoto, Peter Rask Møller, Tohru Naruse, and staff of the Tropical Biosphere Research Center, Iriomote Station, University of the Ryukyus; at Ishigaki Island 2018 of Keiichi Kakui, Masaru Mizuyama, Peter Rask Møller; at Okinawa Island 2019 of Mark Christian Allentoft-Larsen, Feran Palero, Danny Eibye-Jakobsen, Kyo Yunokawa and staff of the Sesoko Marine Lab.

## Funding

Expeditions to South Korea and Japan from 2015 to 2019 were financially supported by Ragna Rask Nielsens Grundforskningsfond and Japan Society for the Promotion of Science (grant no. S18162)

to KW; Scandinavia-Japan Sasakawa Foundation (grant no. GA19-0348) to MJH and KW; National Institute of Biological Resources, Korea to TP (grant no. NIBR201501111); VILLUM Foundation, Experiment grant (project no. 17467) to JO; and JSPS Grant-in-Aid for Scientific Research (B) (No. 20H03313) to YF. Confocal microscopy examinations were supported by the Carlsberg Foundation (Grant Nos. CF15-0946 and CF20-0458).

## Compliance with ethical standards

### Conflict of interest

The authors declare that they have no conflict of interest.

### Ethical approval

All applicable international, national, and/or institutional guidelines for animal testing, animal care and use of animals were followed by the authors.

### Sampling and field studies

All necessary permits for sampling and observational field studies have been obtained by the authors from the competent authorities and are mentioned in the acknowledgements, if applicable. The study is compliant with CBD and Nagoya protocols.

## Data availability

The datasets generated and analysed during the current study are available in the GenBank database with the accession numbers PQ149815-PQ149832 for 28S rRNA, PQ149833-PQ149851 for 18S rRNA, PQ421126-PQ421140 for H3 and PQ570583-PQ570603 for COI. Final alignments and raw trees can be found online in Figshare (https://doi.org/10.6084/m9.figshare.28758929).

## Author contribution statement

KW conceptualized and designed the study. TP organized the sampling trips to South Korea in 2015 and 2018, by coordinating the dives and research vessels, and obtaining collection permits. YF helped organize the collecting in Japan in 2018. JO and YF organized the sampling trip in Japan in 2019 by coordinating the cave dives and all related logistics, as well as obtaining collection permits. Apart from ED, all authors participated in at least one collecting trip and KW in all. YF and KW did all of the cave scuba diving collections, assisted by MJH in Okinawa, and KW and TP did the scuba diving collections in Jeju Island. KW, MJH, TP, YF, JO and JP sorted out specimens. KW identified and fixed the specimens. MJH, JP, ED & KW performed light microscopy and confocal laser scanning microscopy on specimens. Scanning electron microscopy was undertaken by KW. Morphological measurements and assessment, molecular sequencing, and phylogenetic analyses were performed by MJH, KW and ED. KW, MJH and ED drafted the manuscript. The other co-authors have all read and commented on the manuscript.

## References

Atherton S. & Jondelius U. 2020. Biodiversity between sand grains: Meiofauna composition across southern and western Sweden assessed by metabarcoding. *Biodiversity Data Journal* 8: e51813. https://doi.org/10.3897/BDJ.8.e51813

Boaden P.J.S. 1961. *Meganerilla swedmarki* nov. gen. nov. spec. an archiannelid of the family Nerillidae. *Arkiv för Zoologi* 13: 553–559.

Brown S., Rouse G., Hutchings P. & Colgan D. 1999. Assessing the usefulness of histone H3, U2 snRNA and 28S rDNA in analyses of polychaete relationships. *Australian Journal of Zoology* 47 (5): 499–516. https://doi.org/10.1071/ZO99026

Chan B.K.K., Xu G., Kim H.K., Park J. & Kim W. 2018. Living with marginal coral communities: Diversity and host-specificity in coral-associated barnacles in the northern coral distribution limit of the East China Sea. *PloS ONE* 13 (5): e0196309. https://doi.org/10.1371/journal.pone.0196309

Chiu R.W.T., Iwatani H., Kitamura A., Yasuhara M. & Fujita K. 2017. Response of subtropical submarine-cave ecosystem to Holocene cave development and Asian monsoon variability. *Paleobiology* 43: 425–434. https://doi.org/10.1017/pab.2016.53

Chough S.K., Lee H. & Yoon S.H. 2000. *Marine Geology of Korean Seas*. Elsevier Science B.V.

Cohen B.L., Améziane N., Eleaume M. & de Forges B.R. 2004. Crinoid phylogeny: a preliminary analysis (Echinodermata: Crinoidea). *Marine Biology* 144: 605–617. https://doi.org/10.1007/s00227-003- 1212-7

Colgan D.J., McLauchlan A., Wilson G.D., Livingston S.P., Edgecombe G.D., Macaranas J., Cassis G. & Gray M.R. 1998. Histone H3 and U2 snRNA DNA sequences and arthropod molecular evolution. *Australian Journal of Zoology* 46 (5): 419–437. https://doi.org/10.1071/ZO98048

Colgan D.J., Hutchings P.A. & Brown S. 2001. Phylogenetic relationships within the Terebellomorpha. *Journal of the Marine Biological Association of United Kingdom* 81 (5): 765–773. https://doi.org/10.1017/S002531540100457X

Curini-Galletti M., Artois T., Delogu V., De Smet W.H., Fontaneto D., Jondelius U., Leasi F., Martínez A., Meyer-Wachsmuth I., Nilsson K.S., Tongiorgi P., Worsaae K. & Todaro M.A. 2012. Patterns of diversity in soft-bodied meiofauna: dispersal ability and body size matter. *PloS ONE* 7 (3): 1–13. https://doi.org/10.1371/journal.pone.0033801

Di Domenico M., Lana P., Martínez A. & Worsaae K. 2014. Molecular and morphological phylogeny of Saccocirridae (Annelida) reveals two cosmopolitan clades with specific habitat preferences. *Molecular Phylogenetics and Evolution* 75: 202–218. https://doi.org/10.1016/j.ympev.2014.02.003

Eisma D. 2010. *South Korea. In*: Bird E.C.F. (ed.) *Encyclopedia of the World's Coastal Landforms*: 1207–1212. Springer Netherlands, Dordrecht. https://doi.org/10.1007/978-1-4020-8639-7_222

Fujikura K., Kitazato H., Lindsay D., Nishida S. & Shirayama Y. 2010. Marine biodiversity in Japanese waters. *PloS ONE* 5: e11836. https://doi.org/10.1371/journal.pone.0011836

Fujimoto S. 2015. *Quisarctus yasumurai* gen. et sp. nov. (Arthrotardigrada: Halechiniscidae) from a submarine cave, off Iejima, Ryukyu Islands, Japan. *Zootaxa* 3948: 145–150. https://doi.org/10.11646/zootaxa.3948.1.10

Fujimoto S. & Miyazaki K. 2013. *Neostygarctus lovedeluxe* n. sp. from the Miyako Islands, Japan: The first record of Neostygarctidae (Heterotardigrada: Arthrotardigrada) from the Pacific. *Zoological Science* 30: 414–419. https://doi.org/10.2108/zsj.30.414

Fujita K., Arakaki T., Denda T., Hidaka M., Hirose E. & Reimer J. 2015. *Nature in the Ryukyu Archipelago: Coral Reefs, Biodiversity, and the Natural Environment*. International Research Hub Project for Climate Change and Coral Reef/Island Dynamics, Faculty of Science, University of the Ryukyus.

Fujita Y. & Naruse T. 2024. A new genus and species of a submarine cave crab of the family Plagusiidae Dana, 1851 (Crustacea: Brachyura: Grapsoidea) from Okinawa Island, Ryukyu Islands, southwestern Japan. *Zootaxa* 5410 (3): 408–418. https://doi.org/10.11646/zootaxa.5410.3.8

Gallagher S.J., Iryu Y., Itaki T., Kitamura A., Koizumi I. & Hoiles P.W. 2015. The Pliocene to recent history of the Kuroshio and Tsushima Currents: a multi-proxy approach. *Progress in Earth and Planetary Science* 2 (1): 17. https://doi.org/10.1186/s40645-015-0045-6

Giere O. 2009. *Meiobenthology: The Microscopic Motile Fauna of Aquatic Sediments*. Springer-Verlag, Berlin Heidelberg. https://doi.org/10.1007/b106489

Giribet G., Carranza S., Baguña J., Riutort M. & Ribera C. 1996. First molecular evidence for the existence of a Tardigrada + Arthropoda clade. *Molecular Biology and Evolution* 13 (1): 76–84. https://doi.org/10.1093/oxfordjournals.molbev.a025573

Gonzalez B.C., Martínez A., Worsaae K. & Osborn K.J. 2021. Morphological convergence and adaptation in cave and pelagic scale worms (Polynoidae, Annelida). *Scientific Reports* 11: 10718. https://doi.org/10.1038/s41598-021-89459-y

Hayami I. & Kase T. 1993. Submarine cave Bivalvia from the Ryukyu Islands: Systematics and evolutionary significance. *The University Museum, The University of Tokyo, Bulletin* 35: 1–133.

He L., Mukai T., Chu K.H., Ma Q. & Zhang J. 2015. Biogeographical role of the Kuroshio current in the amphibious mudskipper *Periophthalmus modestus* indicated by mitochondrial DNA data. *Scientific Reports* 5: 15645. https://doi.org/10.1038/srep15645

Higgins R. & Thiel H. 1988. *Introduction to the Study of Meiofauna*. Smithsonian Institution Press, Washington DC.

Hillis D.M. & Dixon M.T. 1991. Ribosomal DNA: molecular evolution and phylogenetic inference. *The Quarterly Review of Biology* 66 (4): 411–453. https://doi.org/10.1086/417338

Hoang D.T., Chernomor O., von Haeseler A., Minh B.Q. & Vinh L.S. 2018. UFBoot2: Improving the ultrafast bootstrap approximation. *Molecular Biology and Evolution* 35 (2): 518–522. https://doi.org/10.1093/molbev/msx281

Ibrahim A.K., Gamil I.S., Abd-El baky A.A., Hussein M.M. & Tohamy A.A. 2011. Comparative molecular and conventional detection methods of *Babesia equi* (*B. Equi*) in Egyptian equine. *Global Veterinaria* 7 (2): 201–210.

Ise Y., Vacelet J., Mizuyama M. & Fujita Y. 2023. New lithistid sponge of the genus *Sollasipelta* (Porifera, Demospongiae, Tetractinellida, Neopeltidae) from submarine caves of the Ryukyu Islands, southwestern Japan, with redescription of *S. sollasi*. *Zootaxa* 5285 (2): 293–310. https://doi.org/10.11646/zootaxa.5285.2.4

Jimi N. 2024. The polychaetous annelids of Japan: Updated checklist of known species. *Species Diversity* 29 (2): 337–377. https://doi.org/10.12782/specdiv.29.337

Jouin C. 1968. Sexualité et biologie de la reproduction chez *Mesonerilla* Remane et *Meganerilla* Boaden (Archiannélides Nerillidae). *Cahiers de Biologie Marine* 9: 31–52.

Jouin C. 1971. Status of the knowledge of the systematics and ecology of Archiannelida. *Smithsonian Contributions to Zoology* 76: 47–56.

Jouin C. & Swedmark B. 1965. *Paranerilla limicola* n. g., n. sp., Archiannélide Nerillidae du benthos vaseux marin. *Cahiers de Biologie Marine* 6: 201–218

Kakui K. & Fujita Y. 2018. *Haimormus shimojiensi*s, a new genus and species of Pseudozeuxidae (Crustacea: Tanaidacea) from a submarine limestone cave in Northwestern Pacific. *PeerJ* 6: e4720. https://doi.org/10.7717/peerj.4720

Kakui K. & Fujita Y. 2023. New sea spider species (Pycnogonida: Austrodecidae) from a submarine cave in Japan. *Journal of the Marine Biological Association of the United Kingdom* 103: e44. https://doi.org/10.1017/S002531542 10.1017/S002531542

Kang T. & Kim D. 2020. Meiobenthic community structure on the Northeast coastal area of Jeju Island, Korea. *Ocean and Polar Research* 42 (1): 1–13. https://doi.org/10.4217/OPR.2020.42.1.001

Katoh K. & Standley D.M. 2013. MAFFT Multiple sequence alignment software version 7: improvements in performance and usability. *Molecular Biology and Evolution* 30 (4): 772–780. https://doi.org/10.1093/molbev/mst010

Katoh K., Kuma K., Misawa K. & Miyata T. 2002. MAFFT: A novel method for rapid multiple sequence alignment based on fast Fourier transform. *Nucleic Acids Research* 30 (14): 3059–3066. https://doi.org/10.1093/nar/gkf436

Kim D., Je J. & Lee J. 2000. The community structure and spatial distribution of meiobenthos in the Kanghwa tidal flat, west coast of Korea. *Ocean and Polar Research* 22: 15–23.

Kimura M. 1980. A simple method for estimating evolutionary rates of base substitutions through comparative studies of nucleotide sequences. *Journal of Molecular Evolution* 16 (2): 111–120. https://doi.org/10.1007/BF01731581

Koike K. 2010. *Japan. In*: Bird E.C.F. (ed.) *Encyclopedia of the World's Coastal Landforms*: 1213–1224. Springer Netherlands, Dordrecht. https://doi.org/10.1007/978-1-4020-8639-7_223

Kojima S., Iijima A., Kamimura S., Kimura T., Kurozumi T. & Furota T. 2006. Molecular phylogeny and population structure of tideland snails in the genus *Cerithidea* around Japan. *Marine Biology* 149 (3): 525–535. https://doi.org/10.1007/s00227-005-0183-2

Komai T. & Fujita Y. 2018. A new genus and new species of alpheid shrimp from a marine cave in the Ryukyu Islands, Japan, with additional record of *Salmoneus antricola* Komai, Yamada & Yunokawa, 2015 (Crustacea: Decapoda: Caridea). *Zootaxa* 4369 (4): 575–586. https://doi.org/10.11646/zootaxa.4369.4.7

Kumar S., Knyaz C., Li M., Stecher G. & Tamura K. 2018. MEGA X: Molecular evolutionary genetics analysis across computing platforms. *Molecular Biology and Evolution* 35 (6): 1547–1549. https://doi.org/10.1093/molbev/msy096

Lee H., Kang T.W., Rho H.S. & Kim D. 2019. Seasonal distribution characteristics of meiobenthos at Gwangyang Bay, Korea. *The Sea Journal of the Korean Society of Oceanography* 24 (3): 400–421. https://doi.org/10.7850/JKSO.2019.24.3.400

Lévi C. 1953. Archiannélides Nerillidae de la région de Roscoff. *Archives de Zoologie expérimentale et générale* 90 (2): 64–70.

Liu J.Y. 2013. Status of marine biodiversity of the China seas. *PLoS ONE* 8 (1): e50719. https://doi.org/10.1371/journal.pone.0050719

Magagnini G. 1966. Un nouvel Archiannélide Nerillidae des côtes de Roscoff: *Meganerilla clavata* n.sp. *Cahiers de Biologie Marine* 7: 331–335.

Martínez A., Artois T., Curini-Galletti M., Di Domenico M., Fontaneto D., Gobert S., Jörger K.M., Leasi F., Norenburg J., Núñez J., Todaro M.A., Zotto M.D. & Worsaae K. 2019. Patterns of diversity and endemism of soft-bodied meiofauna in an oceanic island, Lanzarote, Canary Islands. *Marine Biodiversity* 49 (5): 2033–2055. https://doi.org/10.1007/s12526-019-01007-0

Mendes S.L. da S.D., Rodrigues J.C. & Rizzo A.E. 2024. A new species of *Paranerilla* Jouin & Swedmark, 1965 (Annelida: Polychaeta) from Brazil. *European Journal of Taxonomy* 943: 144–153. https://doi.org/10.5852/ejt.2024.943.2591

Meyer C.P. 2003. Molecular systematics of cowries (Gastropoda: Cypraeidae) and diversification patterns in the tropics. *Biological Journal of the Linnean Society* 79: 401–459. https://doi.org/10.1046/j.1095-8312.2003.00197.x

Miller M., Pfeiffer W.T. & Schwartz T. 2010. Creating the CIPRES Science Gateway for inference of large phylogenetic trees. *2010 Gateway Computing Environments Workshop (GCE), New Orleans*: 1–8. https://doi.org/10.1109/GCE.2010.5676129

Minh B.Q., Schmidt H.A., Chernomor O., Schrempf D., Woodhams M.D., von Haeseler A. & Lanfear R. 2020. IQ-TREE2: New models and efficient methods for phylogenetic inference in the genomic era. *Molecular Biology and Evolution* 37 (5): 1530–1534. https://doi.org/10.1093/molbev/msaa015

Motokawa M. & Kajihara H. 2017. *Species Diversity of Animals in Japan*. Springer Japan. https://doi.org/10.1007/978-4-431-56432-4

Müller M.C. 2002. *Aristonerilla*: A new nerillid genus (Annelida: Polychaeta) with description of *Aristonerilla* (*Micronerilla*) *brevis* comb. nov. from a seawater aquarium. *Cahiers de Biologie Marine* 43: 131–139. https://doi.org/10.21411/CBM.A.137553DE

Müller M.C. & Worsaae K. 2006. CLSM analysis of the phalloidin-stained muscle system in *Nerilla antennata*, *Nerillidium* sp. and *Trochonerilla mobilis* (Polychaeta; Nerillidae). *Journal of Morphology* 267 (8): 885–896. https://doi.org/10.1002/jmor.10292

Müller M.C., Bernhard J.M. & Jouin-Toulmond C. 2001. A new member of Nerillidae (Annelida: Polychaeta), *Xenonerilla bactericola* gen. et sp. nov., collected off California, USA. *Cahiers de Biologie Marine* 42 (3): 203–217. https://doi.org/10.21411/CBM.A.64923395

Nakae M., Aizawa M., Fujiwara K., Fukui Y., Hagiwara K., Hata H., Jeong B., Koeda K., Senou H., Shinohara G., Motomura H., Tashiro S., Yamakawa T., Yoshida T. & Matsuura, K. 2018. An annotated checklist of fishes of Amami-oshima Island, the Ryukyu Islands, Japan. *Memoirs of the National Museum of Nature and Science* 52: 205–361.

Naruse T. & Fujita Y. 2015. *Lipkemera iejima*, a new cavernicolous crab (Brachyura: Xanthidae) from a submarine cave at Ie Island, central Ryukyu Islands, Japan. *Crustacean Research* 44: 21–27. https://doi.org/10.18353/crustacea.44.0_21

Núñez J., Ocaña O. & Brito M.C. 1997. Two new species (Polychaeta: Fauveliopsidae and Nerillidae) and other polychaetes from the marine lagoon cave of Jameos del Agua, Lanzarote (Canary Islands). *Bulletin of Marine Science* 60 (2): 252–260.

Odani S., Uchiyama Y., Kashima M., Kamidaira Y. & Mitarai S. 2017. Influence of the Kuroshio current on dispersal of coral spawn and larvae around Ryukyu Islands. *Journal of Japan Society of Civil Engineers* 73 (2): 1315–1320. https://doi.org/10.2208/kaigan.73.I_1315

Okanishi M. & Fujita Y. 2018. First finding of anchialine and submarine cave dwelling brittle stars from the Pacific Ocean, with descriptions of new species of *Ophiolepis* and *Ophiozonella* (Echinodermata: Ophiuroidea: Amphilepidida). *Zootaxa* 4377 (1): 1–20. https://doi.org/10.11646/zootaxa.4377.1.1

Osawa M. & Fujita Y. 2019. Submarine cave hermit crabs (Crustacea: Decapoda: Anomura: Paguroidea) from three islands of the Ryukyu Islands, southwestern Japan. *Zootaxa* 4560 (3): 463–482. https://doi.org/10.11646/zootaxa.4560.3.3

Osawa M. & Fujita Y. 2022. A new species of the genus *Eutrichopagurus* Komai, 2015 (Crustacea: Decapoda: Anomura: Paguridae) from a submarine cave in the Ryukyu Islands, southwestern Japan. *Zootaxa* 5214 (3): 440–450. https://doi.org/10.11646/zootaxa.5214.3.6

Park J. 2023. *Systematic Studies on the Korean Interstitial Polychaetes (Annelida) Based on Morphological and Molecular Data*. PhD Thesis, Ewha Womans University, Seoul, Korea.

Pavlyuk O.N. & Trebukhova Y.A. 2011. Intertidal meiofauna of Jeju Island, Korea. *Ocean Science Journal* 46 (1): 1–11. https://doi.org/10.1007/s12601-011-0001-3

Posada D. 2008. jModelTest: Phylogenetic model averaging. *Molecular Biology and Evolution* 25: 1253–1256. https://doi.org/10.1093/molbev/msn083

Rambaut A., Baele G., Drummond A.J., Xie D. & Suchard M.A. 2018. Posterior summarization in Bayesian phylogenetics using Tracer 1.7. *Systematic Biology* 67 (5): 901–904. https://doi.org/10.1093/sysbio/syy032

Reimer J., Biondi P., Lau Y.W., Masucci G.D., Nguyen X., Santos M. & Wee H.B. 2019. Marine biodiversity research in the Ryukyu Islands, Japan: Current status and trends. *PeerJ Preprints* 7: e27029v2. https://doi.org/10.7717/peerj.6532

Riser N.W. 1988. Morphology of a new species of nerillid polychaete from the north shore of Massachusetts Bay, U.S.A. *Transactions of the American Microscopical Society* 107 (2): 171–179. https://doi.org/10.2307/3226459

Ronquist F. & Huelsenbeck J. 2003. MrBayes 3: Bayesian phylogenetic inference under mixed models. *Bioinformatics* 19: 1572–1574. https://doi.org/10.1093/bioinformatics/btg180

Saito T. & Fujita Y. 2022. A new shrimp of the genus *Odontozona* Holthuis, 1946 (Decapoda: Stenopodidea: Stenopodidae) from a submarine cave of the Ryukyu Islands, Indo-West Pacific. *Zootaxa* 5175 (4): 439–452. https://doi.org/10.11646/zootaxa.5175.4.2

Saito Y. & Alino P.M. 2008. *Regional Conditions*. *In*: Mimura N. (ed.) *Asia-Pacific Coasts and their Management: States of Environment*: 255–331. Springer, Dordrecht. https://doi.org/10.1007/978-1-4020-3625-5_5

Saphonov M.V. & Tzetlin A.B. 1988. *Nerilla jouini* sp. n. (Polychaeta, Nerillidae) – a new archiannelid from the Japan Sea. *Zoologicheskii Zhurnal* 67 (6): 839–845.

Saphonov M.V. & Tzetlin A.B. 1997. Nerillidae (Annelida: Polychaeta) from the White Sea, with description of a new species of *Micronerilla* Jouin. *Ophelia* 47 (3): 215–226. https://doi.org/10.1080/00785236.1997.10428672

Sasaki S. 1981. A new species of the genus *Saccocirrus* (Archiannelida) from Hokkaido, Northern Japan. *Annotationes Zoologicae Japonenses* 54 (4): 259–266

Schindelin J., Arganda-Carreras I., Eliceiri K., Frise E., Hartenstein V., Kaynig V., Longair M., Pietzsch T., Preibisch S., Rueden C., Saalfeld S., Schmid B., Tinevez J., Tomancak P., White D.J. & Cardona A. 2012. Fiji: An open-source platform for biological-image analysis. *Nature Methods* 9 (7): 676–682. https://doi.org/10.1038/nmeth.2019

Schmidt H. & Westheide W. 1998. RAPD-PCR experiments confirm the distinction between three morphologically similar species of *Nerilla* (Polychaeta: Nerillidae). *Zoologischer Anzeiger* 236: 277–285.

Shimada D. & Kajihara H. 2014. Two new species of free-living marine nematodes of *Adoncholaimus* Filipjev, 1918 (Oncholaimida: Oncholaimidae: Adoncholaiminae) from Hokkaido, northern Japan, with a key to species and discussion of the genus. *Nematology* 16: 437–451. https://doi.org/10.1163/15685411-00002776

Shimada D., Kajihara H. & Mawatari S. 2009. Three new species of free-living marine nematodes (Nematoda: Enoplida) from Northern Japan. *Species Diversity* 14: 137–150. https://doi.org/10.12782/specdiv.14.137

Shimada D., Kakui K. & Fujita Y. 2023. A new species of free-living marine nematode, *Fotolaimus cavus* sp. nov. (Nematoda, Oncholaimida, Oncholaimidae), isolated from a submarine anchialine cave in the Ryukyu Islands, southwestern Japan. *Zoosystematics and Evolution* 99: 519–533. https://doi.org/10.3897/zse.99.109097

Shimomura M. & Fujita Y. 2017. First description of the female of *Heteromysoides simplex* Hanamura & Kase, 2001 (Mysidacea: Mysidae) collected from a submarine cave on Ie-jima Island, Ryukyu Islands, southwestern Japan. *Proceedings of the Biological Society of Washington* 130: 75–83. https://doi.org/10.2988/17-00001

Shimomura M. & Fujita Y. 2021. *Seborgia cavernicola* sp. nov. from a submarine cave on Okinawa Island, Ryukyu Islands, southwestern Japan (Crustacea, Amphipoda, Seborgiidae). *Zootaxa* 4927 (1): 133–142. https://doi.org/10.11646/zootaxa.4927.1.9

Shimomura M., Fujita Y. & Naruse T. 2012. First record of the genus *Thetispelecaris* Gutu & Illife, 1998 (Crustacea: Peracarida: Bochusacea) from a submarine cave in the Pacific Ocean. *Zootaxa* 3367 (1): 69–78. https://doi.org/10.11646/zootaxa.3367.1.7

Sterrer W. & Iliffe T. 1982. *Mesonerilla prospera*, a new Archiannelid from marine caves in Bermuda. *Proceedings of the Biological Society of Washington* 95: 509–514.
Available from https://www.biodiversitylibrary.org/page/34964823 [accessed 17 Jul. 2025].

Swedmark B. 1959. Archiannélides Nerillidae des côtes du Finistère. *Archives de Zoologie expérimentale et générale* 98: 26–42.

Takayasu K. 1978. Ryukyu Limestone of Okinawa-Jima, South Japan: A stratigraphical and sedimentological study. *Memoirs of the Faculty of Science, Kyoto University*. *Series of Geology and Mineralogy* 45 (1): 133–175.

Tzetlin A.B. & Larionov V.V. 1988. Morphology of a new Archiannelid *Akessoniella orientalis* gen. et sp. n. (Nerillidae). *Zoologicheskii Zhurnal* 67: 846–857.

Tzetlin A.B. & Saphonov M.A.V. 1992. *Trochonerilla mobilis* gen. et sp. n., a meiofaunal nerillid (Annelida, Polychaeta) from a marine aquarium in Moscow. *Zoologica Scripta* 21 (3): 251–254. https://doi.org/10.1111/j.1463-6409.1992.tb00329.x

Uchida T. 1935. Eine neue Urannelidenart, *Polygordius pacificus* n. sp. *Proceedings of the Imperial Academy* 11: 119–120. https://doi.org/10.2183/pjab1912.11.119

Veron J.E.N. 1992. Hermatypic corals of Japan. *Australian Institute of Marine Science, Monograph Series* 9: 1–234. https://doi.org/10.5962/bhl.title.60634

Vonnemann V., Schrödl M., Klussmann-Kolb A. & Wägele H. 2005. Reconstruction of the phylogeny of the Opisthobranchia (Mollusca: Gastropoda) by means of 18S and 28S rRNA gene sequences. *Journal of Molluscan Studies* 71 (2): 113–125. https://doi.org/10.1093/mollus/eyi014

Wang P., Li Q. & Li C. 2014. *Geology of the China Seas*. Developments in Marine Geology 6. Elsevier.

Weese D.A., Fujita Y. & Santos S.R. 2016. Looking for needles in a haystack: Molecular identification of anchialine crustacean larvae (Decapoda: Caridea) from the Shiokawa Spring, Okinawa Island, Ryukyu Islands, Japan. *Journal of Crustacean Biology* 36 (1): 61–67.

Westheide W. 2008. *Polychaetes: Interstitial Families, Keys and Notes for the Identification of the Species*. Synopses of the British Fauna (New Series) 44, 2nd Edition. Linnean Society, London.

Westheide W. & Purschke G. 1996. *Leptonerilla diplocirrata*, a new genus and species of interstitial polychaetes from the island of Hainan, South China (Nerillidae). *Proceedings of the Biological Society of Washington* 109 (3): 586–590. Available from https://www.biodiversitylibrary.org/page/34645193 [accessed 17 Jul. 2025].

Wilke U. 1953. *Mesonerilla intermedia* nov. sp., ein neuer Archiannelide aus dem Golf von Neapel. *Zoologischer Anzeiger* 150: 211–215.

Worsaae K. 2005a. Systematics of Nerillidae (Polychaeta, Annelida). *Meiofauna Marina*: 49–74.

Worsaae K. 2005b. Phylogeny of Nerillidae (Polychaeta, Annelida) as inferred from combined 18S rDNA and morphological data. *Cladistics* 21 (2): 143–162. https://doi.org/10.1111/j.1096-0031.2005.00058.x

Worsaae K. 2020. Annelida (excluding Clitellata and Sipuncula). *In*: Schmidt-Rhaesa A. (ed.) *Guide to the Identification of Marine Meiofauna*: 239–270. Verlag Dr. Friedrich Pfeil.

Worsaae K. 2021 (2014, Online version). 7.9 Errantia incertae sedis: Nerillidae Levinsen, 1883. *In*: Purschke G., Böggemann M. & Westheide W. (eds) *Handbook of Zoology. Annelida Volume 3: Pleistoannelida, Sedentaria III and Errantia I*: 215–227. DeGruyter, Berlin. https://doi.org/10.1515/9783110291704-011

Worsaae K. & Kristensen R.M. 2005. Evolution of interstitial Polychaeta (Annelida). *In*: Bartolomaeus T. & Purschke G. (eds) *Morphology, Molecules, Evolution and Phylogeny in Polychaeta and Related Taxa*. Developments in Hydrobiology 179: 319–340. Springer Netherlands, Dordrecht. https://doi.org/10.1007/1-4020-3240-4_18

Worsaae K. & Müller M.C.M. 2004. Nephridial and gonoduct distribution patterns in Nerillidae (Annelida: Polychaeta) examined by tubulin staining and cLSM. *Journal of Morphology* 261 (3): 259–269. https://doi.org/10.1002/jmor.10153

Worsaae K. & Rouse G. 2009. *Mesonerilla neridae* n. sp. (Nerillidae): First meiofaunal annelid from deep-sea hydrothermal vents. *Zoosymposia* 2: 297–303. https://doi.org/10.11646/ZOOSYMPOSIA.2.1.20

Worsaae K., Sterrer W. & Iliffe T. 2004. *Longipalpa saltatrix*, a new genus and species of the meiofaunal family Nerillidae (Annelida: Polychaeta) from an anchialine cave in Bermuda. *Proceedings of the Biological Society of Washington* 117 (3): 346–362.
Available from https://www.biodiversitylibrary.org/page/35515799 [accessed 17 Jul. 2025].

Worsaae K., Martínez A. & Núñez J. 2009. Nerillidae (Annelida) from the Corona lava tube, Lanzarote, with description of *Meganerilla cesari* n. sp. *Marine Biodiversity* 39 (3): 195–207. https://doi.org/10.1007/s12526-009-0027-2

Worsaae K., Mikkelsen M.D. & Martínez A. 2019a. Description of six new species of *Mesonerilla* (Nerillidae, Annelida) and an emended description of *M. intermedia* Wilke, 1953, from marine and cave environments. *Marine Biodiversity* 49 (5): 2141–2165. https://doi.org/10.1007/s12526-019-00984-6

Worsaae K., Armenteros M., Gonzalez B.C., Iliffe T.M., Jørgensen J.T., Kerbl A., Nielsen S.H. & Martínez A. 2019b. Diversity and evolution of the stygobitic *Speleonerilla* nom. nov. (Nerillidae, Annelida) with description of three new species from anchialine caves in the Caribbean and Lanzarote. *Marine Biodiversity* 49 (5): 2167–2192. https://doi.org/10.1007/s12526-018-0906-5

Worsaae K., Kerbl A., Di Domenico M., Gonzalez B.C., Bekkouche N. & Martínez A. 2021a. Interstitial Annelida. *Diversity* 13 (2): 77. https://doi.org/10.3390/d13020077

Worsaae K., Hansen M.J., Axelsen O., Kakui K., Møller P.R., Osborn K.J., Martínez A., Gonzalez B.C., Miyamoto N. & Fujita Y. 2021b. A new cave-dwelling genus and species of Nerillidae (Annelida) from the Ryukyu Islands, Japan. *Marine Biodiversity* 51: 67. https://doi.org/10.1007/s12526-021-01199-4

Xia X. 2018. DAMBE7: New and improved tools for data analysis in molecular biology and evolution. *Molecular Biology and Evolution* 35 (6): 1550–1552. https://doi.org/10.1093/molbev/msy073

Yamanishi R. 1983. Preliminary report on the fauna of interstitial polychaetes (Annelida) of Japan. *Benthos Research* 24: 41–48. https://doi.org/10.5179/benthos1970.1983.41

Printed versions of all papers are deposited in the libraries of four of the institutes that are members of the *EJT* consortium: Muséum national d'Histoire naturelle, Paris, France; Meise Botanic Garden, Belgium; Royal Museum for Central Africa, Tervuren, Belgium; Royal Belgian Institute of Natural Sciences, Brussels, Belgium. The other members of the consortium are: Natural History Museum of Denmark, Copenhagen, Denmark; Naturalis Biodiversity Center, Leiden, the Netherlands; Museo Nacional de Ciencias Naturales-CSIC, Madrid, Spain; Leibniz Institute for the Analysis of Biodiversity Change, Bonn – Hamburg, Germany; National Museum of the Czech Republic, Prague, Czech Republic; The Steinhardt Museum of Natural History, Tel Aviv, Israël.

## Supplementary file

**Supp. file 1.** Pairwise genetic distances for 18S, 28S, H3, and COI gene fragments (values in %).
https://doi.org/10.5852/ejt.2025.1021.3075.13715